ROLES OF THE PRESYNAPTIC CHOLINE TRANSPORTER IN SUSTAINING CHOLINERGIC SIGNALING AS REVEALED USING GENETICALLY ALTERED MICE

By

David Randall Lund

Dissertation

Submitted to the Faculty of the

Graduate School of Vanderbilt University

in partial fulfillment of the requirements

for the degree of

DOCTOR OF PHILOSOPHY

in

Neuroscience

December, 2010

Nashville, Tennessee

Approved:

Professor Craig H. Kennedy

Professor Randy D. Blakely

Professor Danny G. Winder

Professor P. Jeffery Conn

Professor David H. Wasserman

To Steve and Kathryn, without whom I would never have come to graduate school

ACKNOWLEDGEMENTS

A long and stimulating journey such as my graduate career has left me with more people to thank than can possibly fit in these pages, but the following people deserve special recognition.

First and foremost, my wife Sabata Lund, who saw me through the pleasure and pain of graduate school. She could brighten up any day whether the experiment went wrong (most days), or was happy to celebrate even the most minor accomplishments. I am lucky that I have someone who, after enduring 6 years of intense education, thinks it will be fun if I do 3 more. She has also been of great scientific assistance through nursing me back to health after breaking my ankle (even if she helped improve the situation on the way to the ER) and in developing qPCR assays for the transgenic mice. The rest of my family has been important to nurture my scientific spirit: my mother Marilyn, the only other bench scientist, and my father Randall, and brothers Brian and Bradley, the engineers who constantly remind me of the practical end of our work.

I would also like to thank Randy. A thesis project is only as good as the guiding mentor. I am particularly thankful that he would take the time to seriously consider any potential project or experiment no matter how difficult or expensive it might be. Of course, most of these wild-eyed projects died before they got started (awake mouse pharmacological functional magnetic resonance imaging), but occasionally they bring new and powerful techniques to the lab (synaptopHlourin

mice). In addition to being a scientific mentor, he has also been an excellent teaching mentor helping me to develop other scientific minds.

Without my excellent committee, this project would not have progressed this smoothly. Craig Kennedy, my committee chair, ensured that I never veered off track from my intended goals. Danny Winder provided excellent assistance in developing my NRSA submission as well as guidance in developing behavioral studies. The fatigue and EMG experiments would still be large question marks if not for the contributions of David Wasserman, who was willing to meet on weekends to discuss the project. Jeff Conn provided a solid context to my work, informing me of useful parts of Mihaela and Shawn's work that otherwise would have been lost to history.

Team choline members, past and present, have been instrumental to my graduate success. Alicia Ruggierio, Brett English, and Lily Zurkovsky have been particularly helpful for scientific ideas and general lab camaraderie. Mihaela Bazalakova is responsible for getting me started in the lab, and I would have been completely lost without her. The majority of this work, the Hb9:CHT mouse, was started by Shawn Ferguson without whom I could not have developed this project. Although not presented in this work, the vesicle hypothesis strongly depends upon the work of Dawn Matthies. Jane Wright and Sarah Whitaker have been outstanding resources in the lab both for their technical expertise and experimental assistance. My knowledge has been passed on to my mentees, Peter Reisz, Lise Harbom, Katie Louderback, and Rolicia Martin, who have helped me as either undergraduates or graduate rotation students. Like any mentor, I am sure that I have learned more from them than they have learned from me.

I am of course extremely grateful to the friends that I have developed in the lab for their moral support and scientific insight from beyond the choline transporter. Ana Carniero brought me into the Nashville hockey world and was excellent company during late nights in the lab. In the numerous vain attempts to quantify CHT expression levels in the Hb9:CHT mouse, her biochemistry expertise was invaluable. Julie Field showed me the path to graduation both as classmate and bench partner. Better than anyone else, she would push me to have the clearest, most well-reasoned interpretations possible.

Tammy Jessen and Chris Svitek have been excellent lab managers. Furthermore, they have each been good friends of mine whether shooting arrows across a field or biting the heads off of chocolate penguins. Shannon Hardie, Michelle Carter, and Leda Ramoz have been wonderful lab mates and hockey buddies.

The briefly mentioned synaptopHlourin mice were developed by the lab of Dr. Rita Balice-Gordon at the University of Pennsylvania. I would like to thank her for allowing me to visit her lab to learn the techniques and bring them back to our lab. Dr. Chris Hayworth not only helped me with the experiments but also took me in when I was trapped in Philadelphia due to a strong snowstorm. I hope and expect that this will be a long and fruitful collaboration.

Many of the experiments could not have been accomplished without strong support from the rest of the lab staff, other labs, or core facilities. Great thanks to Qiao Han, Angela Steele, Tracy Moore-Jarret and Kathryn Lindler for excellent laboratory support. I would like to like to thank Dr. Amanda Peltier, Dr. David

Robertson, and Dr. Martin Appalsamy for training and equipment related to the CMAP experiments, and Dr. James Sutcliffe for assistance with copy number determination. Treadmill experiments were performed through the use of the Murine Neurobehavioral Core lab at the Vanderbilt University Medical Center, managed by Dr. John D. Allison. Imaging experiments, analysis, and presentation of confocal images were performed largely through the use of the Vanderbilt University Medical Center Cell Imaging Shared Resource, with particular thanks to Sean Schaffer. This work was supported by NIH award MH073159 and Zenith Award from the Alzheimer's Association and NIH training grant T32 MH64913.

TABLE OF CONTENTS

LIST OF FIGURES

LIST OF ABBREVIATIONS

+/+	Wild-type at the defined locus
+/-	Heterozygous Null Genotype
-/-	Homozygous Null Genotype
ABCA1	ATP binding cassete transporter, sub-family A, member 1
AcOH	Acetate
ACh	Acetylcholine
AChE	Acetylcholinesterase
AChR	Acetylcholine Receptor
ADHD	Attention-Deficit Hyperactivity Disorder
AP-3	Adaptor Protein-3
ANOVA	Analysis of Variance
ANS	Autonomic Nervous System
APP	Amyloid Precursor Protein
ATP	Adenosine Triphosphate
BAC	Bacterial Artificial Chromosome
BMP-4	Bone Morphogenetic Protein 4
CAM	Chloramphenicol
cAMP	3'-5' Cyclic Adenosine Monophosphate
CBF	Cholinergic Basal Forebrain
cDNA	Reverse Transcribed Copy DNA
ChAT	Choline Acetyltransferase

CHT	Choline Transporter
CMAP	Compound Muscle Action Potential
CMS-EA	Congenital Myasthenic Syndrome with Episodic Apnea
CNS	Central Nervous System
CoA	Coenzyme A
DAT	Dopamine Transporter
DB	Diagonal Band of Broca
df	Degrees of Freedom
DNA	Deoxyribonucleic Acid
ECL	Enhanced Chemilumenescence
EDTA	Ethylenediaminetetraacetic Acid
EGFP	Enhanced Green Fluorescent Protein
ENS	Enteric Nervous System
EPM	Elevated Plus Maze
EPP	End Plate Potential
FDB	Flexor Digitorum Brevis
GPCR	G-Protein Coupled Receptor
HACU	High Affinity Choline Uptake
HC-3	Hemicholinium-3
hDB	Horizontal Limb of the Diagonal Band of Broca
HEPES	4-(2-hydroxyethyl)-1-piperazineethanesulfonic acid
HSD	Honestly Significant Difference
IML	Interomedial Lateral Column

IRES	Internal Ribosome Entry Site
KRB	Krebs' Ringers Bicarbonate Buffer
KRH	Krebs' Ringers HEPES Buffer
LB	Luria Broth
LDTg	Lateral Dorsal Tegmentum
LEMS	Lambert-Eaton Myasthenic Syndrome
M1, ..., M5	mAChR subtypes 1 to 5
mAChR	Muscarinic Acetylcholine Receptor
mCHT	Mouse CHT
mEPP	Miniature End Plate Potential
MG	Myasthenia Gravis
mRNA	Messenger Ribonucleic Acid
MS	Medial Septum
nAChR	Nicotinic Acetylcholine Receptor
NBM	Nucleus Basalis of Meynert
NGF	Nerve Growth Factor
NMJ	Neuromuscular Junction
OAc	Acetyl Group
PBS	Phosphate Buffered Saline
PBS-T	PBS containing Tween-20
PBS-X	PBS containing Triton-X100
PCR	Polymerase Chain Reaction
PKA	Protein Kinase A

PKC	Protein Kinase C
PNS	Peripheral Nervous System
polyA	Polyadenylation Signal
PPTg	Pedunculopontine Tegmentum
PS1	Presenilin 1
PSNS	Parasympathetic Nervous System
qPCR	Quantitative Polymerase Chain Reaction
RNS	Repetitive Nerve Stimulation
RRP	Readily Releasable Pool
SCG	Superior Cervical Ganglion
SDH	Succinate Dehydrogenase
SDS	Sodium Dodecyl Sulfate
SNS	Sympathetic Nervous System
spH	SynaptopHlourin
SV	Synaptic Vesicle
VAChT	Vesicular Acetylcholine Transporter
vDB	Vertical Limb of the Diagonal Band of Broca

CHAPTER I

CHT AND CHOLINERGIC MECHANISMS

Introduction

Acetylcholine (ACh) is a neurotransmitter utilized throughout the central and peripheral nervous systems that supports diverse physiological functions. Despite being one of the first neurotransmitters discovered in a classic set of experiments by Otto Loewi (Loewi, 1921), ACh constitutes only a small portion of the neurons in the central nervous system (CNS). ACh is more prevalent in the peripheral nervous system (PNS), being substantial components of the parasympathetic (PSNS, and the original source for Loewi's experiments), sympathetic (SNS), and enteric (ENS) nervous systems. Commensurate with the large variety of cholinergic neurons, deficits in cholinergic function contribute to several known pathologies, including Alzheimer's Disease (Schliebs and Arendt, 2006), myasthenic disorders (Meriggioli and Sanders, 2009), and various autonomic dysfunctions (Vernino, 2009). Consequently, therapies targeted to cholinergic systems have been developed, but are limited by off-target and intolerable side effects (Birks, 2006). To contribute to the understanding of the functions of this neurotransmitter and its potential use as a therapeutic target, I have endeavored to alter synaptic cholinergic signaling by examining increasing and decreasing expression levels of the presynaptic choline transporter (CHT). The impact of these changes on cholinergic signaling will be analyzed and discussed.

The cholinergic synapse and the role of CHT

Cloning and characterization of CHT

CHT was initially thought to be cloned in Mayser et al. (Mayser, 1992), but further research showed that the protein encoded was actually a creatine transporter (Happe and Murrin, 1995). 8 years later, rat CHT was cloned followed shortly by the cloning of the mouse and human CHT genes (Apparsundaram, 2000; Okuda, 2000; Apparsundaram, 2001). Surprisingly, unlike the misidentified CHT (which was part of the SLC6 family of well-known neurotransmitter transporters such as the dopamine and serotonin transporters), the correct CHT was part of the SLC5 family of glucose transporters (Okuda, 2000). Other choline transporters and transport systems have been identified, although these other transporters are not thought to contribute to ACh synthesis. The SLC44 family of "choline transporter-like" proteins (CTL1 to CTL5) are present on neurons and elsewhere and are likely involved in phosphotidylcholine synthesis and methyl-donor metabolism (Yuan, 2006). A well-characterized blood-brain choline transport system has been characterized both for supplying free choline to the brain and as a potential CNS drug delivery system (Allen and Lockman, 2003; Geldenhuys, 2010). However, the protein mediator of blood-brain choline transport has not been identified with organic cation transporter 2 (OCT, OCT2) being a candidate in addition to CTL family proteins (Murakami, 2000; Tomi, 2007).

In addition to the underlying function, there are several distinguishing characteristics of these transport systems. Before the cloning of CHT, it was

recognized that in brain tissue, and likely within individual neurons, that there are two choline transport systems, commonly referred to as the "high affinity, low capacity" and "low affinity, high capacity" systems (Michel, 2006). The choline transport system that supports ACh synthesis is Na^+-dependent, hemicholinium-3 (HC-3) sensitive, with a high affinity for choline (K_m) and low capacity for transport (V_{max}). Conversely, the other choline transport system is Na^+-independent, inhibited by HC-3 only at very high concentrations with a lower affinity for choline and much higher capacity for transport. CHT is the only choline transporter thus far found that has the properties of the "high affinity, low capacity" system that supplies choline for ACh synthesis (mouse brain synaptosomes: K_m=0.62μM, V_{max}=2.1pmol/mg protein/min) (Ferguson, 2003). Both the CTL and OCT systems more closely resemble the "low affinity, high capacity" choline transport system. The clearest example from brain is rat CTL1 from cultured astrocytes (K_m=35μM, V_{max}=49pmol/mg protein/min) (Inazu, 2005). Additionally, rat CTL1 has a wide variance in reported choline affinity from 5μM in transfected COS-7 cells (Yuan, 2004) up to 130μM in an immortalized placental cell line (Lee, 2009). The K_m for rat OCT2 also varies depending on its expression system, with values ranging from 183μM in choroid plexus to 442μM in oocytes (Sweet, 2001).

Although it was odd when CHT turned out to be an SLC5 family member instead of an SLC6 family member, it is more structurally similar to the other known neurotransmitter transporters than the other choline transport proteins (Abramson and Wright, 2009). CHT has 13-transmembrane domains with a very short, extracellular N-terminus and a long intracellular C-terminus (Ferguson, 2003),

whereas CTL1 has between 8 and 11 transmembrane domains (Yuan, 2004). The higher number of transmembrane domains allows a prokaryotic homolog of CHT to assume a tertiary structure similar to SLC6 family transporters with a pesudo-two-fold symmetry composed of halves with 5 transmembrane helices each (Faham, 2008). OCT family members also have two-fold symmetry, but it is direct and each half contains 6 transmembrane helices (Abramson, 2003; Schmitt, 2009).

Synaptic proteins in cholinergic signaling and metabolism

CHT is essential for the proper functioning of chemical synapses that use ACh as a neurotransmitter by bringing choline into the presynaptic terminal for the synthesis of ACh (Figure 1). In order to move choline up its concentration gradient, transport is coupled to the sodium gradient across the plasma membrane (Yamamura and Snyder, 1973; Iwamoto, 2006). Because CHT has the highest affinity for choline of the detectable choline transport systems, its transport process is specifically referred to as high-affinity choline uptake (HACU). Choline is then used for the synthesis of ACh by choline acetyltransferase (ChAT). The acetate group for ACh is derived from acetyl-coenzyme A (acetyl-CoA) supplied by the mitochondria (Jope and Jenden, 1980). ACh is then imported into the synaptic vesicle (SV) by the vesicular acetylcholine transporter (VAChT). A large electrochemical gradient exists across the vesicular membrane where the lumen of the vesicle is both more positive and more acidic than the cytoplasm. VAChT exchanges 2 protons for each ACh molecule in order to use the electrochemicalgradient to concentrate ACh within the vesicle (Nguyen, 1998). ACh,

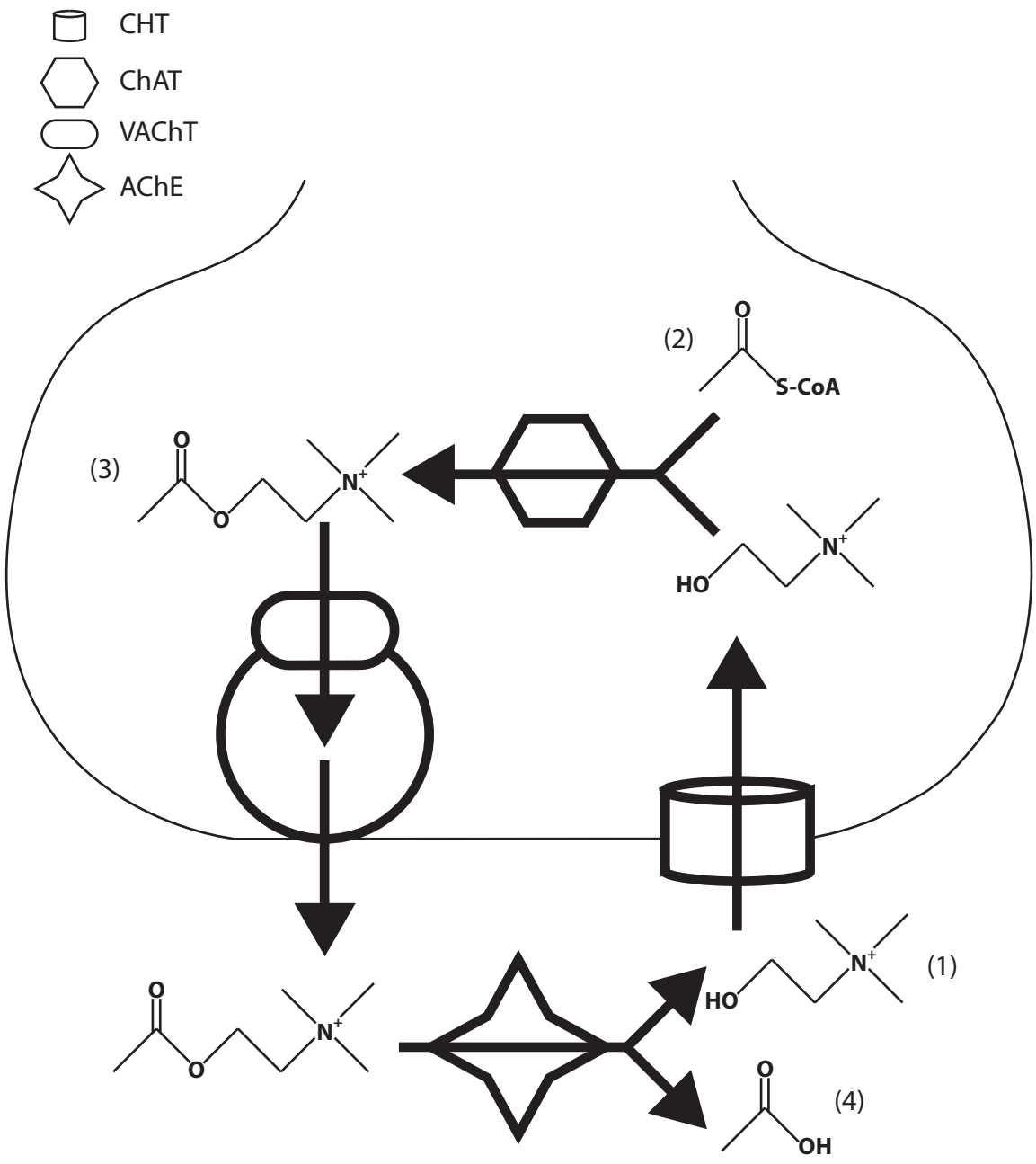

Figure 1. Metabolic cycle of ACh with molecular structures. Extracellular choline (1, principally supplied by recycling or from the blood) is imported into the presynaptic terminal by CHT. An acetyl moiety is then added to choline by ChAT, producing ACh (3). The acetyl moiety is delivered from acetyl-CoA (2) made in metabolic processes of the mitochondria. ACh is then packaged into vesicles and released. ACh in the synapse (either before or after acting on an AChR) is then rapidly degraded by AChE to choline and free acetate (4). Choline produced by AChE is predominantly recycled for further rounds of synthesis and release. The fate of free acetate is currently unknown.

like all other known neurotransmitters, is released by fusion of the ACh containing vesicle with the plasma membrane (Sudhof, 2004). After release, ACh can then act on pre- and post- synaptic ACh receptors (AChRs).

AChRs can be divided into two types based on their mechanism of signal transduction. Nicotinic AChRs (nAChRs) are ligand-gated cation channels that are activated by the sequential binding of two (or more, depending on the subunit composition) ACh molecules. Muscarinic AChRs (mAChRs) are metabotropic receptors that belong to the G-protein coupled receptor (GPCR) superfamily. nAChRs are composed of five subunits arranged around a central non-selective cation channel (Dani and Bertrand, 2007). There are five mAChRs (M1-5) that fall into two subtypes. M1, M3, and M5 are coupled to the phospholipase-C signaling pathway through $G_{\alpha q}$ and ultimately activates protein kinase C (PKC). M2 and M4 are generally inhibitory and, via $G_{\alpha i/o}$, reduce the synthesis of 3'5'-cyclic-adenosine monophoshpate (cAMP) and reduce the activity of protein kinase A (PKA) (Volpicelli and Levey, 2004).

After eliciting its action, the ACh signal is terminated by enzymatic degradation by acetylcholinesterase (AChE) present in the synaptic cleft that is either attached to a basement membrane (NMJ) or attached to the extracellular face of the presynaptic or postsynaptic membrane (central termianals) (Schatz and Veh, 1987; Rotundo, 2003). Due to the location and efficiency of AChE, a substantial amount of the ACh released is also degraded before it reaches an AChR (Chang, 1985; Bazelyansky, 1986). AChE breaks down ACh into acetate and free choline. Whereas the fate of the acetate molecule is currently unknown, choline derived

from AChE is mostly recycled by CHT for reuse as newly synthesized ACh (Collier and Katz, 1974). The other major source of choline for ACh synthesis comes from dietary choline transported across the blood brain barrier and present in the extracellular space (Klein, 1998).

The transport of choline by CHT is the rate-limiting step in ACh synthesis, particularly during periods of afferent nerve stimulation causing moderate to strong Ach releasev (Haga, 1971; Barker and Mittag, 1975); therefore, elevation of HACU is thought to increase ACh release. In the perfused cat superior cervical ganglion (SCG) model, stimulation of the afferent nerve results in the continued release of ACh. Addition of either eserine (an AChE inhibitor), or HC-3, results in a gradual rundown in the amount of ACh released. These findings suggested that the loss of available choline for ACh synthesis was a primary driver of reduced ACh release (Birks and MacIntosh, 1961). Later studies with more kinetic detail would show that the transport step was rate-limiting by its control of the intracellular availability of choline (Simon and Kuhar, 1975).

Regulation of CHT

The best understood aspect of CHT regulation is trafficking to and from the plasma membrane. Classical studies showed an increase in HACU and HC-3 binding after neuronal stimulation (Simon and Kuhar, 1975; Lowenstein and Coyle, 1986; Saltarelli, 1987). Despite the well-characterized role of CHT in HACU, only a small proportion of CHT is present on the plasma membrane although the exact percentage varies with brain region (Ferguson, 2003; Holmstrand, 2010) (Figure 2).

Part of the reason for this small proportion of surface of CHT is that CHT is rapidly endocytosed (Ribeiro, 2003). In its C-terminal tail, CHT possesses an endocytic motif, DKTILV, that is very similar to the classical dileucine motif (Ribeiro, 2005a). Mutation of the LV residues to AA results in an endocytosis deficient mutant.

Several proteins are known to facilitate or restrict CHT endocytosis and trafficking. The signaling molecule PKC has been well studied and yielded mildly contradictory results. Short incubations in SH-SY5Y cells with a PKC activator appear to result in increased HACU that reduced to baseline after 15 minutes. Increased HACU was mainly caused by a reduction in CHT endocytosis (Black, 2010). However, another study using mouse brain synaptosomes showed no changes in HACU after a 5 minute incubation with a PKC activator but reduced HACU at time periods >15 minutes (Gates, 2004). The observed effects on HACU of PKC activation were similar to effects of protein phosphotase 1/2A inhibtion (Gates, 2004). One potential cause of such discrepancies is the nature of vesicle pools in different systems (Ivy, 2001). Amyloid Precursor Protein (APP), faciliates endocytosis of CHT (Wang, 2007). Adaptor protein 3 (AP-3), a protein that assists clathrin in the formation of trafficking vesicles, is critical in the trafficking of CHT to the synapse as well as endosomal sorting within the synapse (Misawa, 2008).

Although the trafficking of CHT has been the focus of substantial research, comparably little is known about the regulation of the endogenous activity of CHT. Trafficking studies have revealed inconsistencies between the amount of change of surface expression and the amount of change in HACU showing that the activity of

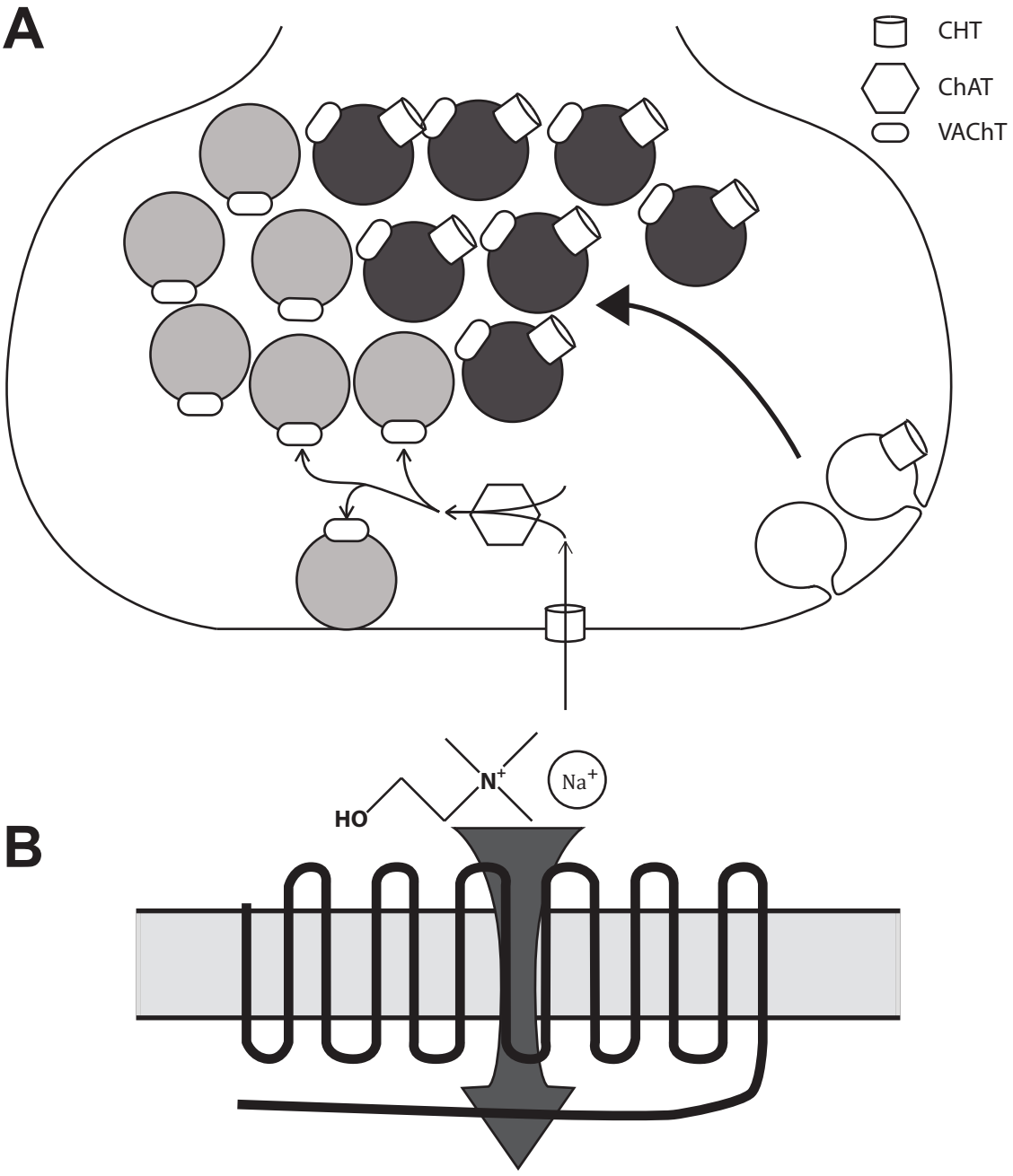

Figure 2. CHT properties at the synapse. (A) Synpatic localization of CHT. CHT is present on the presynaptic membrane to import choline for ACh synthesis (thin arrows). Additionally, CHT is present on a subset of synaptic vesicles where synaptic vesicles are defined as those small vesicles that contain VAChT (CHT containing synaptic vesicles, dark gray; CHT lacking synaptic vesicles, light gray). Due to the tightly regulated quality of CHT endocytosis, we hyopthesize that the functional segregation of CHT containing and CHT lacking vesicles begins at the initial endocytic step (thick arrows). (B) Schematic of CHT in the plasma membrane. CHT cotransports uses the Na^+ gradient to move choline into the presynaptic terminal with Na^+.

variant (I89V) has been reported that reduces the activity of CHT by 50% (Okuda, 2002). CHT has a pH dependence where more a more acidic environment will block transport (Iwamoto, 2006).

Several steps in the regulation of CHT expression have been identified. 3'-5' cyclic adenosine monophosphate (cAMP) reduces the amount of CHT messenger ribonucleic acid (mRNA) through the Epac/Rap pathway, not the more commonly associated PKA pathway (Brock, 2007). Nerver growth factor (NGF) and bone morphogenetic protein 4 (BMP-4) both upregulate CHT expresssion, consistent with the role of these growth factors in the trophic support of cholinergic neurons (Mobley, 1985; Berse, 2005). Later work focusing on the NGF pathway revealed activity through Akt/PKB (Madziar, 2008). In the symapthetic ganglion, a signaling molecule derived from the postsynaptic neuron is required for CHT expression (Rassadi, 2005). Production of the retrograde signaling molecule is dependent upon active, postsynaptic $\alpha 3$ nAChRs, although the identity of the signaling molecule is not yet known (Krishnaswamy and Cooper, 2009). Surprisingly, all the other molecules that are necessary for cholinergic signaling, such as VAChT and ChAT, are present without the retrograde signal.

In addition to growth factors, other physiological circumstances are known to affect CHT expression. Genetically altered mice with reduced cholinergic tone (such as reduced levels of ChAT), cause an increase in CHT expression (Brandon, 2004). A similar increase in CHT levels is observed in rats that are deprived of choline *in utero* (Mellott, 2007). In the striatum, where the function of cholinergic

and dopaminergic systems are substantially integrated, increased levels of dopaminergic signaling result in a reduction of CHT expression (Parikh, 2006).

Functionally defined SV pools

After the molecular cloning of CHT (Apparsundaram, 2000; Okuda, 2000; Apparsundaram, 2001), early work on the transporter showed that an intracellular store of CHT is mobilized after stimulation of cholinergic terminals (Ferguson, 2003). This has led to an ongoing hypothesis that CHT associates exclusively with one of the SV pools that have been defined by their likelihood of release after single or sustained neuronal signaling (Ferguson and Blakely, 2004). Other methods of categorizing vesicle pools have been established based on specific molecular steps that are required of all vesicles to fuse with the plasma membrane, but these likely do not reflect the sustained probability of release and thus will not be discussed here.

Recent mammalian definitions of SV pools have depended almost entirely on functional characterizations initiated by the use of fluorescent styryl dyes (Betz and Bewick, 1992; Betz, 1996; Rizzoli and Betz, 2005) (Figure 3). Functional definitions have received some contribution from morphological (Garcia, 1998; Van der Kloot, 2003) and anatomical (Schikorski and Stevens, 2001; Rizzoli and Betz, 2004) considerations. The studies leading to these definitions have identified 3 distinct pools of vesicles at the presynaptic terminal: a readily releasable pool (RRP), a recycling pool, and a reserve pool (Figure 4). The RRP is best defined as the vesicles

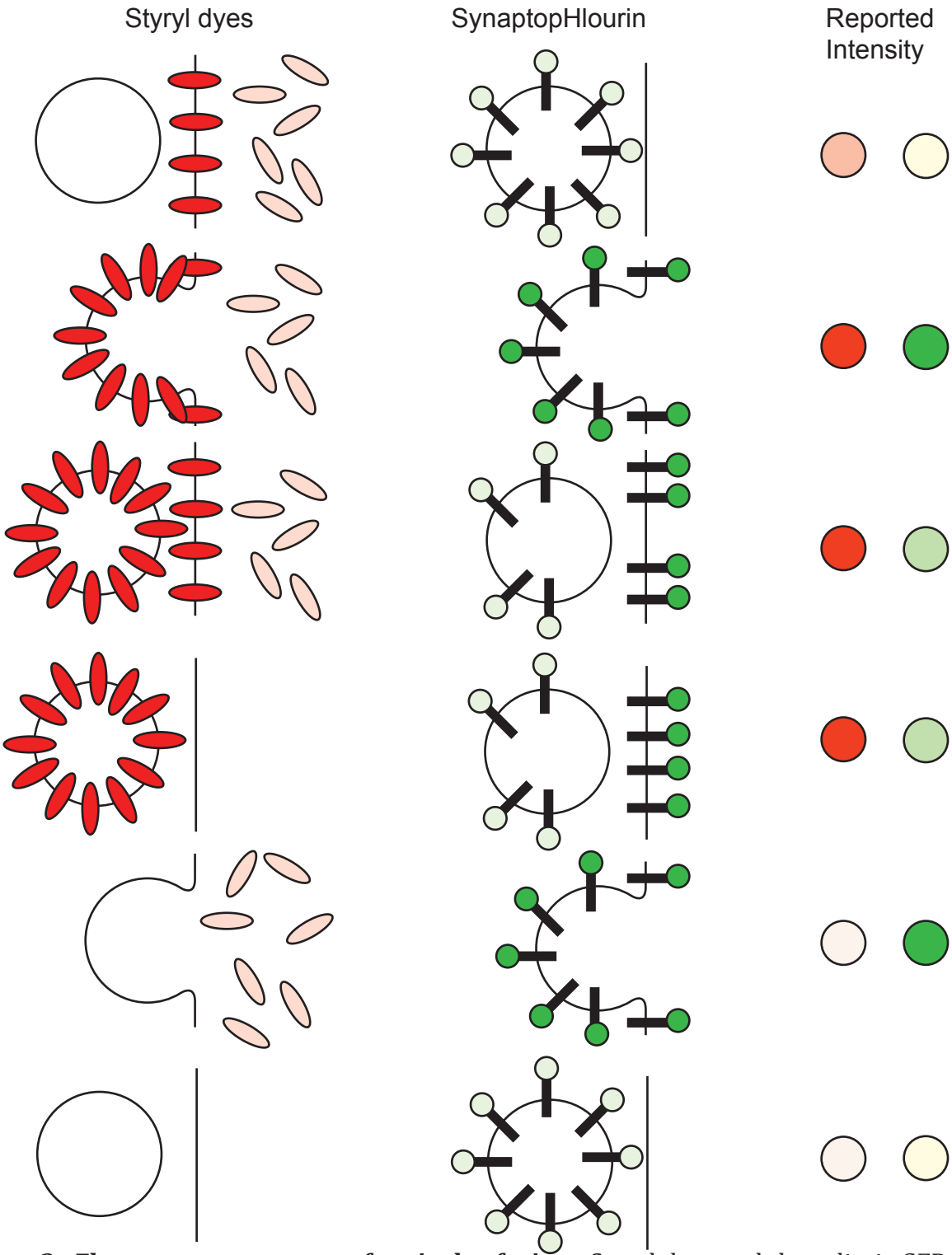

Figure 3. Fluorescent reporters of vesicular fusion. Styryl dyes and the ecliptic GFP fusion protein synaptopHlourin (SpH) can be used to monitor different stages of vesicular release. Styryl dyes need to be loaded into vesicles, fluoresce in the membrane and are lost to the medium after veiscular release. Therefore, styryl dyes can only report vesicular fusion once. SpH is always present and only fluoresces on the plasma membrane. SpH can therefore report on repeated cycles of endocytosis and exocytosis.

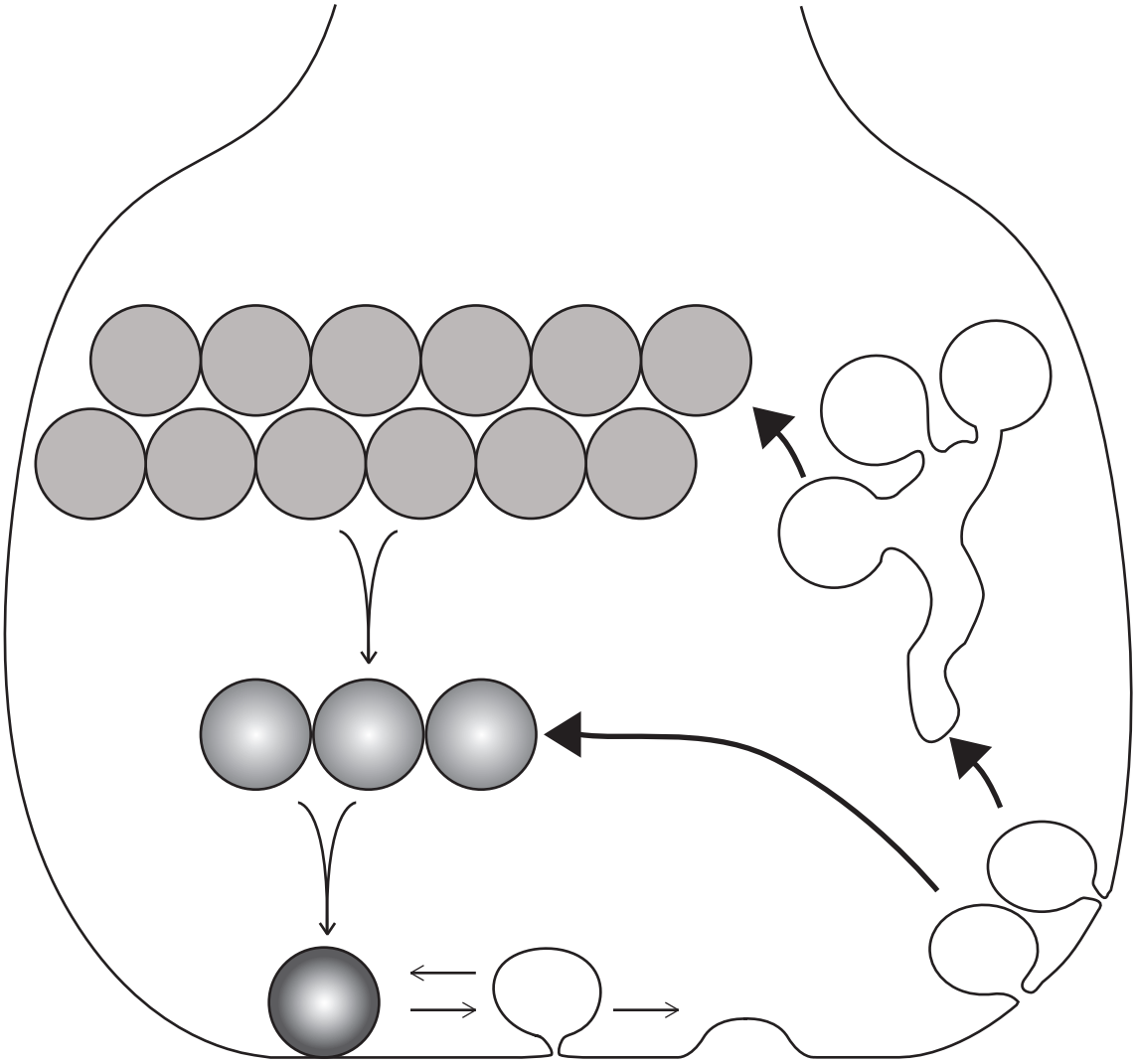

Figure 4. Synaptic vesicle cycling. Synaptic vesicles belong to one of three functional pools, through which they can move (thin arrows) before fusing with the synaptic membrane; reserve (solid light gray), recycling (light gradient), and readily releasable (dark gradient). Upon arrival of an action potential, only vesicles from the RRP are released. After several action potentials, vesicles from the recycling pool can migrate to the readily releaseable pool and fuse with the synaptic membrane. Only during periods of intense stimulation, reserve pool vesicles can sustain vesicular release of neurotransmitter. In all systems so far studied, the size of the reserve pool is greater than the recycling pool which is in turn, greater than the RRP. While the pools can be filled by exchange between themselves, they are predominantly filled by sorting upon endocytosis (thick arrows). The fastest and most rapid from is when the identity of the vesicle is never compromised becuase it never undergoes full fusion. In additon to direct filling by vesicles budded from the plasma membrane, vesicles can go through intermediate endosome steps to facilitate sorting. Neither of these endocytic pathways are exclusive, but direct endocytosis tends toward the recycling pool, and endomsomal pathways tend towards the resreve pool.

that release their contents upon arrival of an action potential at the presynaptic terminal (Richards, 2000; Richards, 2003). Rapid fusion of these vesicles requires that they be docked with the plasma membrane and potentially have changes that prime them for release (Nagy, 2004). The recycling pool contains those vesicles that can fuse with the membrane under mild, physiologically relevant stimulation conditions and possess little if any specific localization within the presynaptic terminal (Fernandez-Alfonso and Ryan, 2004). Reserve pool SV cannot be released except under extreme stimulation protocols that may not occur in a physiological context. Although functional definitions have been useful, they remain inexact in a variety of preparations where pools cannot be easily separated (Trommershauser, 2003). For example, at the frog neuromuscular junction (NMJ), the RRP cannot be distinguished from the recycling pool (Greengard, 1993) and will sometimes be collectively referred to collectively as the releasable pool.

Two divergent lines of evidence have emerged suggesting that CHT associates with a functionally-defined subset of SVs. An older line of evidence used HC-3 and other pharmacological means of observing CHT function to track when and how HACU is present after synaptic stimulation in intact as well as *in vitro* systems and argues for a reserve pool like localization of CHT. The best example comes from Simon et al. where reduced HACU in the hippocampus was induced pharmacologically and, the loss of HACU could be reversed, but only by strong septo-hippocampal stimulation for a sufficiently long (>4min) period of time (Simon, 1976). Other lines of evidence showed that stimulation under unaltered conditions also increased HACU, although less attention was given to the time and

stimulation intensity dependence of the increase in HACU (Rommelspacher, 1974; O'Regan and Collier, 1981). A newer line of evidence using biochemical techniques, possible after the development of CHT antibodies, suggests a RRP localization of CHT. However, this evidence is exclusively in cell culture models (therefore, not synapses) and only compromised a small portion of the available CHT (Ribeiro, 2007).

Cholinergic systems and pathways

Central Cholinergic Nuclei and Projections

In the brain, cholinergic terminals are present in nearly every brain region even though the number of cholinergic nuclei and cells is small (Woolf, 1991). There are two clusters of cholinergic projection nuclei that are responsible for the majority of known functions of central ACh in addition to a major population of cholinergic interneurons. In the ventromedial portion of the forebrain are the nucleus basalis of Meynert (NBM), medial septum (MS), olfactory tubercle, vertical and horizontal limbs of the diagonal band of Broca (vDB and hDB respectively or DB when not distinguished). Neurons in all these nuclei project to the cortex and hippocampus to influence aspects of cognition such as attention and memory. These nuclei are often referred to together as the cholinergic basal forebrain (CBF) and have received much attention due to evidence of degeneration in Alzhemier's Disease (Whitehouse, 1982; Coyle, 1983). The second cluster of cholinergic nuclei is located in the midbrain, mostly composed of the lateral dorsal tegmentum (LDTg)

and the pedunculopontine tegmentum (PPTg). These nuclei send both ascending and descending projections and are thought to be involved in sleep and arousal, reward and addiction, respiratory rhytmogenesis, and other autonomic functions. In the caudate nucleus a population of large, aspiny cholinergic interneurons is present that functions to balance dopaminergic inputs and regulate motor behaviors, reward, and procedural memory.

In addition to the better known and characterized cholinergic nuclei, there are a number of small cholinergic clusters that have restricted or poorly characterized properties, including the following: medial habenula, deep cerebellar nuclei, and hindbrain non-motor neurons. Despite the large array of tools available to characterize cholinergic neurons, a small group of interneurons in the cortex has been described but remains controversial since ChAT is the only cholinergic protein that has been identified in these neurons (Bhagwandin, 2006; von Engelhardt, 2007).

Peripheral Cholinergic Systems

Peripheral ACh is present in both the SNS and PSNS branches of the autonomic nervous system (ANS) as well as the ENS. Postganglionic neurons of the PSNS are entirely cholinergic whereas only the neurons of a small subset of postganglionic neurons are cholinergic in the SNS (Anderson, 2006). Both branches use ACh in their preganglionic neurons. Preganglionic SNS neuron somata are located mainly in the spinal cord along the interomedial lateral column (IML) with ganglion typically located nearer to the spinal cord than the target organ. PSNS

somata are located in the caudal end of the spinal cord or the brain with ganglion located in or near the target organ.

Although ACh is predominantly understood as a neurotransmitter, it has many other functions throughout the body. This will only be a brief and partial catalogue of those functions. The lung epithelium, like several other tissues, uses ACh as a growth factor with signaling mediatd by α7 nAChR (Maouche, 2009). Dysregulation of this cholinergic system appears to be an important step in small cell lung cancer (Song, 2003). Several immune cells contain nicotinic receptors and can synthesize ACh during periods of activation (Kawashima, 2007), likely as part of a negative feedback loop (Wessler, 1999). The ENS contains both neuronal and non-neuronal ACh transmission with all components of cholinergic signaling present (Harrington; Mandl, 2003; Harrington, 2007). Several other systems use ACh, a molecule that is part of intercellular communication from prokaryotes to humans, with several of these facets reviewed elsewhere (Wessler, 1999). Because of this diversity, it is important to keep in mind that cholinergic interventions and cholinergic genetic variation will likely have effects outside the nervous system.

CHT in cholinergic systems

With the exception of the controversial cortical, cholinergic interneurons, CHT has been observed in all other cholinergic neurons (Ferguson, 2003), including all major cholinergic nuclei (Figure 5). CHT has also been detected in both neuronal and non-neuronal peripheral systems. In the mouse heart, CHT has a much greater localization to the cardiac ganglion compared to AChE, but may also present in the

1.525 mm
from midline

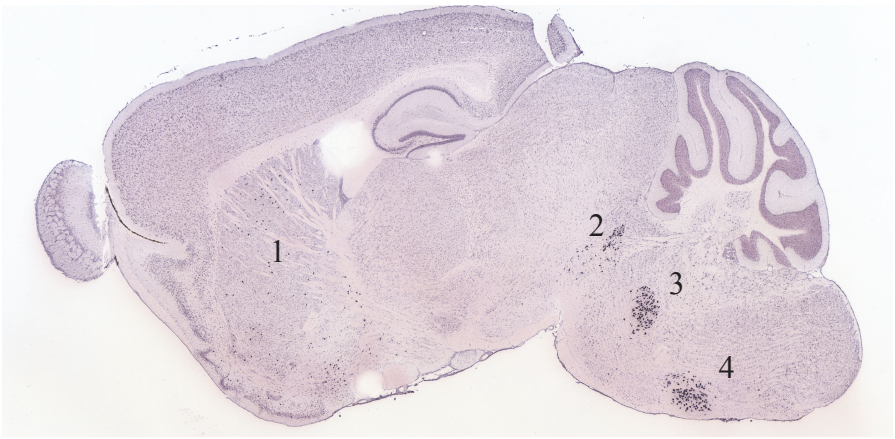

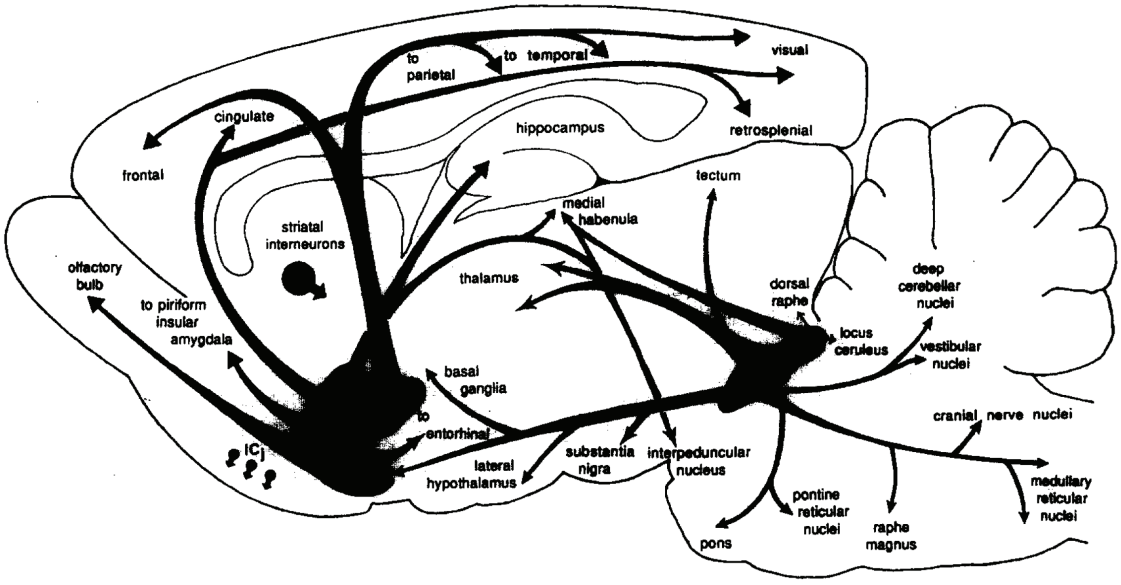

0.675mm
from midline

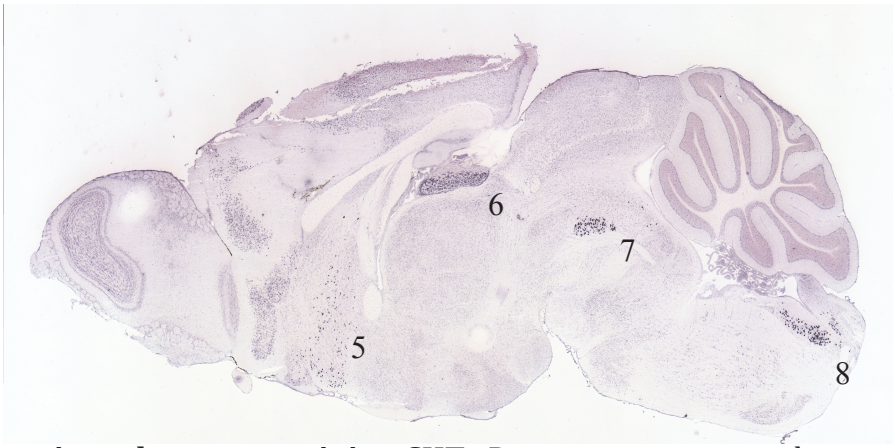

Figure 5. Cholinergic pathways containing CHT. Representative sagittal images from the Allen Brain Atlas showing cells expressing CHT. The projections are given in the diagram (adapted from Woolf, 1991). (1) Striatal interneurons. (2) Pedunculo-pontine Tegmentum (3) Cranial motor nucleus - V (4) Cranial motor nucleus - VII (5) Medial septum (6) Medial habenula (7) Lateral dorsal tegmentum (8) Cranial motor nucleus - XII.

arterial wall (Lips, 2003; Hoover, 2004). Other organs, such as the skin and lungs, also contain neuronal and non-neuronal cells expressing CHT (Pfeil, 2003). In these organs, CHT supports ANS communication with the target tissues and local functions such as the differentiation of keratinocytes mediated by the release of ACh from hair follicle root sheath cells (Haberberger, 2002) or the control of epithelial cell proliferation in the lung (Horiguchi, 2009). Neuronal CHT is also important in the gut where it is part of both the input from the PSNS and the intrinsic neurons of the ENS (Harrington, 2010). CHT has been found in enteric neurons in all layers of the ENS including neuromuscular synapses onto smooth muscle although CHT is not always found in the same neurons with ChAT or VAChT in the myenteric plexus (Harrington, 2007).

ACh at the Neuromuscular Junction

The most well-studied mammalian cholinergic synapse is the NMJ, where release of ACh from the motor neuron causes a depolarization of the muscle fiber followed by forceful contraction of the muscle. The NMJ is referred to as a tripartite synapse due to the role of a surrounding glia cell in NMJ function. Motor neurons are located in the ventral horn of the spinal cord and project through the ventral root to the target muscle. Motor neurons typically have recurrent collaterals that synapse on themselves as well as other spinal cord neurons.

NMJs have several specializations that are not found in other mammalian synapses. They are substantially larger both in contact area and synaptic cleft distance than central synapses (Wilson and Deschenes, 2005). The size of the

synaptic cleft allows for a basement membrane of extracellular matrix to exist between the terminal and the muscle. The basement membrane inserts itself into another unique feature of the NMJ, postsynaptic folds. The folding of the target membrane is thought to provide enhanced surface area to maintain a greater number of receptors for ACh binding that can amplify the signal generated by ACh molecules and increase the control of transmission by AChE (Anglister, 1994).

As the NMJ is often used as a model synapse to study synaptogenesis, there have been several studies that investigated the role of ACh in this process. ACh has a strong influence on the localization of nAChR clusters present on the myotube (Lin, 2005). Lack of ACh (caused by deletion of the synthetic enzyme ChAT), causes formation of synapses across the entire width of the diaphragm suggesting that neuronally released ACh leads to proper removal of nAChR clusters (Brandon, 2003). During gestation, complete loss of CHT produces less severe phenotypes than the loss of ChAT because CHT-/- mice have ACh whereas the ChAT mice do not have ACh (Brandon, 2003; Ferguson, 2004). In particular, the CHT-/- have only a slighly wider NMJ band in the diaphragm (Ferguson, 2004).

Several previous studies have shown how adjusting CHT levels can alter the strength of communication at cholinergic synapses. Direct reduction of CHT levels in either homozygous (Ferguson, 2004) or heterozygous (Bazalakova, 2006) knockout mice impairs cholinergic signaling, resulting in neonatal lethality or physical challenge-induced motor deficits respectively. Consistent with physical challenge eliciting deficits, the CHT+/- mice have reduced heart-reate recovery after a forced treadmil execise (English, 2010). CHT is also modulated in response to

reductions in other parts of the cholinergic system. Reduction in the levels of choline acetyltransferase (ChAT) causes an increase in the amount and activity of CHT (Brandon, 2004). Even hypocholinergic models where synaptic choline is elevated, such as acetylcholinesterase (AChE) transgenic mice, have increased CHT levels as an apparent compensatory mechanism for the loss of cholinergic signaling (Beeri, 1997). AChE knockout mice, also increase CHT due to the dysregulation of cholinergic signaling (Volpicelli-Daley, 2003). Furthermore, challenging behavioral tasks, such as sustained attention, can increase the surface expression and capacity of CHT (Apparsundaram, 2005b). Because CHT appears to have a strong ability to control the strength of cholinergic synapses, I have chosen to test how CHT accomplishes the regulation of cholinergic signaling.

Hypothesis and experimental overview

Given the role of ACh in numerous systems and pathologies, ACh has been the target of several therapeutic strategies. Although the AChRs, ChAT, VAChT, and AChE have been known and well-studied for decades, there is comparatively little research on the role of CHT in cholinergic function and disease. To enhance our understanding of the function of CHT, I have studied the effects of increased and decreased expression of CHT on different aspects of cholinergic signaling. These mouse models should inform us as to the possible roles of CHT in both pathology (underexpression) and therapeutics (overexpression) in cholinergic systems.

In addition to HACU, CHT has been postulated to reside on the reserve pool of synaptic vesicles. However, its contribution to SV pools in mammalian synapses

has not been well studied or defined. There are two possible hypotheses if CHT considered in this thesis. First, CHT may be cargo on otherwise defined reserve pool vesicles. In this case, deletion or overexpression of CHT should have a minimal effect on ACh release other than changes in ACh concentration. Second, CHT may participate in the formation of reserve pool vesicles. Under this hypothesis, even in conditions where ACh concentrations are equivalent, ACh release can be altered due to altered quantal content or a loss of a pool of releasable vesicles, which may vary depending on the stimulation conditions. These two possibilities are discussed and explored in the following chapters.

In Chapter II, the previously characterized CHT heterozygous knockout (CHT+/-) model is used to examine the effects of underexpression on ACh release and develop future hypotheses for the overexpression models. ACh release is measured by [3H]-ACh outflow under suprafusion conditions. Ca^{2+}-mediated ACh release is not different between wild-type (CHT+/+) and CHT+/- mice so other methods that could explore the stronger reserve pool definition hypothesis were tested. First, Ca^{2+} was substituted for Sr^{2+} or Ba^{2+}, cations that alter the release properties of vesicles. One of these alterations is to increase the proportion of release of slower, reserve pool SV. Although Ba^{2+} did not generate enough release to observe an effect, Sr^{2+}-mediated release suggests a possible reduction of reserve pool release in the CHT+/- mice. Second, the pool of ACh labeled with tritium was altered to increase labeling of reserve pool ACh. This result showed a clear deficit in ACh release in the CHT+/- mice, suggesting a functional role in producing reserve pool vesicles.

Previous work on presynaptic neuromuscular plasticity has focused on signaling pathways that can alter the release properties of vesicles (Coleman and Bykhovskaia, 2009) or the amount of ACh per vesicle (Yu and Van der Kloot, 1991). In chapter III, I examine whether a direct manipulation of ACh cycling pathways can augment cholinergic signaling at the NMJ. We generated a mouse that specifically overexpresses CHT in motoneurons by producing a transgenic mouse where CHT is under control of the motor neuron specific Hb9 promoter (Hb9:CHT). To test for cholinergic function at the behavioral level, mice were forced to exercise until exhaustion. Hb9:CHT mice performed significantly better than littermate controls. Analysis of the compound muscle action potential (CMAP) revealed that elevated CHT might cause two distinct effects at the neuromuscular junction. Two populations of basal CMAP were observed where there was only one population in the CHT+/+ mice. The higher of the two populations in the Hb9:CHT mice also recovered faster from a high frequency stimulation. At both the behavioral and physiological level, elevated CHT is able to sustain neuromuscular function during and after periods of high demand.

Chapter IV extends the overexpression model to the CNS and higher order behaviors. The model contains a transgene composed of a large region of mouse genomic DNA around the SLC5A7 locus derived from a commercially available bacterial artificial chromosome (BAC); the BAC-CHT mouse. Despite strongly elevated protein levels, no increase in uptake was observed at either baseline or under stimulation. However, behavioral phenotypes were observed in spontaneous alternation (Y-maze), anxiety (elevated plus maze, EPM), and possibly social

memory (Crawley 3-chamber task). The lack of correlation between changes in uptake and behavior is consistent with the hypothesis that CHT has a function beyond choline transport.

Chapter V links the results from these 3 models together to produce a general model of the role of CHT in supporting cholinergic function. Connections are drawn between each of the models and related disease states and the utility of CHT as a therapeutic target. Specifically, the role of elevated expression is discussed with respect to both choline transport and reserve pool biogenesis. Reduced expression is discussed with regards to previous work on choline transport and the current work on reserve pool release. Furthermore, I hyopthesize that these functions are likely not independent and the modes of interaction are discussed in the context of future experiments.

CHAPTER II

EFFECT OF REDUCED CHT ON THE RELEASE OF [3H]-ACH

Introduction

Previous studies with the CHT+/- mice

Previous work on CHT+/- and CHT-/- mice, as well as classic biochemistry, initiated the hypothesis that CHT may do more than supply choline for ACh synthesis; it also contributes to a vesicle's functional identity (Ferguson, 2003; Ferguson and Blakely, 2004). Specifically, CHT may be a necessary component of reserve pool SV formation. The two functions of CHT are expected to have opposite effects on basal activity: lower CHT levels should impair cholinergic activity through reduced ACh synthesis and potentially augment basal cholinergic acitivy through increased RRP vesicle availability. It is, therefore, difficult to predict the directionality of the effects of altered CHT on many behaviors. Previous work using the CHT+/- mice demonstrated one possible category of phenotypes where basal cholinergic function is identical, but challenges to cholinergic signaling reveal a deficit (Bazalakova, 2006), presumably due to reduced reserve pool capacity. This work has provided a hypothesis that links the two functions of CHT to possible phenotypes: CHT maintains ACh synthesis, release, and signaling predominantly at times of high ACh demand. Experiments in this chapter will address this hypothesis by examining ACh release from CHT+/- brain slices.

Established role of CHT in supporting ACh release

Although work predating the cloning of CHT examined the relationship between CHT function and ACh release (Haga, 1971), the lack of more recent tools (such as CHT targted antibodies allowing for the use of biochemical techniques) has hampered the ability to distinguish between the roles of CHT as a transport protein and a vesicle pool formation molecule. Early work on CHT showed that transport could be elevated by activity, but later work showed that CHT was delivered from intracellular pools and that strong, constitutive endocytosis is responsible for this intracellular location (Ribeiro, 2003; Ribeiro, 2005b). Birks and MacIntosh (Birks and MacIntosh, 1961) produced the most comprehensive study of synaptic ACh metabolism and the role of HACU in sustaining ACh signaling during periods of quiescence and intense stimulation, using the perfused cat SCG as a model. Without choline from hydrolyzed ACh or from external sources, ACh release rapidly decayed to very low levels, with only "released choline from other sources" available for continuing ACh synthesis. Continuous release was completely abolished when HACU was directly inhibited by the use of HC-3. The loss of ACh release when choline transport was inhibited was only observed when release was ongoing, as the initial rate of release was the same with or without HC-3. The most interesting finding in this study was an elevation in total ganglionic ACh after prolonged stimulation. Because prolonged stimulation would be expected to decrease ACh levels, it was argued that HACU was elevated during stimulation supporting the observed increase in ganglionic ACh. Birks and MacIntosh further noticed that based on the concentration of choline in plasma (one of the perfusion fluids used),

choline uptake must have an affinity lower than 7μM, and that systemic, biological sources of choline were relevant to ACh synthesis.

Since the cloning of CHT and the development of antibodies against it, it has been possible to show where the increase in HACU comes from and how this increase is regulated. Biochemical studies have shown that CHT moves to the surface in response to stimulation providing the source for the increased uptake (Ferguson, 2003). Studies in adaptor protein-3 (AP-3) deficient mice, where one mode of synaptic endocytosis is impaired, showed that CHT trafficking is regulated by mechanisms linked to vesicle budding (Misawa, 2008). Importantly, AP-3 is thought to be involved in making reserve pool vesicles (Scheuber, 2006; Danglot and Galli, 2007).

Link between divalent cations and neurotransmitter release

As mentioned above, functional vesicle pools were only discovered 20 years ago (Betz and Bewick, 1992), but several older bodies of work (Dowdall and Zimmermann, 1974), particularly on the role of divalent cations in making synaptic vesicle available for release, supported this idea (Zengel and Magleby, 1977). The fusion of synaptic vesicles with the plasma membrane is a Ca^{2+} regulated event, thought to be mediated by the protein synaptotagmin (Sugita, 2002). Ca^{2+} is also a major signaling molecule for several other steps in synaptic vesicle formation and function (Cousin, 2000; Sugita, 2002). Significantly, the mobilization of reserve pool vesicles and the steps that make a vesicle fusion competent are also known to be

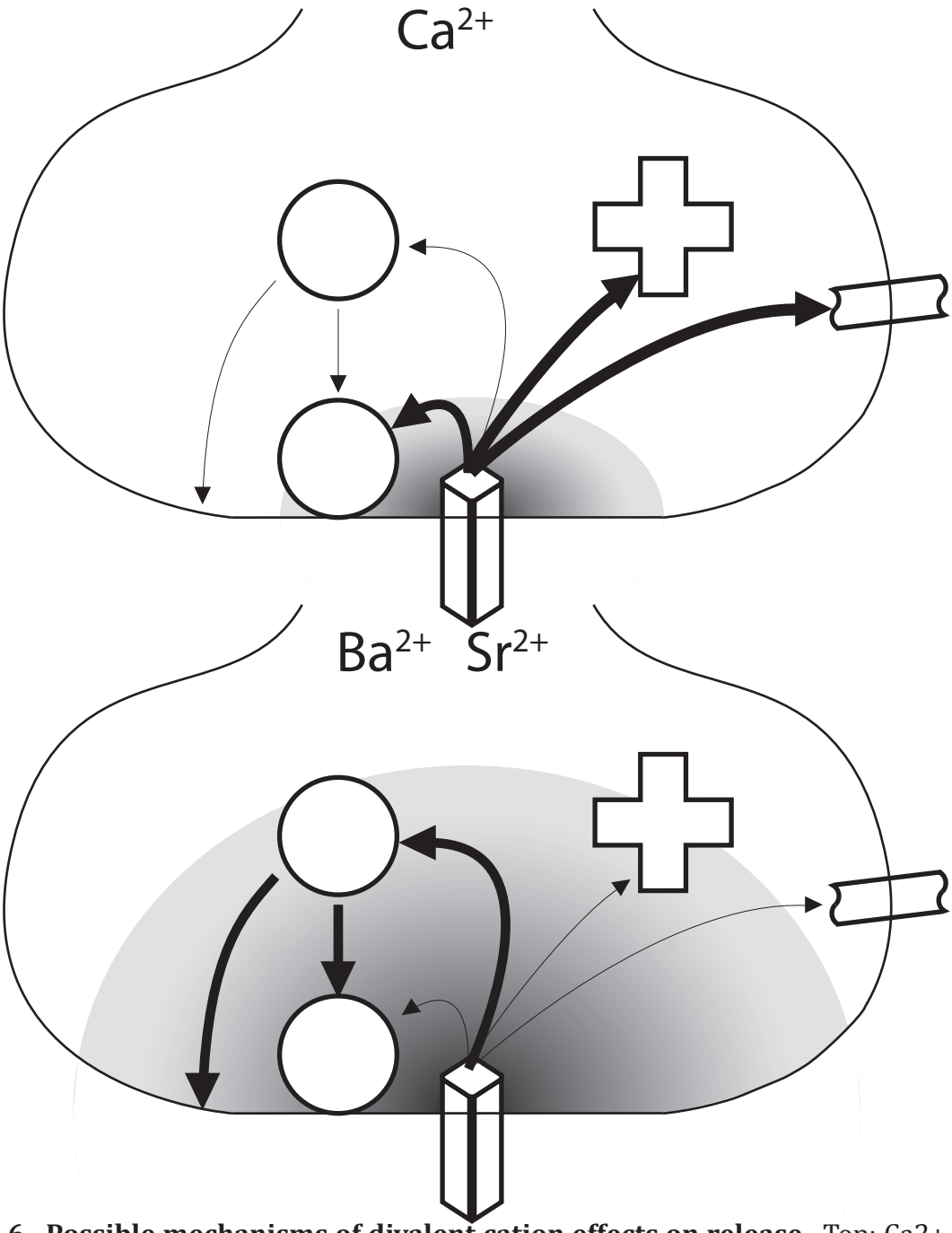

Figure 6. Possible mechanisms of divalent cation effects on release. Top: Ca2+ enters the synapse through voltage gated Ca2+ channels. Because of the transient opening of the channel and effecient Ca2+ buffering and clearing capacities of the synapse, effective concentrations of Ca2+ are typically only present around RRP vesicles and do not promote the release or trafficking of reserve pool vesicles. Bottom: Ca2+ sensitive synaptic proteins have different affinities for other divalent cations altering the net output of the synapse. Sr2+ and Ba2+ are less efficiently buffered and cleared resulting in higher conenctrations in a greater volume of the synapse. This activates signaling pathways on reserve pool vesicles to either induce fusion and release or traffick these vesicles to the RRP.

regulated by Ca^{2+} (Kuromi and Kidokoro, 2002). Several experiments have utilized other divalent cations to test how well they substitute for Ca^{2+}. Due to the different permeability of other divalent cations (Ba^{2+} and Sr^{2+}) (Nachshen and Blaustein, 1982), their differential effects on Ca^{2+}-dependant signaling molecules (Robinson and Dunkley, 1983), and their different clearance rates (Tillotson and Gorman, 1983), Ba^{2+} and Sr^{2+} behave very differently than Ca^{2+} in regulating synaptic vesicle function (Figure 6). It has been suggested that these different properties bias the release of synaptic vesicles from the reserve pool when Ba^{2+} and Sr^{2+} are used in the place of Ca^{2+} (Neves, 2001), although promotion of asynchronous release has also been postulated as an effect of these other cations (McLachlan, 1977).

The creation of mice with altered expression of CHT has enabled the use of older neurochemical tools to directly study the role of CHT in synaptic vesicle function (Ferguson, 2004; Bazalakova, 2006). This section will detail a series of physiological experiments that address the effects of reduced CHT on ACh release and the proposed cellular cause of the phenotypes observed in the overexpressing mice.

Materials and Methods

Suprafusion of brain slices and measurement of [3H]-ACh release

CHT+/- mice have been described previously (Ferguson, 2004), and were housed under the same conditions as the Hb9:CHT and BAC-CHT mice. Animals were sacrificed by rapid decapitation and brains immediately dissected out and

placed on ice. The striatum and cortex were dissected by hand. For striatum, careful attention was paid to not take basal forebrain (MS-DB) or olfactory tubercle as part of the dissection. This introduces a small bias in the tissue taken to have a greater amount of caudatoputamen (dorsal striatum) as opposed to nucleus accumbens (ventral striatum). Cortex, as dissected, contains the dorsal and lateral (not ventral) aspects of cortex present forward of bregma. Tissue was manually sliced with stainless steel razor blades at 4°C and placed into release-Krebs-Ringer-Bicarbonate (r-KRB) buffer (concentrations, in mM: NaCl 118, KCl 4.8, NaH_2PO_4 1.2, $CaCl_2$ 2.2, $MgCl_2$ 1.2, Glucose 10, $NaHCO_3$ 25, Na_2EDTA) bubbled for 1 hour with O_2/CO_2 (95%/5%). Tissue was then passed through a P1000 pipette tip 3 times. [3H]-choline was added sufficient to make the final concentration 100nM and incubated at 37° for 30 minutes in a water bath with periodic shaking. The entire sample was then split into 2 (stimulated load) or 3 (divalent cation) chambers of a Brandel Suprafusion apparatus. Reagent bath and air environment were maintained at 37°C. Chambers were closed at both the input and output with Whatman GF/B glass fiber filters. Samples were washed for 1 hour at 0.4mL/min with buffer in the experimental divalent cation prior to the initiation of the experiment. All buffers during the wash and experiment contained 100uM eserine sulfate. Fractions during experiments were taken every 5 minutes and collected in 8mL polyethylene scintillation vials. All stimulations were done using 25mM KCl (stim-KRB) by substitution of NaCl to maintain osmolarity. At the completion of the experiment, filters and sample remaining in the chamber were collected to determine radioactivity remaining in the sample and dissolved with 20% SDS for 15

minutes at ambient temperature. 5mL of EcoScint XR was added to all samples including the final and incubated shaking overnight at ambient temperature. Samples were then counted on a liquid scintillation counter. To normalize the results, all data are presented as the fraction of [3H] released that was present at the beginning of the fraction.

$SrCl_2$ and $BaCl_2$ substituted for $CaCl_2$ beginning with the wash. For tissue stimulated prior to [3H]-choline loading ("stimulated load" experiments), sliced tissue was collected in KRB, it was centrifuged at 3000rpm for 3 minutes at 4°C. Tissue was then resuspended in stim-KRB and incubated at 37°C for 20 minutes in a water bath with periodic shaking. Tissue was then recentrifuged and resuspended in 250μL of KRB prior to the addition of [3H]-choline and initiation of experiment.

Statistical analysis of ACh release experiments

Statistics were calculated using SPSS Statistics 19 (IBM, Somers, NY). Initial analysis was conducted using a general linear model with time and cation as fixed-effects. Time and cation were both significant ($P<0.01$) while genotype was not significant ($P>0.05$). Due to insuffcient degrees of freedom for genotype, a 2-way ANOVA was used for analysis to allow *post hoc* tests to be conducted. Of all possible comparisons, the only 2 analyzed were 1) cation x time and 2) cation x genotype. The latter was performed at 3 separate timepoints using the ACh pooled from 3 fractions to generate the data and compared using all 3 cations. Therefore, "baseline" is the ACh from 0 to 15 minutes, "peak" is the ACh from 30 to 45 minutes, and "tail" is the ACh from 60 to 75 minutes. Although presented as comparisons

between Ca^{2+} and a single divalent cation, all analyses were performed using all 3 cations to match the performed experimental design. For the stimulated load experiment, only a 2-way ANOVA was necessary. Individual *post hoc* comparisons were performed using the Bonferroni post-test and group *post hoc* comparisons were performed using the Tukey's honestly significant difference (HSD) test.

Results

Sr^{2+} and Ba^{2+} have different ACh release properties compared to Ca^{2+} in frontal cortex

ACh release was measured by loading slices of each brain region with [3H]-choline, which the tissue then converts to [3H]-ACh. Previous work has demonstrated that nearly all further [3H] (>90%) obtained from the sample is from released [3H]-ACh (Zhang, 2002). In tissue slices from frontal cortex, Sr^{2+} and Ba^{2+} are capable of supporting ACh release evoked by high K^+ (Figures 7-8). However, the peak ACh release was significantly lower for both cations (2-way ANOVA, P(cation)=0.0103, P(time)<0.0001, P(interaction)<0.0001) and the peak ACh release occurred faster (first fraction after stimulation versus second) than release with Ca^{2+} (Figures 7A and 8A). Basal release, as well as the release continuing after the termination of stimulation, were also compared between cations. There was a minimal effect of Sr^{2+} on release during periods prior to stimulation (2-way ANOVA (cation x time), P(Ca^{2+} x Sr^{2+})>0.05 5 minute to 35 minute fractions) although return to baseline was possibly slower. Ba^{2+} produced several other changes relative to Ca^{2+}. An ongoing release both before and after stimulation (2-way ANOVA (cation x

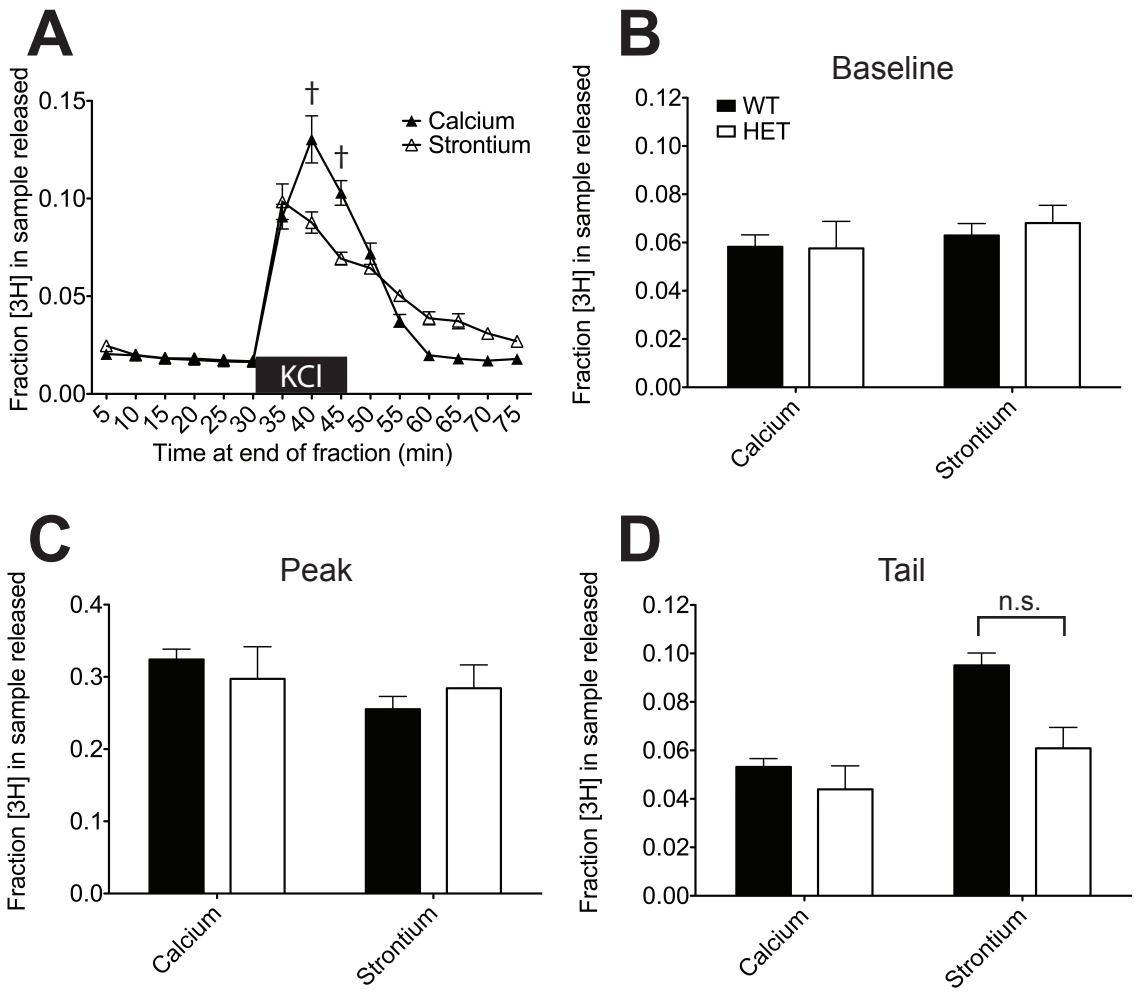

Figure 7. Sr2+-mediated ACh release from cortical slices. (A) Timecourse in CHT+/+ mice of [3H]-ACh release with stimulation by elevated KCl as indicated. Release in the presence of Sr^{2+} was significantly lower and occurred sooner compared to Ca^{2+}. The apparent difference in release with Sr^{2+} after the cessation of stimulation was not statistically significant. 2-way ANOVA (cation x time, n=3). †P<0.001 Bonferroni post-test. Comparison between genotypes of release during the 3 periods of the experiment: baseline (B), peak (C), and tail (D). All comparisons between genotypes were not significant (n.s., P>0.05, Bonferroni post-test). All comparisons between cations were not significant (P>0.05, Tukey's HSD post-test).

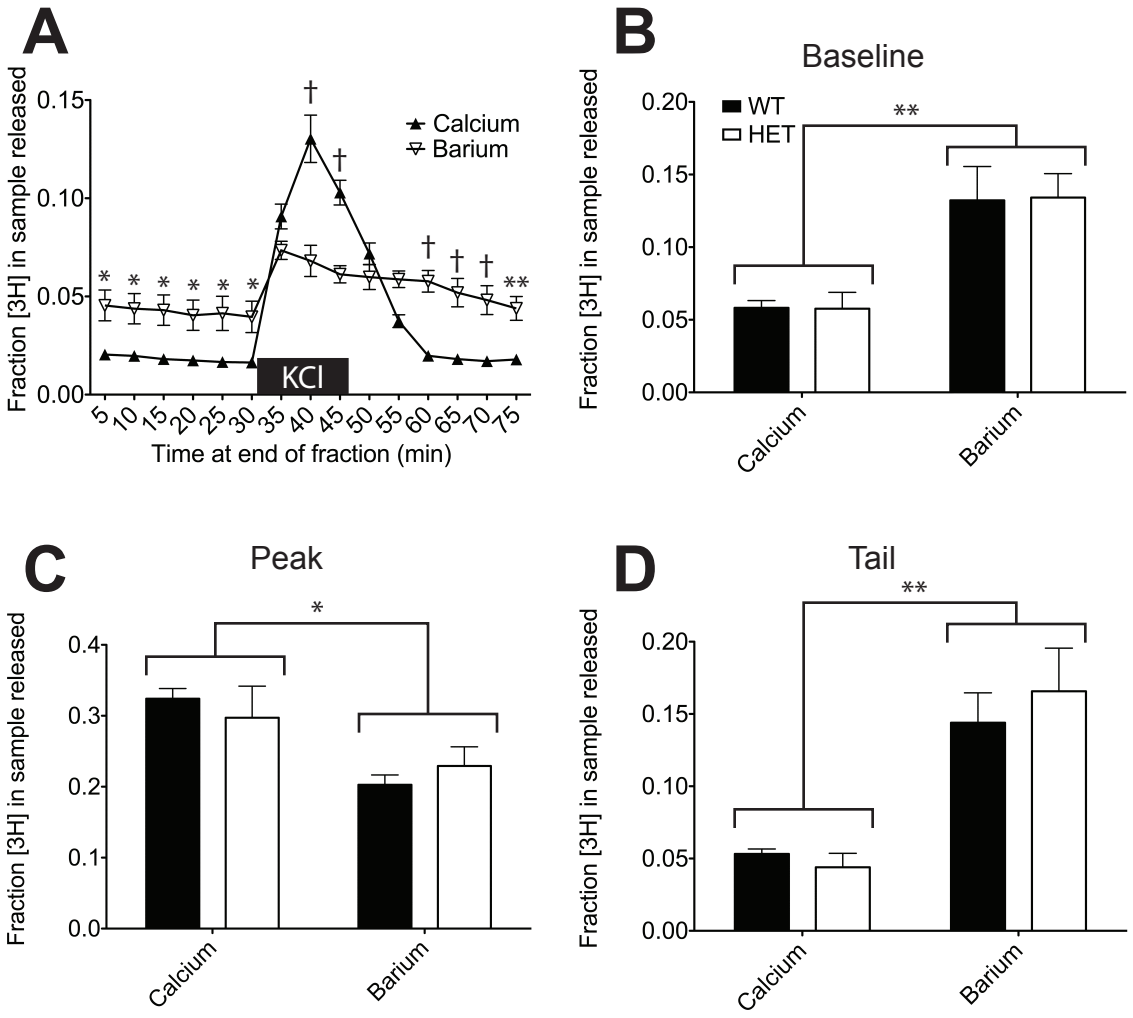

Figure 8. Ba2+-mediated ACh release from cortical slices. (A) Timecourse in CHT+/+ mice of [3H]-ACh release with stimulation by elevated KCl as indicated. Release in the presence of Ba^{2+} was significantly lower and occurred sooner compared to Ca^{2+}. There was also a noticeable release of [3H]-ACh during periods without stimulation. 2-way ANOVA (cation x time, n=3). *P<0.05, **P<0.01, †P<0.001 Bonferroni post-test. Comparison between genotypes of release during the 3 periods of the experiment: baseline (B), peak (C), and tail (D). Ba^{2+}-mediated release was significantly different during all 3 phases of the experiment (*P<0.05, **P<0.01, Tukey's HSD post-test). All comparisons between genotype were not significant (P>0.05, Bonferroni post-test).

time), $P(Ca^{2+} \times Ba^{2+})<0.05$ for baseline fractions and $P(Ca^{2+} \times Ba^{2+})<0.01$ for tail fractions) was induced by the presence of Ba^{2+}. Furthermore, the decay after stimulation was also much slower for Ba^{2+} than Sr^{2+}. ACh release was declining during the moment that stimulation was ended, so a direct, kinetic analysis of decay would be inappropriate. However, comparing release in later fractions to the peak release shows that release in Ba^{2+} did not significantly differ from peak until the final fraction whereas both Sr^{2+} and Ca^{2+} had decayed from peak prior to the end of stimulation (2-way ANOVA (cation x time), Ba^{2+}: P(peak fraction X time)>0.05 for all fractions except 75 minutes, Sr^{2+}: P(peak fraction x time)<0.001 beginning 2 fractions after peak, Ca^{2+}: P(peak fraction x time)<0.001 beginning 1 fraction after peak).

In order to compare between genotypes and ions, each phase of the experiment (baseline, peak, and continuing post-stimulation release) was pooled and compared individually. No significant genotype effect was observed at any time period regardless of cation. The pooled analysis showed some evidence of a difference in the effect of genotype for Sr^{2+} during the continuous release suggesting a reduced ability of Sr^{2+} to prolong release relative to Ca^{2+} (2-way ANOVA (cation x genotype), tail, P(CHT+/+ vs. CHT+/- in Sr^{2+})>0.05 during tail) (Figure 7D. The pooled analysis also confirmed the effects of Ba^{2+} although the effect of Sr^{2+} on peak release was obscured by pooling (2-way ANOVA (cation x genotype), P(Ca^{2+} vs Sr^{2+})>0.05 at peak) (Figure 7C).

Ba^{2+} mediated ACh release is different in striatum from frontal cortex while Sr^{2+} mediated release is similar

Although both Sr^{2+} and Ba^{2+} could both support ACh release in cortex, only Sr^{2+} could support stimulated release in striatum (Figure 9A). Like cortex, Sr^{2+}-mediated release in striatum was impaired compared to Ca^{2+} while also having no elevated baseline and possibly slower return to baseline (2-way ANOVA (cation x time), $P(Ca^{2+} \times Sr^{2+})<0.05$ for 40 minute fraction, $P(Ca^{2+} \times Sr^{2+})>0.05$ for all other fractions) . Ba^{2+}, however, was unable to support K^+ stimulated release in striatum like it was able to do in cortex (2-way ANOVA (cation x time), Ba^{2+}: P(5 minute fraction vs. time)>0.05 for all fractions) (Figure 10A). Although individual fraction variability with Ba^{2+} in the striatum obscured a possible difference, spontaneous release was still detected with the pooled analysis (2-way ANOVA (cation x genotype, $P(Ca^{2+} \times Ba^{2+})<0.01$ at peak, $P(Ca^{2+} \times Ba^{2+})<0.001$ at baseline and tail) (Figure 10B-D). The possible elevation of tail release mediated by Sr^{2+} seen in cortex was detected in striatum (2-way ANOVA (cation x genotype), $P(Ca^{2+} \times Sr^{2+})<0.05$ during tail) (Figure 9D). However, where there was a suggested Sr^{2+}-mediated genotype effect in cortex (Figure 1D), no such interaction is evident in striatum (2-way ANOVA (cation x genotype), tail, P(CHT+/+ vs. CHT+/- in Sr^{2+})>0.05 during tail) (Figure 9D).

Both Ba^{2+} and Sr^{2+} have clear effects on the release of ACh. Ba^{2+}, when substituting for Ca^{2+}, causes an increase in basal ACh release and significantly impairs stimulated release of ACh. Sr^{2+} produces no effect on basal release but significantly prolongs the duration of K^+-stimulated ACh release. Slight differences

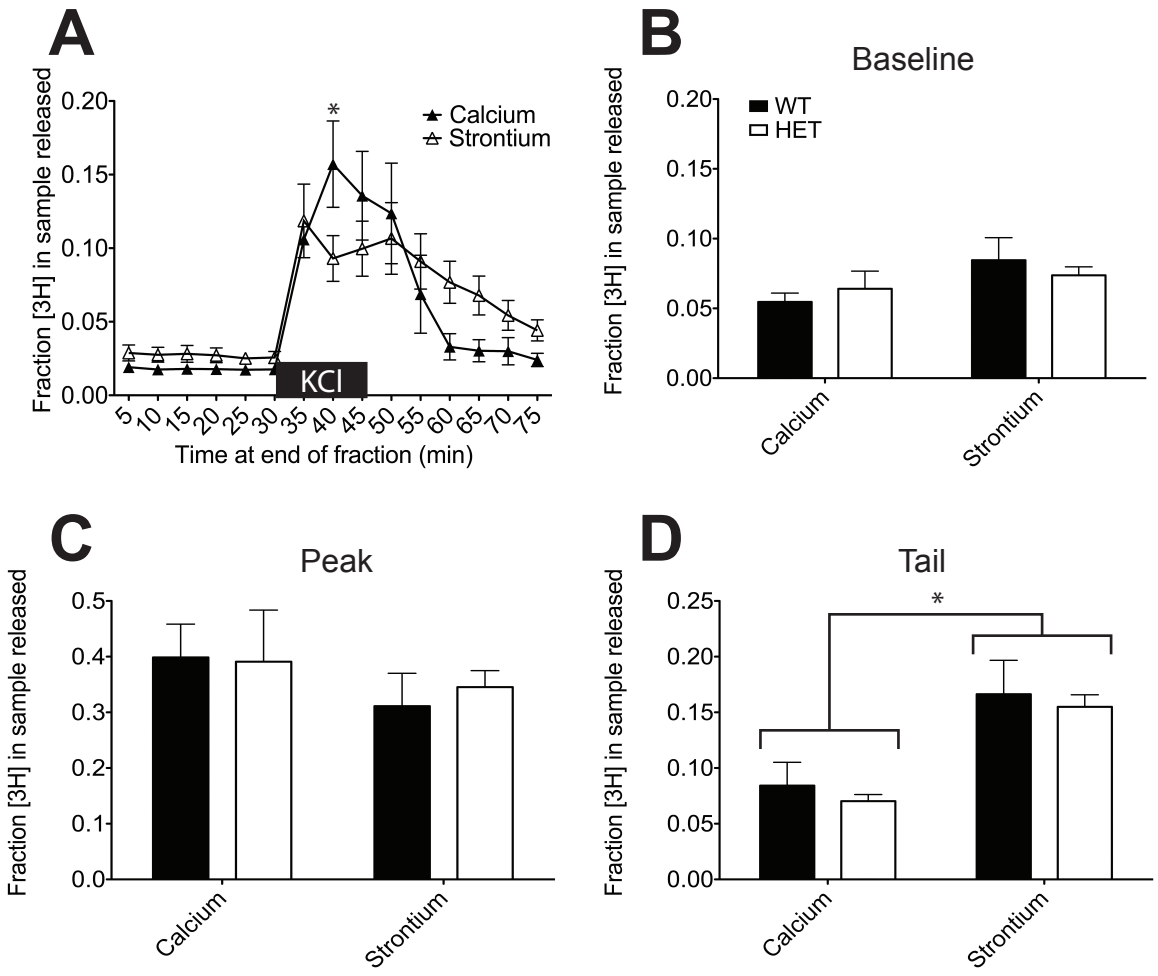

Figure 9. Sr2+-mediated ACh release from striatal slices. (A) Timecourse in CHT+/+ mice of [3H]-ACh release with stimulation by elevated KCl as indicated. Release in the presence of Sr^{2+} was significantly lower and occurred sooner compared to Ca^{2+}. The apparent elevation of release after the cessation of stimulation was not statistically significant. 2-way ANOVA (cation x time, n=3). *, $P<0.05$ Bonferroni post-test. Comparison between genotypes of release during the 3 periods of the experiment: baseline (B), peak (C), and tail (D). All comparisons between genotypes were not significant ($P>0.05$, Bonferroni post-test). All comparisons between cations were not significant ($P>0.05$, Tukey's HSD post-test).

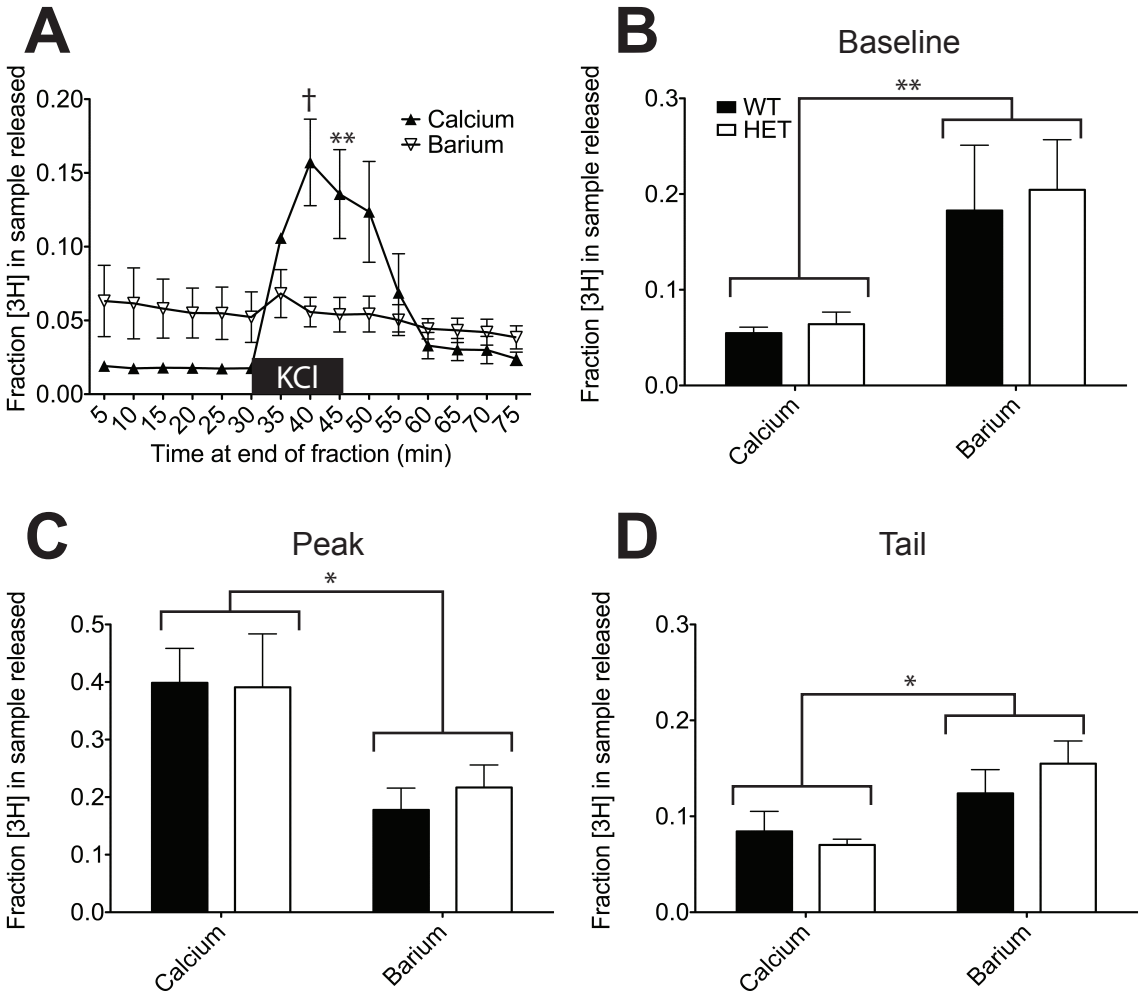

Figure 10. Ba2+-mediated ACh release from striatal slices. (A) Timecourse in CHT+/+ mice of [3H]-ACh release with stimulation by elevated KCl as indicated. Release in the presence of Ba^{2+} was significantly lower and likely non-existent. The apparent elevation of release during baseline was not statistically significant. 2-way ANOVA (cation x time, n=3). **P<0.01, †P<0.001 Bonferroni post-test. Comparison between genotypes of release during the 3 periods of the experiment: baseline (B), peak (C), and tail (D). Ba2+-mediated release was significantly different during all 3 phases of the experiment (*P<0.05, **P<0.01, Tukey's HSD post-test). All comparisons between genotype were not significant (P>0.05, Bonferroni post-test).

in the degree of the cation effect between genotypes were also observed. Although no statistically significant genotype effects were observed, there was one trend where Sr^{2+}-mediated [3H]-ACh release in cortex showed a possible reserve pool impairment in CHT+/- mice (Figure 7D).

Stimulation of vesicle turnover prior to [3H]-choline loading reveals an ACh release deficit in CHT+/- mice

Previous work, particularly in non-mammalian systems, has shown that vesicle loading of newly synthesized ACh is not uniform (Gracz, 1988). I therefore utilized a new paradigm predicted to change which vesicles are loaded with [3H]-ACh and to potentially show genotype differences between early and late release. To change which vesicles were loaded, tissue slices were incubated in the high-K^+ stimulation buffer prior to loading to induce vesicle release and increase endocytosis. Furthermore, slices were stimulated twice for ACh release to try to separate early release from late release.

ACh release was strong in both genotypes during both periods of stimulation. Unlike the comparisons between divalent cations and the ability to support ACh release, when loading occurred immediately after a period of stimulation, there was a significant ACh release deficit in the CHT+/- mice (2-way ANOVA (genotype x time), $P(\text{time})<0.0001$, $P(\text{genotype})=0.0115$, and $P(\text{interaction})=0.0359$). This deficit was only present during stimulation demonstrating that the difference was in vesicular ACh release instead of an unregulated release or leakage (Figure 11A). Furthermore, [3H] content of the slices at the beginning and end of the experiment

was not different (Figure 11B) and all data were normalized to the [3H] present in the sample at the beginning of the fraction so the result is unlikely to be caused by a difference in the uptake of [3H]-choline and the total amount of [3H]-ACh in the sample.

Discussion and Conclusions

Utility of CHT+/- mice for studying effects of reduced CHT on ACh release

CHT+/- mice provide a unique opportunity to study how the amount of CHT at the synapse affects cholinergic function. Due to reduced CHT on CNS cholinergic synapses, it is possible to measure the amount of ACh released from cholinergic terminals. Molecular changes in CHT levels and activity have been previously characterized allowing the development of precise hypotheses regarding ACh release. Therefore, the CHT+/- mice were used to assess the role of CHT in regulating ACh release.

The initial and obvious hypothesis is that reduced CHT should reduce ACh release under all measured conditions. The rationale is that reduced CHT should reduce choline uptake. As choline transport is rate-limiting for ACh synthesis (Haga, 1971; Barker and Mittag, 1975), reduced HACU should result in reduced ACh levels available for release. If all ACh is equally available for release, then reduced ACh release (the outcome measured here) and reduced cholinergic function should be detectable. However, HACU is rate-limiting for ACh synthesis and is necessary to support release only during prolonged stimulation (Birks and MacIntosh, 1961), but

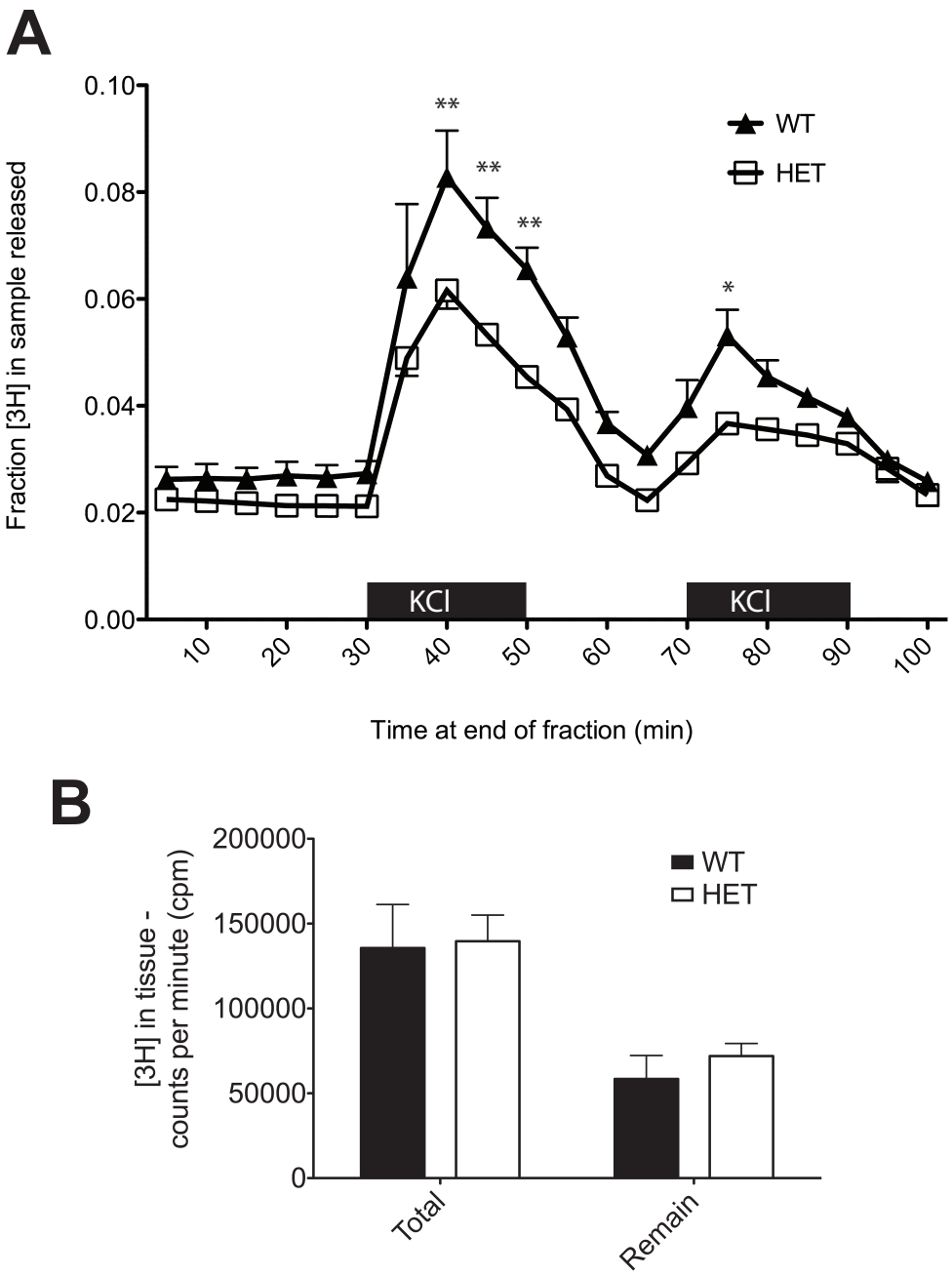

Figure 11. ACh release from striatal slices that were stimulated with 25mM KCl for 30 minutes prior to loading. (A) Timecourse of [3H]-ACh release with stimulation by elevated KCl as indicated. Stimulated release of [3H]-ACh was reduced during both stimulations in the CHT+/- mice. There was no difference in release of [3H]-ACh during periods without stimulation. 2-way ANOVA (cation x time, n=3). *P<0.05, **P<0.01 Bonferroni post-test. (B) Total amount of [3H] present in the tissue slices of each genotype both at the beginning (total) and end (remain) of the experiment. No difference was observed between genotypes at either time period. 2-way ANOVA (n=3) with Bonferroni post-test.

ACh synthesis will not be rate-limiting for ACh release when the amount of vesicular release at the presynaptic terminal is sufficiently low. During these periods, ACh will accumulate in the synapse and synaptic vesicles. If the amount of CHT on the surface is similar between CHT+/+ and CHT+/- mice, then accumulated ACh levels will also be similar between genotypes. Therefore, reduced ACh release in CHT+/- mice would only be expected during conditions when ACh synthesis is rate-limiting for ACh release.

Previous results already suggested that changes in ACh release would not be as simple as reduced CHT causing reduced ACh synthesis and reduced ACh release. Although CHT protein is reduced by 50% in CHT+/- mice, basal uptake and HC-3 binding in the CHT+/- mice are unchanged from CHT+/+ mice undercutting the first assumption in impaired ACh release (Ferguson, 2004). However, bulk tissue ACh levels are reduced suggesting that ACh release may still be impaired (Bazalakova, 2006). Furthermore, surface CHT at baseline is similar between genotypes, but after stimulation, CHT+/- have reduced surface CHT (Martin Sarter, personal communication). Because there is less bulk, stored ACh that can be released, and reduced capacity to refill ACh pools despite similar levels of HACU at baseline, I expected that ACh release should be impaired. As behavioral and cardiovascular work with the CHT+/- mice had shown that a challenge was necessary to elicit phenotypes (Bazalakova, 2006; English, 2010), I reasoned that an ACh release deficit would only be detectable under stimulation conditions that reflected a challenge.

Possible roles of Sr^{2+} and Ba^{2+} in reserve pool mobilization and asynchronous release

I have hypothesized that the relationship of CHT to the reserve pool might play a role in the necessity of challenge for elicited phenotypes in the CHT+/- mice. However, the work that has characterized the different vesicle pools has relied almost entirely on optical techniques to differentiate these pools (Betz and Bewick, 1992; Richards, 2000; Rizzoli and Betz, 2004). These studies have also revealed that stimulation conditions can bias release in favor of one pool or another (Gaffield, 2006). One such study used the goldfish retina biopolar neuron and used fluorescent intensity to count vesicles released. Based on the number of vesicles, it was concluded that Sr^{2+} resulted in far greater release of the reserve pool, and reduced release of the readily releasable pool, compared to release with Ca^{2+} (Neves, 2001). Many others have suggested that the change in release when Ca^{2+} is replaced with either Sr^{2+} or Ba^{2+} is between synchronous and asynchronous release and not between functional pools, but this appears to be based on the stimulation paradigm and not the cations themselves (McLachlan, 1977; Zengel and Magleby, 1981). Additionally, these hypotheses are not mutually exclusive. Asynchronous release is widely acknowledged to depend on replenishment of the releasable pool rather than on preexisting vesicles. Support in the literature exists for a wide range of sources including immediate recycling of readily releasable vesicles (Stevens and Williams, 2007), modulation of the size of the RRP (Zhao and Klein, 2004), filling from the reserve pool (Otsu and Murphy, 2004), or the presence of an overlapping but larger RRP (Hagler and Goda, 2001). Therefore, the mode of action of Sr^{2+} and

Ba^{2+} could be to both bias in favor of reserve pool release and increase asynchronous release.

One of the most common paradigms used to measure asynchronous release is high frequency stimulation, where residual Ca^{2+} causes asynchronous release. The mechanism for the divalent cation substitution bias to reserve pool vesicles is thought to be impaired clearance of the non-physiological ions resulting in prolonged action similar to continuous activity in the presence of Ca^{2+}. If this proposed mechanism is correct, the role of Ba^{2+} and Sr^{2+} would be consistent with what is known about mobilization of reserve pool vesicles. In particular, prolonged intracellular Ca^{2+} promotes reserve pool mobilization, possibly through a synapsin IIa mediated process (Coleman, 2008; Gitler, 2008).

Divalent cation substitution alters ACh release and may reveal a reserve pool impairment in CHT+/- mice

Because Ba^{2+} and Sr^{2+} should preferentially release reserve pool vesicles, it should be possible to detect a difference using bulk ACh release instead of optical or electrophysiological techniques that look at vesicles more directly. Results comparing ACh release by divalent cation substitution confirmed that this approach changes the release properties in the expected ways. In particular, peak release was blunted with both cations, consistent with the idea that Sr^{2+} and Ba^{2+} fail to elicit readily releaseable pool release at the same rate as Ca^{2+}. Release is maintained longer than with Ca^{2+} as well, which is consistent with impaired clearance of the substitute cations. Only one possible difference was observed in CHT+/- mice. A

trend of decreased ACh release after cessation of stimulation in the presence of Sr^{2+} was observed although not statistically signficant.

Selective labeling of ACh pools reveals a clear deficit in ACh release of CHT+/- mice

Despite the demonstrated potential of this approach, no effect of genotype was observed in spontaneous, peak, or continuous release, with the possible exception of Sr^{2+} mediated post stimulation release. As this certainly has the potential to be a real effect, more focused experiments, such as substituting Sr^{2+} for Ca^{2+} at a later timpoint or pairing substitution with the stimulated loading conditions, will likely elicit a stronger and more pronounced effect of the CHT+/- genotype on Sr^{2+} mediated release. Whereas the general absence of genotype effect could reflect a lack of relationship between CHT and release of vesicle pools, it could also reflect a limit of the methodology. As we measured ACh release by labeling with [3H]-choline, we are only measuring ACh that had been synthesized during the course of the experiment. Reserve pool vesicles are likely to have been filled to capacity before the experiment began due to their low release probability and thus, long duration in the synaptic terminal. Previous work has shown a distinct bias in the releasability of newly synthesized ACh to be preferentially released (Gracz, 1988). It is thus plausible that the loading bias is working against the bias of cation to show the effects of the CHT genotype on ACh release.

To test this hypothesis, I altered the loading conditions to cause reserve pool turnover prior to loading. This was done using the same stimulation conditions used to evoke ACh release so that any vesicle that could release detectable ACh

would have been stimulated for loading as well. Using these conditions, release of ACh by the CHT+/- was reduced compared to CHT+/+. This difference is the first demonstration that reduction in CHT protein levels and consequent reduction in ACh levels in the CHT+/- mice results in reduced ACh release. Furthermore, since this deficit was only seen under one set of conditions but not another, it lends further support to the hypothesis that CHT has a functional effect on vesicles dependent on stimulation conditions.

Potential compensations in CHT+/- mice

One caveat with all reverse-genetic approaches is the possible confound of compensatory changes. This concern is particularly acute when an alteration, such as the reduction of CHT in the CHT+/- mice, is present during the entire developmental process. Most of the expected compensatory changes in CHT+/- mice have been previously tested. CHT+/- mice have no change in the activity of either ChAT or AChE showing that CHT+/- mice do not alter ACh metabolism in response to reduced CHT and ACh (Bazalakova, 2006).

CHT+/- mice have changes in AChR receptor levels that may result in compensatory downstream effects. Specifically, M1 and M2 mAChRs are lower in CHT+/- mice in a brain region dependent manner (Bazalakova, 2006). Reduced mAChR levels manifests behaviorally as an impairment in hyperlocomotion induced by the mAChR antagonist scopolamine (Bazalakova, 2006). Presynaptic mAChR can modulate ACh release (Zhang, 2002). Due to the high flow rate of the superfusion apparatus and the consequently low ACh concentrations even during stimulation,

the likelihood that differential activation of mAChRs is responsible for the observed genotype difference is low. However, a difference between genotypes caused by compensatory changes in mAChR signaling cannot be ruled out.

Future experiments can more narrowly determine the selective effect of CHT on ACh release

Further experiments using these bulk ACh methods are likely to yield useful results to show the effect of CHT on ACh release. Shorter stimulation times or multiple stimulation pulses with Sr^{2+} substitution would elucidate the possible effect seen during the ongoing release. Also using the divalent cation substitution with the stimulated loading conditions would also be expected to strengthen the possible difference observed between CHT+/+ and CHT+/- mice during Sr^{2+} substitution. Regarding the stimulated loading experiment, there are several variations that would also be useful contributions following the work already done. Introducing a delay between stimulation and loading would likely label a different subset of ACh containing vesicles than the paradigm used here. Similar experiments have been done using styryl dyes, although those experiments would not identify preformed vesicles that could be labeled with [3H]-ACh. Comparing which conditions yield a difference between genotypes and which do not could help identify which synaptic vesicle pools are most impacted by altered levels of CHT.

Of course, the most promising extensions of the experiments here are experiments that do not require labeling of the ACh. Attempts were made to perform the basic release experiments using the endogenous ACh, but the absolute ACh concentration that was recovered was too low to be easily detected. Several

alternate approaches were tested including altering the perfusion conditions and tetraphenylborate precipitation, but results were inconsistent.

The data that have been generated here represent a useful first step in directly examining ACh release alterations by altered CHT. Although the hypothesis that initiated these experiments was based on a simple understanding of the role of CHT, the data actually suggest something much more profound: a meaningful role for CHT regarding synaptic vesicle pools. Furthermore, the data suggest that a stronger version of the hypothesis of CHT and reserve pool vesicles is warranted, which will be discussed in Chapter V.

CHAPTER III

NEUROMUSCULAR ELEVATION OF CHT

Introduction

Acetylcholine (ACh) serves as a neurotransmitter throughout the central and peripheral nervous systems and supports diverse physiological functions. In the brain, cholinergic terminals are present in nearly every brain region, even though the number of cholinergic nuclei and cells is relatively small (Woolf, 1991). Peripherally, ACh is utilized in both the sympathetic and parasympathetic branches of the autonomic nervous system, as well as the enteric nervous system. The most well-studied mammalian cholinergic synapse is the neuromuscular junction (NMJ), where release of ACh from motor neurons produces a depolarization of muscle fibers, triggering contraction of the muscle.

The presynaptic, high-affinity, choline transporter (CHT, *SLC5A7*) is essential for proper signaling at cholinergic synapses due to the transporter's rate-limiting uptake of choline that is required to sustain ACh synthesis and release, particularly at high firing rates (Birks and MacIntosh, 1961; Haga, 1971; Barker and Mittag, 1975; Ferguson and Blakely, 2004). Interestingly, despite the known function of CHT to transport choline, the majority of CHT is present on synaptic vesicles (Nakata, 2004). In turn, multiple studies have documented that manipulation of CHT activity alters the strength of cholinergic signaling (Bazalakova and Blakely, 2006). Thus, genetically induced loss of CHT levels in either homozygous

(Ferguson, 2004) or heterozygous (Bazalakova, 2006) knockout mice impairs cholinergic signaling, resulting in neonatal lethality or physical challenge-induced motor deficits respectively. Pharmacological manipulation of CHT also impacts cholinergic signaling; for example, treatment of NMJ synapses with the lethal CHT antagonist hemicholinium-3 (HC-3) reduces the level of ACh in NMJ presynaptic vesicles (Yu and Van der Kloot, 1991). CHT is also responsive to modulation of other elements that support cholinergic signaling. Reductions in the levels of choline acetyltransferase (ChAT) produce an increase in the level and activity of CHT (Brandon, 2004). Other models of impaired cholinergic function, such as acetylcholinesterase (AChE) transgenic overexpressing (Beeri, 1997) and knockout (Volpicelli-Daley, 2003) mice, demonstrate increased CHT levels that appear to represent a compensatory alteration to offset a loss of cholinergic signaling. Additionally, Krishnaswamy and Cooper recently demonstrated that presynaptic CHT downregulation is triggered by genetic elimination of nicotinic receptors on postganglionic neurons (Krishnaswamy and Cooper, 2009).

Pharmacological augmentation of cholinergic tone by enhancement of CHT expression and/or activity may be of benefit in disorders with cholinergic deficits, including myasthenia gravis, attention-deficit hyperactivity disorder (ADHD) and Alzheimer's Disease. Currently, we lack small molecule, positive modulators of CHT that can inform as to the impact of elevated CHT expression or activity *in vivo*. We took advantage of the Hb9 promoter's capability of driving motor neuron-specific gene expression (Arber, 1999; Thaler, 1999) to enhance CHT expression at NMJ synapses. In the CHT-/- mouse, that dies 30-60 min after birth, Hb9:CHT transgenic

animals demonstrated significantly enhanced viability. In a CHT+/+ background, Hb9:CHT transgenic mice demonstrated altered physiological and behavioral motor phenotypes. Strikingly, studies of evoked responses of muscle fibers from the latter animals revealed a shift of excitatory events from a single population of summed action potential amplitudes to two populations, with either enhanced or diminished excitation. We discuss these findings with respect to a dual impact of overexpressed CHT to NMJ synaptic events, mediated either by an enhanced production of ACh, or a reduction in the readily-releasable pool of cholinergic synaptic vesicles.

Experimental Procedures

Generation and genotyping of Hb9:CHT mice

All animal procedures were approved by the Vanderbilt University Institutional Care and Use Committee. pHb9-MCS-IRES-EGFP (Figure 12A) was a kind gift of Dr. Thomas Jessell and contains a 9kb fragment of the Hb9 promoter, a 5' splicing substrate, an internal ribosome entry sequence (IRES), enhanced green fluorescence protein (EGFP), and a bovine polyadenylation (polyA) signal (Arber, 1999; Wilson, 2005). BamHI/HindIII blunted cDNA encoding the mouse CHT (mCHT) (Apparsundaram, 2001) was cloned into the PmeI site, resulting in the expression construct pHb9:CHT-IRES-EGFP. DNA was sequenced using primer-directed Sanger sequencing in the DNA Core of the Vanderbilt Division of Human Genetics, Department of Medicine. To produce transgenic founders, the plasmid was first linearized and vector sequences removed using XhoI, and then purified and

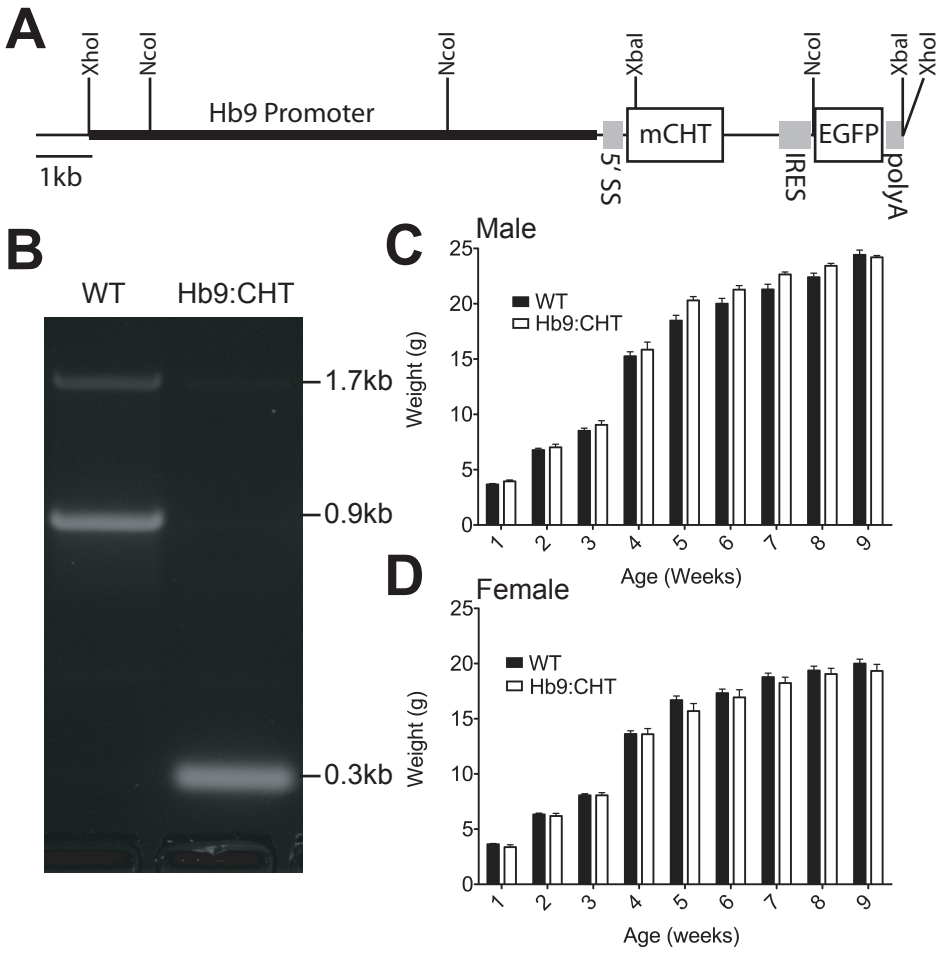

Figure. 12. Generation of Hb9:CHT mice. (A) Schematic of Hb9:CHT transgene showing all elements that allow expression including a 5' splice substrate (5'SS), CHT cDNA (mCHT), internal ribosome entry site (IRES), enhanced green fluorescent protein (EGFP), and a bovine polyadenylation signal (polyA). (B) PCR demonstrating presence of transgene. The 0.3kb band is derived from the cDNA for CHT and the 0.9kb band is derived from the genomic DNA for CHT. An aberrant 1.7kb band was also observed. (C) and (D) Growth curves for male (C) and female (D) mice (male: CHT+/+ n=12, Hb9:CHT n=4; female: CHT+/+ n=12, Hb9:CHT n=6, p>0.1 for genotype effect).

injected into the pronucleus of C57BL/6 single cell embryos in the ES/Transgenic Core of the Vanderbilt Stem Cell Center. Founders were screened by Southern blotting and PCR to identify carriers of exogenous mCHT cDNA or EGFP. DNA for genotyping was obtained by tail biopsy and processed using the RED Extract-n-Amp kit (Sigma; St. Louis, MO). Primers for PCR were 5'-ACACATGGGTTGGAGGAGG-3' and 5'-CTAATGCAGAGAAAATTGC-3', targeting the 5' end of exon 3 and the 3' end of exon 4 respectively. Products were analyzed using agarose gel electrophoresis. Quantitative PCR (qPCR) was performed using a LightCycler 480 (Roche) with SybrGreen fluorescence. Primers for qPCR were directed at 2 locations on the Hb9 promoter (5'-TGACCATCCACCAGGCTAAC-3' with 5'-AGGGGCTCTTGATACAACCTC-3' and 5'-GCGACAAAAATTGTCTGCCTA-3' with 5'-TGATGCACACCAFCATCATA-3') and 1 location in the mCHT cDNA in exon 3 (5'-GGGTTGGAGGAGGCTACATC-3' with 5'-CTAGCCCAAGCTAGACCAC-3'). The reference primer was directed at a location 80kb upstream from genomic CHT (5'-CTGCTAACCTGGATGAAGCA-3' with 5'-GCCTGTGAGAGCCTAGCTGA-3').

Mice, breeding strategy, and survival analysis

CHT+/- and CHT-/- mice have been previously described (Ferguson, 2004; Bazalakova, 2006). C57BL/6NHsd breeding females were obtained from Harlan (Harlan Laboratories; Indianapolis, IN). Mice were housed with 2 to 5 animals per cage on a 12-hour light/dark cycle with lights on at 0600h. Food and water were provided *ad libitium* (Purina Rodent Chow 5001). For staining and survival experiments, Hb9:CHT;CHT+/- males were bred to CHT+/- females. For treadmill

and some CMAP experiments Hb9:CHT;CHT+/- males were bred to C57BL/6 females. For the remaining CMAP experiments, Hb9:CHT;CHT+/+ males were bred to C57BL/6 females. For neonatal experiments, multiple breeding triplets were established with the males removed after 5 days. Beginning on day 19 after the establishment of breedings, females were observed each hour beginning at 2200h, and if no pups were born, observation ended at 0900h the following day. If pups were born, litters were observed every 30 minutes for the first 6 hours and every hour subsequently up to 72 hours with the time of death recorded as the time the pup was found dead. All litters observed were completely born within 1 hour. For neonatal staining experiments, animals were taken 4 hours after birth or when observed as dead.

Tissue processing and immunofluorescence

Mice were deeply anaesthetized with Nembutal™ and euthanized by decapitation. For brain tissue, mice were perfused with 4% paraformaldehyde, brains removed and post-fixed for up to 1 week in 4% paraformaldehyde. Tissue was cryoprotected in 20% sucrose and sliced at 40µm using a freezing microtome. Pups were euthanized by decapitation if necessary. Diaphragms with attached ribs were pinned down at tension slightly above resting tension on Sylgard-lined (Ellsworth Adhesives; Germantown, WI) plates and fixed for 30 minutes in 4% paraformaldehyde. NMJs were labeled with 1ug/mL alphaBungarotoxin-alexa488 (Invitrogen; Eugene, OR) for 30min. NMJs and floating brain sections were washed and then blocked with 3% normal donkey serum, 0.2% Triton X-100 in PBS for 1

hour. Primary antibodies (chick anti-Neurofilament-M, chick anti-Neurofilament-H, goat anti-ChAT (Millipore; Temecula, CA), rabbit anti-CHT (Ferguson, 2003)) were incubated overnight at 4^{o}C in blocking medium. After washing, sections were stained with the appropriate, fluorescently labeled secondary antibodies, mounted with Aqua PolyMount, and imaged using a Zeiss LSM Meta 510 laser scanning confocal microscope.

NMJ area analysis

Flexor digitorum brevis (FDB) was processed for alphaBungarotoxin-alexa488 as disaphragm. Projection images from a confocal stack were thresholded manually using the ImageJ software (NIH). Area of the image above threshold was then calculated based on the internal scaling from the microscope.

Treadmill testing

Mice between 8 and 11 weeks of age were examined for running endurance on a 6 lane motorized treadmill with an electric shock grid at one end (Columbus Instruments; Columbus OH). All experiments were conducted between 0900h and 1600h. For each mouse, training or trial sessions were ended when they reached a criterion of exhaustion, defined as willingness to receive 15s of shock in any 1 minute interval. On day 1 (training), mice were allowed to explore their lane for 5 minutes without shock followed by 5 minutes where the shock was turned on. All mice received a shock at least once during this stage. The treadmill was then started at 5m/min and accelerated to 15m/min at a rate of 1m/min/30sec. After 1 hour of

running, the treadmill was then increased to 18m/min at 1m/min/30sec. Day 2 (test) began as described for day 1, but the treadmill was accelerated directly from 5m/min to 18m/min at the beginning. At 1 hour of running, the treadmill was accelerated to 20m/min. In these tests, endurance times for both the CHT+/+ ($F(3,12)=15.28$, $P=0.0002$, extra sum-of-squares F test), and the CHT+/+;Hb9:CHT ($F(3,12)=9.650$, $P=0.0016$, extra sum-of-squares F test) mice separated into bimodal distributions for endurance time. To reduce contributions in our data analysis from animals of either genotype with low performance values that likely fail to complete the task for reasons unrelated to physical endurance, we established a minimum criteria for performance for both genotypes. We averaged the minimum criteria for performance for each genotype (mean of the lower component of the bimodal distribution plus 3 standard deviations), and applied the result (28.74 min) to both genotypes.

Compound muscle action potential recording (CMAP)

All recordings were obtained between 1600h and 2330h. A separate cohort of mice from the treadmill between 8 and 11 weeks of age were anaesthetized with 3% isoflurane and maintained at 1.5% isoflurane on a heating pad at 37°C for the duration of the experiment. Experiments are based on protocols from Kaja et al. (Kaja, 2007) and Byun and Delpire (Byun and Delpire, 2007) with minor modifications. Data were collected and analyzed using a TECA Synergy portable electromyography system with platinum/iridium needle electrodes (Viasys Healthcare; Madison, WI). A bipolar stimulating electrode was inserted at the ankle

to stimulate the tibial nerve, the recording electrode was inserted through the paw at the level of attachment for the first and fifth digits, and a reference electrode was inserted distally. A ground surface electrode was wrapped around the paw proximal to the recording electrode and affixed to a styrofoam surface. This allowed us to fix the position of the paw to mostly eliminate movement artifacts and record reliably before and after 50Hz stimulation although a small number of animals could not be analyzed due to the movement. Correct placement of the electrodes was determined by lack of noise >1microV and lack of an initial positive deflection upon stimulation. Stimulation intensity for each recording location was determined by increasing the stimulus intensity gradually during 0.5Hz stimulation until a plateau response was achieved. Suprathreshold stimulation was defined as 150% of the minimum stimulation needed to reach plateau response. This stimulation was recorded as the basal CMAP, and used for the duration of the experiment. High-frequency stimulation (50Hz, 1min) was then applied, immediately followed by test stimulations at 0.5Hz with data recorded every minute. All stimulations were delivered as 0.02ms square pulses and were reliably delivered at less than 4mA. The low-pass acquisition filter was 1Hz and the high-pass filter was 10kHz.

Muscle and muscle fiber cross-sectional analysis

Mice were euthanized by rapid cervical dislocation. The gastrocnemius was rapidly dissected with the distal tendon cut and left attached at the proximal end. The muscle was held at resting length and frozen for 20 seconds in 2-methylbutane cooled in liquid nitrogen. Muscles were then mounted for cryostat sectioning at

20μm and thaw mounted onto superfrost slides (Fisher). Muscle sections were dried for at least 30min, then stained for succinate dehydrogenase activity as previously described (De Paepe, 2009). Briefly, slides were incubated for 30 minutes at 37°C in a reaction buffer containing 100mM Na-succinate and 1.2mM nitroblue tetrazolium in 0.2M Na-phosphate buffer (pH=7.4). Slides were then rinsed and cleared in ascending and descending acetone solutions followed by washes with water. Slides were mounted with Aqua PolyMount and imaged using a Zeiss Discovery V.12 stereo microscope (for whole muscle cross-sectional area) or a Zeiss Axiophot upright microscope (for muscle fiber cross-sectional area).

AChE and ChAT enzyme activities

Gastrocnemius muscles were dissected, frozen on dry ice, and stored at -80°C until use. Muscles were weighed and then placed into 3mL of PBS to be homogenized using a polytron. 3mL of PBS was then added to the initial homogenate and then further homogenized using a dounce homogenizer. A portion of the dounce homogenized tissue was then taken and Triton X-100 was added to a final concentration of 0.5% and frozen at -20°C for later ChAT assays. AChE was determined using the Amplex Red kit (Invitrogen). ChAT was determined by the synthesis of [^{14}C]-ACh from [^{14}C]-Acetyl-CoA using the method of Frick et al (Frick, 2002).

Statistical Analysis

Statistics were computed using Prism 5.0 (GraphPad). Survival curves were analyzed first for all genotypes and, if significant, reanalyzed for the experimental pair using the Mantel-Cox Log-Rank test. To assess the bimodality of the CMAP experiment, CMAPs were binned into 0.75mV intervals and the resulting histogram used to calculate probability density functions. Comparison between models using a single normal distribution or a sum of two normal distributions was performed using the extra sum-of-squares F test. Data for the recovery curves were analyzed by normalizing data to findings obtained from 0 minutes to 5 minutes following stimulation (0% and 100% respectively). A single exponential function was fitted constraining Y0 to 0 and plateau to 100 and the K values of the following equation were compared: Y=Y0 + (Plateau-Y0)*(1-exp(-K*x)).

Results

Motor neuron-specific expression of mCHT transgene.

Of five founder animals generated following pronuclear injection of a pHb9:mCHT-IRES-EGFP construct (Figure 12A), three animals transmitted the Hb9:CHT transgene to offspring. The presence of the transgene was examined by presence of the CHT cDNA (Figure 12B). One line did not achieve stable transmission to successive generations. Of the two remaining lines, we selected the line (Tg2) that exhibited the highest copy number as determined by qPCR (10 copies versus 7 copies in the other line, Tg9) for analysis. Furthermore, Tg9 animals

displayed lower NMJ CHT expression on a CHT -/- background than Tg2 animals, as determined by fewer terminals with CHT and no visible CHT in incoming fibers (data not shown). They also did not display rescue from neonatal lethality, even when possessing the transgene on both chromosomes, suggesting overall low CHT protein expression. Both male and female Hb9:CHT transgenic mice from the Tg2 line grew normally (Figure 12 C-D), and the transgene segregated randomly from CHT with no evidence for lethality (n=80, chi2=7.6, df=5, $P>0.1$).

As the mCHT protein expressed from our transgene does not differ in sequence from the native CHT, we utilized the coexpressed EGFP to examine expression of the transporter in somatic motor neurons. Although the Tg2 line carries multiple copies of the Hb9:CHT transgene, direct EGFP fluorescence signal was not apparent. We therefore utilized anti-EGFP antibody-based detection to examine transgene expression. In Figure 13, we demonstrate colocalization of anti-EGFP immunoreactivity with ChAT in the large majority of hypoglossal nucleus motor neurons (Figure 13C). Consistent with the specificity of the Hb9 promoter, EGFP immunoreactivity was absent from neurons of the cholinergic lateral dorsal tegmental nucleus (Figure 13D-F). Western blotting of brainstem extracts however did not reveal an elevation in CHT levels (data not shown), possibly because of efficient export of transporters to motor neuron terminals. As with others (Wessler and Kilbinger, 1986; Wessler and Sandmann, 1987), we have to date been unsuccessful in immunoblotting or in monitoring CHT activity at the NMJ, most likely due to the limited density of neuronal elements in muscle preparations and the presence of a non-CHT choline accumulation mechanism in muscle tissue.

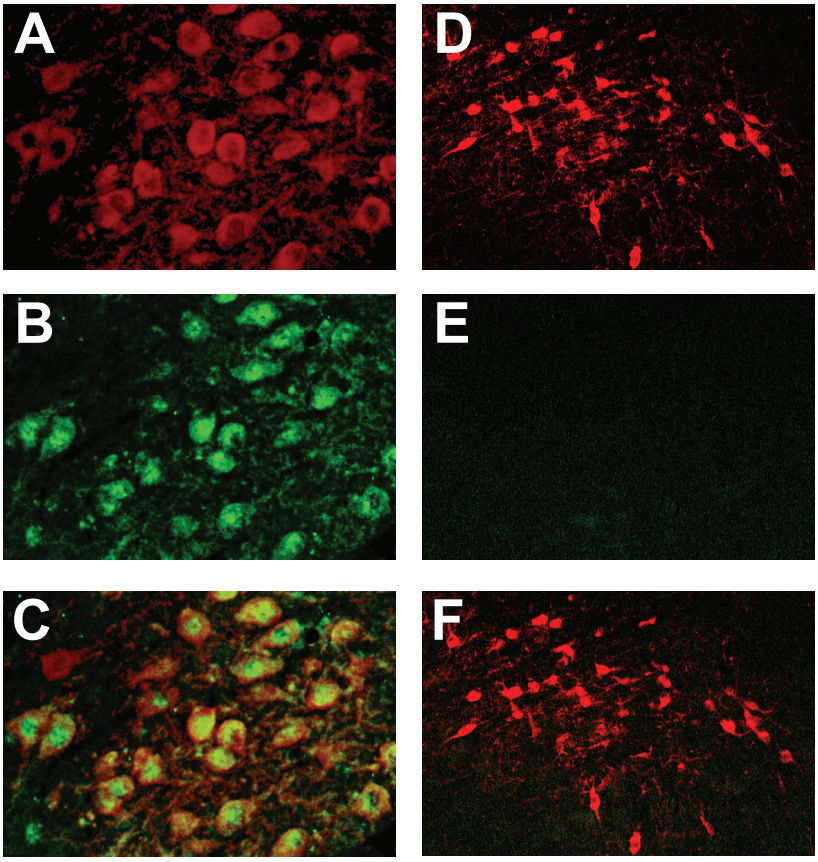

Figure 13. Expression of EGFP from Hb9:CHT Transgene. (A-C) Hindbrain immunostaining for ChAT (A) and EGFP (B) with the merged image (C) showing colocalization in the soma of motor neurons from cranial nerve XII. Scale bar for (A-C) 20μm. (D-F) Midbrain immunostaining for ChAT (D) and EGFP (E) with the merged image (F) showing lack of EGFP in a non motor neuron population of cholinergic neurons in the lateral dorsal tegmentum. Scale bar for (D-F) is 50μm.

Nonetheless, on the CHT-/- background, we could readily detect CHT expression by mmunofluorescence (Figure 14A-I) in CHT-/-;Hb9:CHT diaphragms. In the diaphragm of neonatal, CHT+/+ animals, CHT immunoreactivity colocalized as previously described (Ferguson, 2004) with alpha bungarotoxin-labeled nicotinic receptors (Figure 14A-C). Specificity of labeling for CHT was evident, as seen in a parallel colocalization series produced with nontransgenic CHT -/- mice (Figure 14D-F). In Hb9:CHT transgenic mice on the CHT-/- background (Figure 14G-I), CHT labeling was evident, though weaker than observed in CHT+/+ preparations (compare Figures 14B and 14H) and, as in CHT+/+ specimens, was colocalized with alpha bungarotoxin. Interestingly, the lateral distribution of endplates across the diaphragm of both CHT -/- and Hb9:CHT transgenic mice on the CHT-/- background was more irregular than seen with sections from CHT+/+ animals, and not all terminals labeled for the CHT transgene opposed dense clusters of nicotinic receptors. These findings indicate that although the CHT transgene is present in multiple copies, expression of CHT protein does not reach that of the transporter at the wild-type NMJ.

To explore the capacity of the Hb9:CHT transgene to rescue CHT -/- mice from neonatal lethality (Ferguson, 2004), we monitored the survival of CHT+/+, CHT+/-, and CHT-/-, with or without the Hb9:CHT transgene, all derived from a cross of CHT+/-;Hb9:CHT with CHT+/- parents. As previously observed (Ferguson, 2004), CHT-/- mice died within 30min after birth, becoming progressively paralyzed and cyanotic, presumably due to an inability to contract the diaphragm. As expected, CHT +/- and CHT+/+ littermates exhibited normal growth and survival.

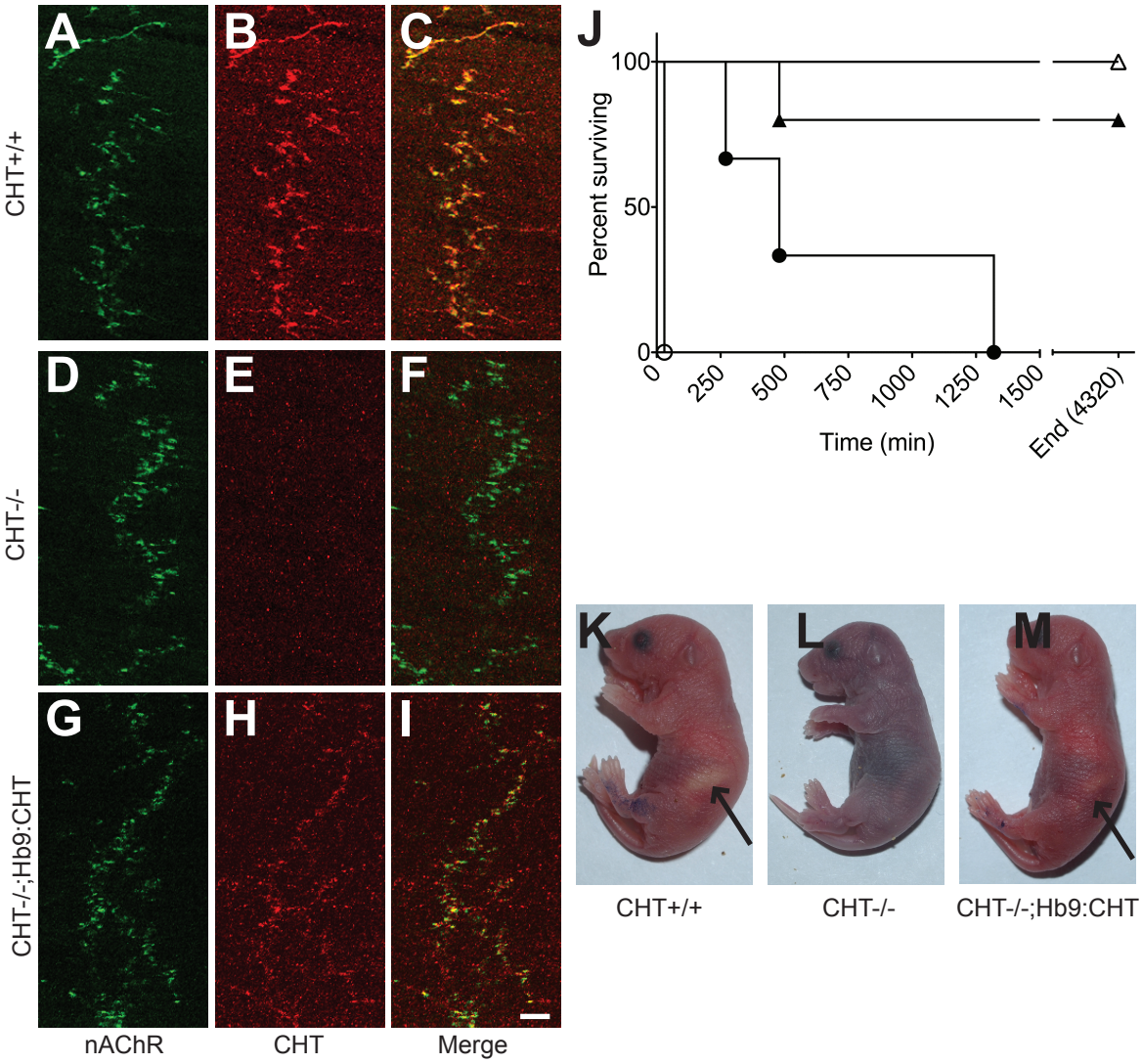

Figure 14. Expression and function of CHT from HB9:CHT demonstrated in Hb9:CHT;CHT-/- neonatal mice. (A-I) Immunostaining for alpha Bungarotoxin and neurofilaments (A, D, G) and CHT (B, E, H) with the merged images (C, F, I) in CHT+/+ (A-C), CHT-/- (D-F) and Hb9:CHT;CHT-/- (G-I) mice. Although weaker than CHT+/+, CHT immunoreactivity is present opposed to α-bungarotoxin staining in CHT-/-;Hb9:CHT diaphragms. Scale bar is 50μm. (J) Survival time from birth for mice of all six possible genotypes (CHT+/+ n=5, CHT+/- n=22, CHT-/- n=5, Hb9:CHT;CHT+/+ n=5, Hb9:CHT;CHT+/- n=22, Hb9:CHT;CHT-/- n=3). CHT+/+ open triangles; CHT+/- not shown, all survived to 4320 min; CHT-/- open circles; Hb9:CHT;CHT+/+ filled triangles; Hb9:CHT;CHT+/- not shown, all survived to 4320 min; Hb9:CHT;CHT-/- filled circles. (K-M) Photographs of mice at 4 hrs after birth. CHT-/-;Hb9:CHT mice have similar color to CHT+/+ mice and occasionally have a milk-spot (indicated by arrows) that is noticeably smaller in this pup.

Strikingly, CHT-/-;Hb9:CHT mice survived up up to 24 hours (Figure 14J), exhibiting normal coloration in the first hour after birth (Figure 14M), grossly normal movements and evidence of nursing behavior.

Hb9:CHT transgenic mice on a CHT+/+ background display enhanced endurance on a treadmill

Our Hb9-based transgenic strategy was designed not only to assess the capacity of motor neuron-specific expression of CHT to rescue lethality of CHT-/- mice, but also to permit evaluation of the functional consequences of supranormal CHT expression when the transgene is placed on a CHT+/+ background. To explore the latter opportunity, CHT+/+ and CHT+/+;Hb9:CHT transgenic mice were assessed for endurance in a paradigm of forced exercise on a motorized treadmill. We have previously shown that CHT+/- mice display an inability to achieve the speeds, or exhibit the endurance, of CHT+/+ mice (Bazalakova, 2006). The distributions of time until exhaustion for CHT+/+ and CHT+/+;Hb9:CHT mice that met performance criteria for inclusion are shown in Figure 15A-B. The mean time until exhaustion for the CHT+/+;Hb9:CHT mice was significantly greater than that of CHT+/+ littermates (two-tailed t-test, P=0.0179) (Figure 15C).

Basal CMAP and CMAP recovery from high frequency stimulation are altered in Hb9:CHT transgenic mice.

With evidence of enhanced endurance in the CHT+/+;Hb9:CHT mice, we sought evidence of altered neuromuscular signaling that might contribute to our

behavioral observations by examining evoked compound muscle action potentials (CMAP). We observed no genotype effect on the amplitude of the baseline evoked CMAP (Mann-Whitney U test, *P*=0.8294) (Figure 16A). However, recordings from the CHT+/+;Hb9:CHT mice revealed a clear shift from the unimodal distribution of values evident in CHT+/+ animals (Figure 16B) to a bimodal distribution (*P*=.0023, F(3,5)=23.04, extra sum-of-squares F-test) (Figure 16C). Both the low and high amplitude Hb9:CHT;CHT+/+ groups were significantly different than the CHT+/+ group *P*<0.001, ANOVA with Bonferroni post-test).

To further explore the properties of the high and low amplitude groups described above, we examined the CMAP recovery rates following prolonged 50Hz stimulation. CHT+/+, low amplitude CHT+/+;Hb9:CHT and high amplitude CHT+/+;Hb9:CHT mice exhibited the same percentage CMAP reduction (~80%) following high frequency stimulation (*P*=0.6047) (Figure 17A). Additionally, the kinetics for CMAP recovery for the low amplitude CHT+/+;Hb9:CHT group was indistinguishable from the CMAP recovery rate of CHT +/+ mice (CHT+/+ K=0.71+/-0.04; CHT+/+;Hb9:CHT(Low) K=0.79 +/- 0.08, *P*=0.3304, F(1,64)=0.9168, extra sum-of-squares F-test) (Figure 17C). In contrast, the high CMAP amplitude, CHT+/+;Hb9:CHT group displayed a significantly faster recovery rate (CHT+/+ K=0.71+/-0.04; CHT+/+;Hb9:CHT(High) K=0.95+/- 0.06, *P*=0.0017, F(1,88)=10.54, extra sum-of-squares F-test) (Figure 17B).

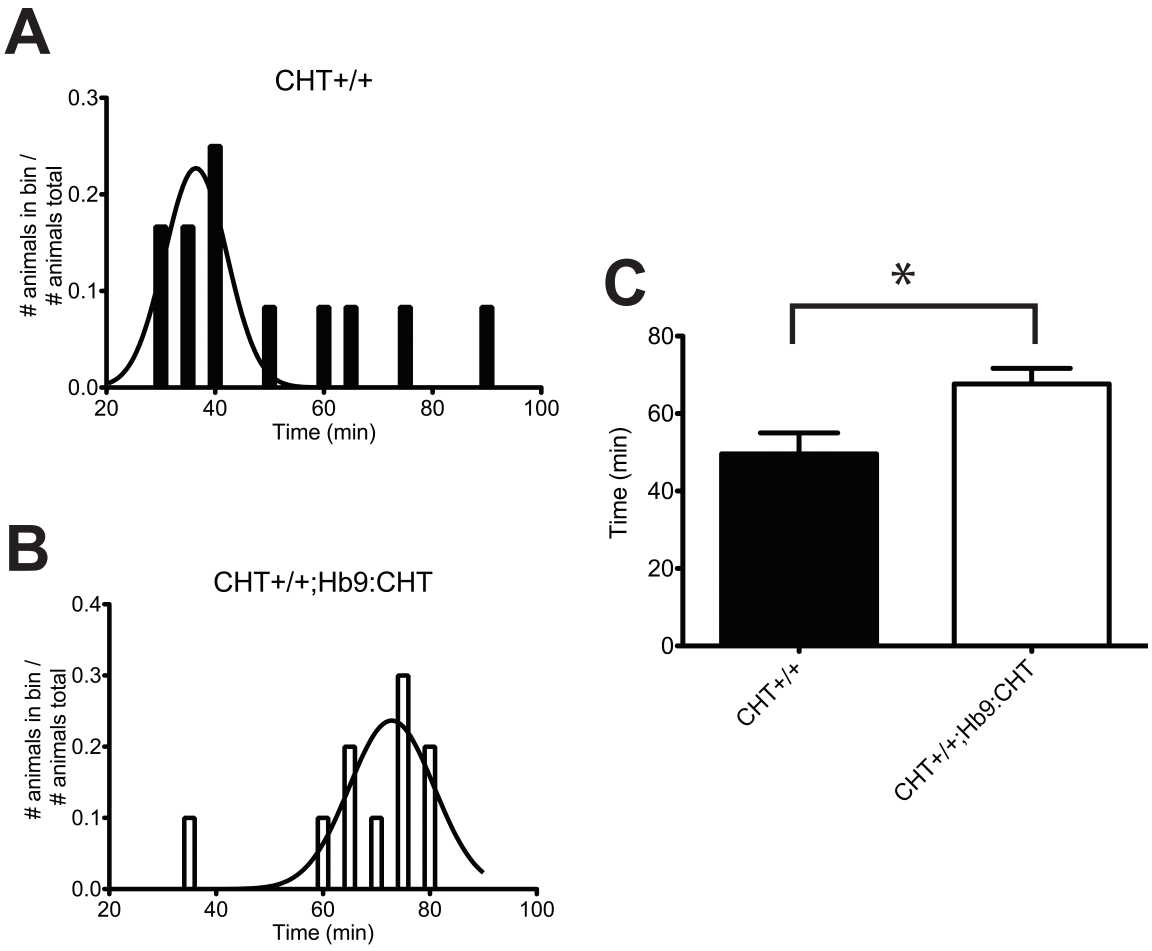

Figure 15. Endurance of Hb9:CHT mice during a forced treadmill exercise paradigm. (A and B) Distributions for running times of CHT+/+ (A) and CHT+/+;Hb9:CHT (B) mice that met performance criteria. The fitted curve is the probability density function for a Gaussian distribution of the performing mice. (C) Comparison of running times for each genotype. CHT+/+;Hb9:CHT mice are significantly elevated (two-tailed t-test, P=0.0179).

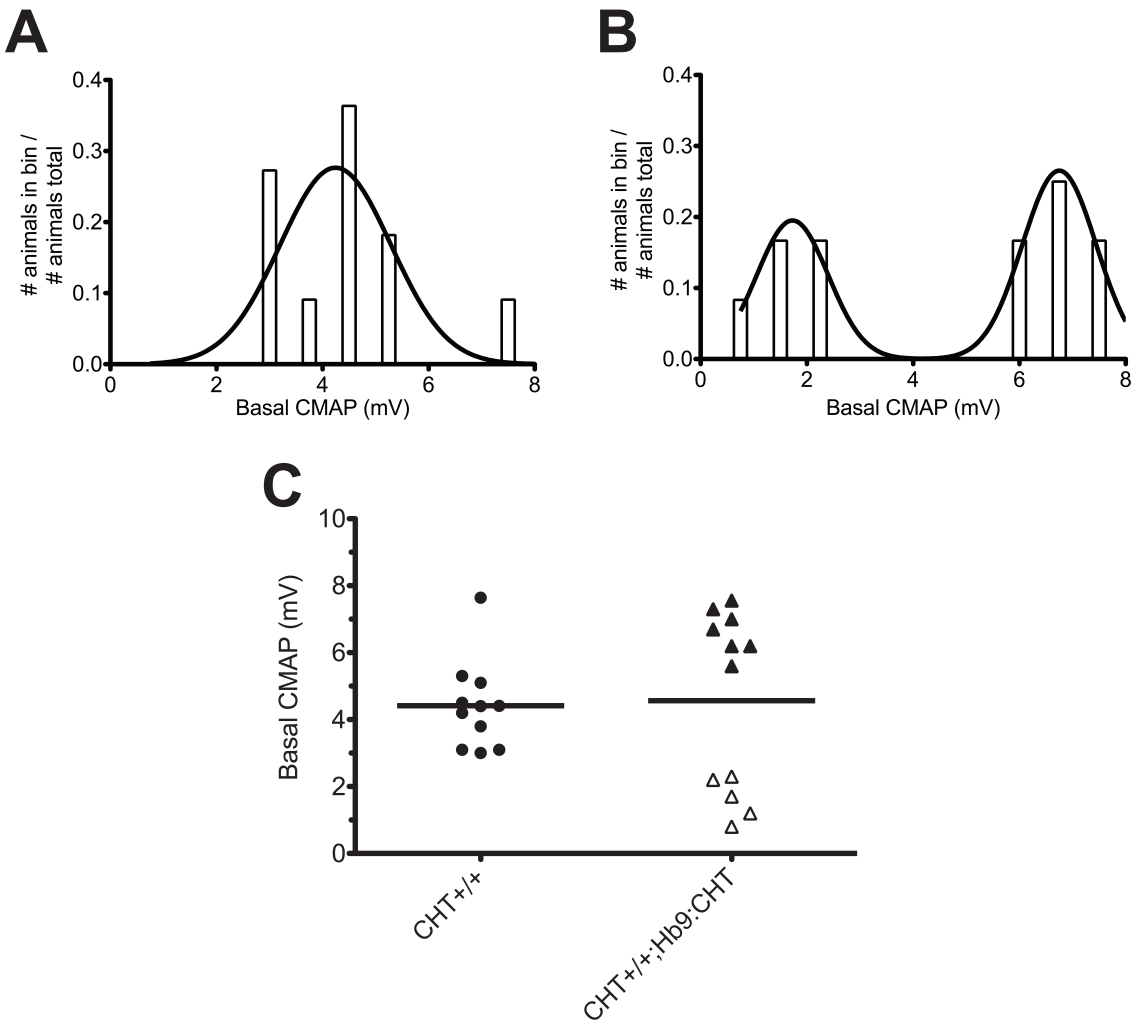

Figure 16. CMAP analysis of the hindlimb paw muscles. (A) Maximal stimulated recorded compound muscle action potential (CMAP) prior to high frequency stimulation (CHT+/+ n=11, Hb9:CHT n=12). Histogram of CMAP amplitudes for CHT+/+ (B) and CHT+/+;Hb9:CHT (C) mice and the resulting probability density functions.

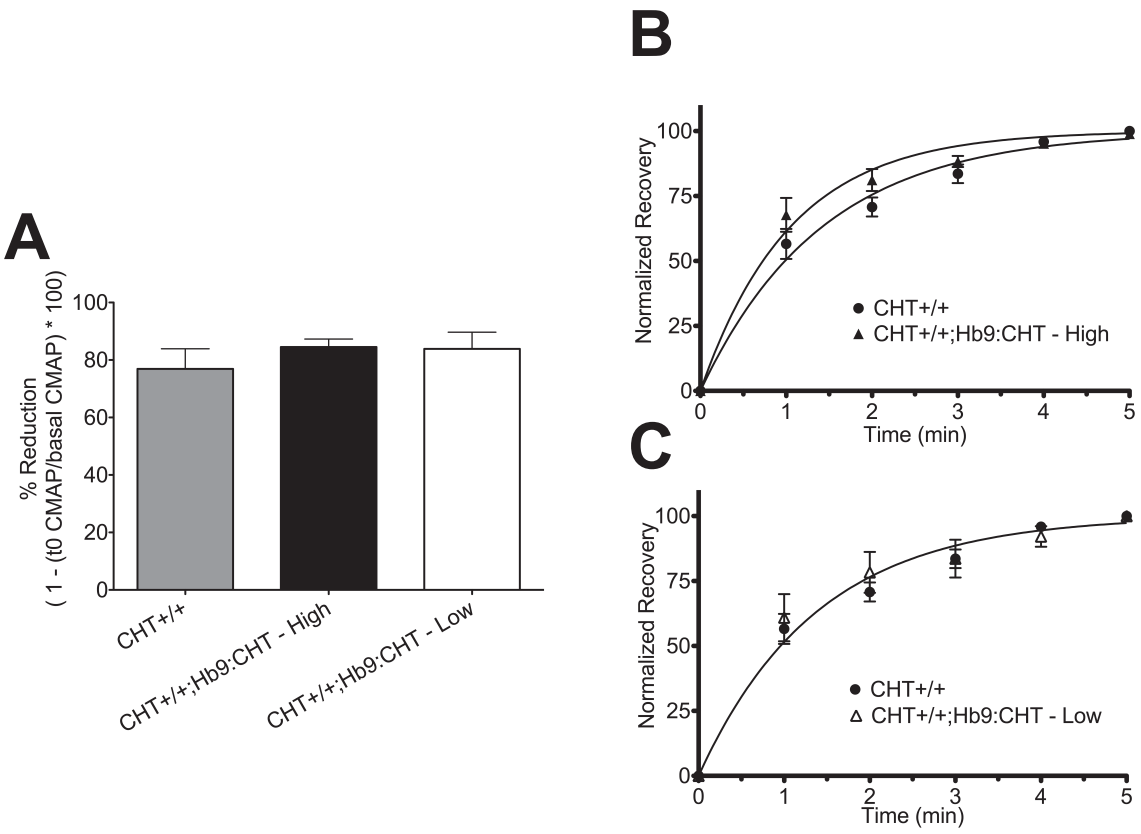

Figure 17. Recovery of stimulated CMAP after 60s of 50Hz stimulation. (A) % reduction of CMAP from basal to first stimulation after high frequency stimulation. (B) and (C) Normalized recovery curves comparing CHT+/+ (n=8) mice against the high (n=7) (B) and low (n=3) (C) CMAP components of CHT+/+;Hb9:CHT mice.

Physical characteristics and enzyme activities of muscles are not changed by the Hb9:CHT transgene

To examine possible structural and compensatory changes related to altered cholinergic signaling, we examined the size of the NMJ and muscles and the activities of enzymes involved in ACh synthesis and degradation. For analysis of NMJ area (Figure 18A-C), we used the FDB near the body of the third metatarsal as this muscle was the predominant muscle for CMAP recording. The NMJ areas of this muscle were not changed between genotypes (two-tailed t-test, P=0.2705) (Figure 18C).

In order to compare the physical aspects of the muscle and enzyme activities, it was necessary to use the gastrocnemius due to its larger size and the ability to generate a complete cross section of the muscle (not possible for FDB). The cross-sectional area of the gastrocnemius was not changed in CHT+/+;Hb9:CHT mice (two-tailed t-test, P=0.8573) (Figure 18G). We also analyzed the cross-sectional area of both Type I / IIa fibers (dark SDH staining) and Type IIb fibers (light SDH staining). In both cases, there was not change in the CHT+/+;Hb9:CHT mice (two-way ANOVA, P=0.7951 for genotype effect) (Figure 18F). Furthermore, there was no change in the activity of either AChE or ChAT (Figure 19).

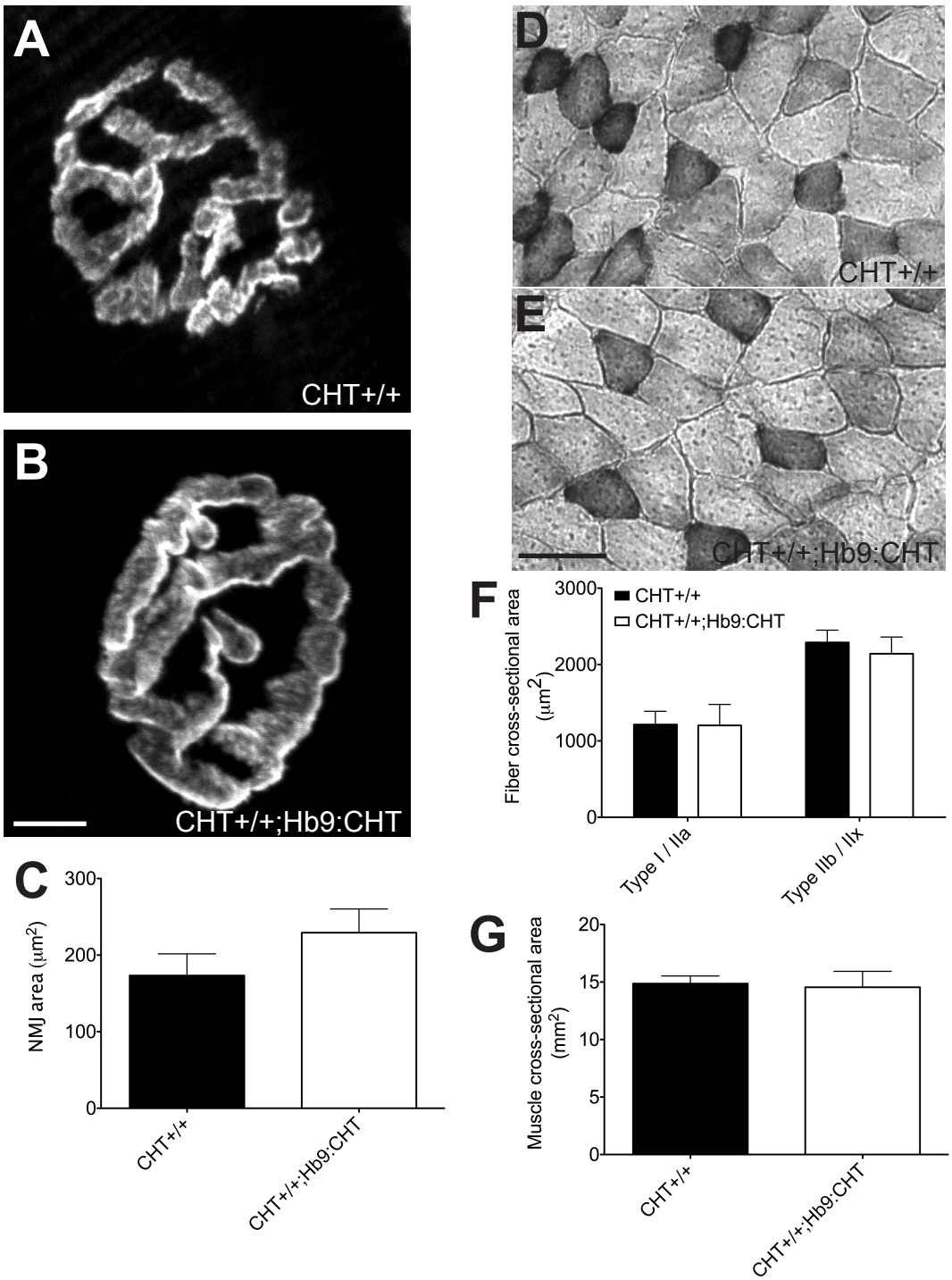

Figure 18. Physical characteristics of NMJ and muscle fibers of Hb9:CHT mice. (A, B) Sample NMJ of CHT+/+ (A) and CHT+/+;Hb9:CHT (B) from the FDB. (C) The NMJ area is not different between genotypes (CHT+/+ n=4, Hb9:CHT n=4; two-tailed t-test, $P>0.1$). (D, E) Sample images of cross-sections of gastrocnemius muscles stained for SDH. (F)Cross-sectional area of each fiber type is not different between genotypes (CHT+/+ n=3, Hb9:CHT n=5; 2-way ANVOA, $P>0.1$). (G) Cross-sectional area of the entire gastrocnemius is also not different between genotypes (CHT+/+ n=4, Hb9:CHT n=5; two-tailed t-test, $P>0.1$). Scale bars are 50μm.

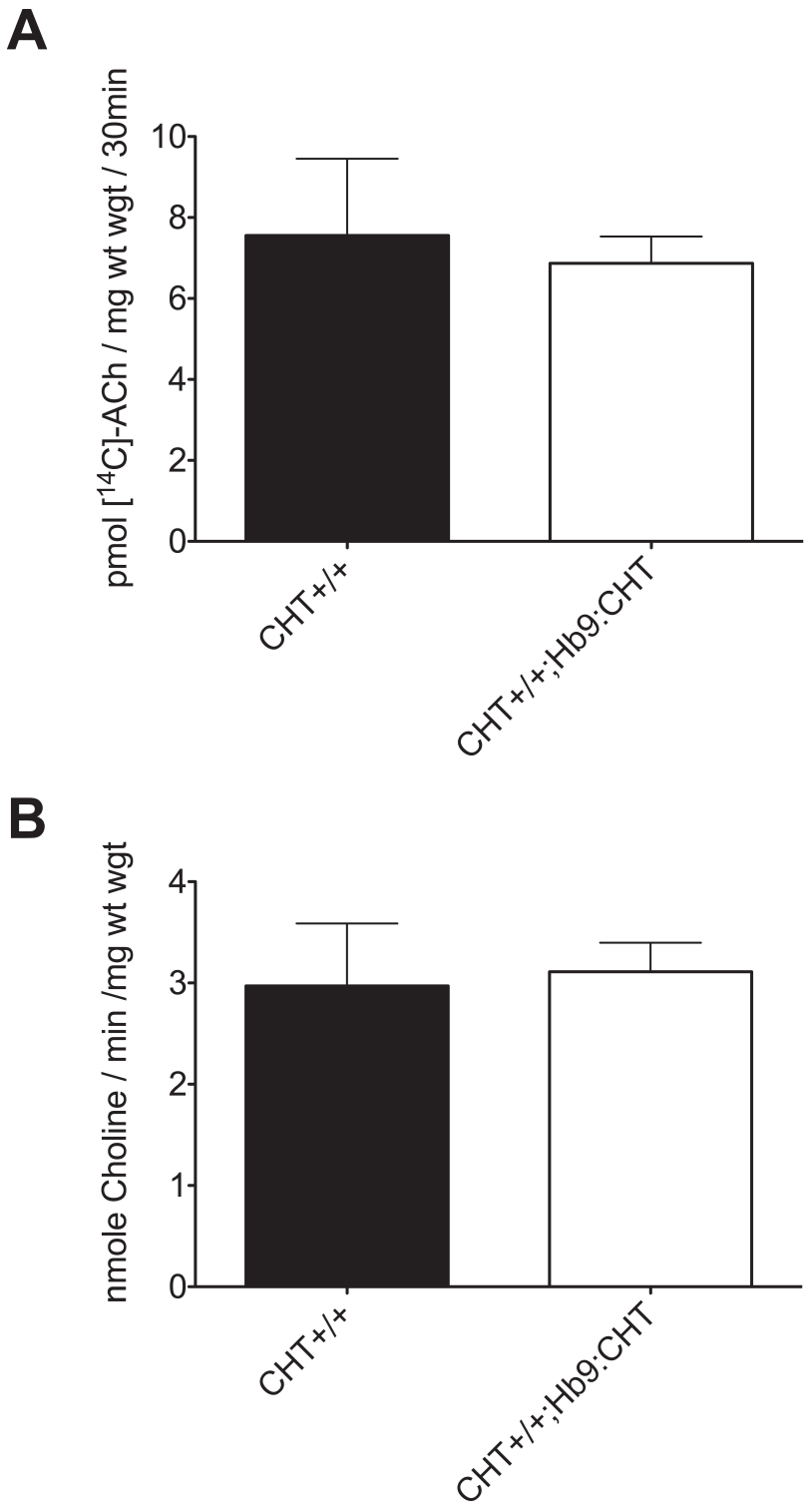

Figure 19. ACh metabolizing enzyme activities of Hb9:CHT mice. (A) ChAT activity is not affected by the Hb9:CHT transgene (CHT+/+ n=3, CHT+/+;Hb9:CHT n=4; two-tailed t-test, *P*>0.1). (B) AChE activity is also not affected (CHT+/+ n=3, CHT+/+;Hb9:CHT n=5; two-tailed t-test, *P*>0.1).

Discussion

Possibility for rescue of CHT-/- mice

Our results provide evidence of successful motor neuron and NMJ expression of CHT in Hb9:CHT transgenic mice. Due to the limitations of measuring CHT levels and activity in motor neurons (Wessler and Kilbinger, 1986; Wessler and Sandmann, 1987), we verified CHT expression of our Hb9:CHT transgene via visualization of transgene expression on a CHT-/- background. Although we detected CHT at the NMJ, staining levels did not reach the levels observed in CHT +/+ mice. We suspect that although we integrated multiple copies of the Hb9:CHT transgene into the genome of these mice, the Hb9 promoter may be intrinsically weaker than the native CHT promoter, or be limited by the site of integration. Qualitative observation of the NMJ region of these mice also displayed morphological characteristics (wider band of NMJ across diaphragm, as seen in Figure 14A-I) seen in mice lacking ACh synthesis (Brandon, 2003) or no CHT expression (Ferguson, 2004), including less compact synaptic zones. Lack of diaphragm function from insufficient ACh release has been shown as the cause of death in mice with severely compromised cholinergic synapses (Misgeld, 2002), including our CHT-/- mice (Ferguson, 2004). Although a full rescue of CHT was not achieved, we did observe a significant extension of lifespan in CHT-/-;Hb9:CHT mice. Pursuit of the basis for limited longevity in these mice is beyond the scope of the current study but may arise from deficits in autonomic signaling supporting normal cardiovascular function (Vaseghi and Shivkumar; Schwartz, 1988). Additionally,

central cholinergic control of motor neuron activity, such as control of respiratory motor neurons by pontine cholinergic neurons (Shao and Feldman, 2005), may be compromised since transgene expression is limited to brainstem and spinal motor neurons (Figure 13A-C).

Relationship between treadmill and CMAP analysis

One of the most striking phenotypes observed in CHT+/- mice was reduced endurance during forced treadmill exercise. We were therefore eager to determine whether the opposite phenotype would emerge when CHT expression was elevated in motor neurons of wild-type animals. Our treadmill paradigm employed for this assessment was designed to ameliorate some anticipated confounds. Specifically, we used a very low amount of training so that we could better identify increases in running time caused by elevated CHT and minimize any training induced plasticity (Massett and Berk, 2005). We also used a lower speed that would be more likely to elicit a challenge-induced phenotype (Bazalakova, 2006). Other groups have used longer training regimens (Lerman, 2002) and more intense testing protocols (Lightfoot, 2001). Our demonstration of enhanced endurance in the Hb9:CHT mice supports the capacity of elevated CHT expression to positively contribute to exercise endurance. Since the haploinsufficiency of our CHT+/- mice is constitutive, we were unable to determine previously (Bazalakova, 2006) whether the reduced endurance of these animals was caused by deficits in neuromuscular, autonomic, or central cholinergic signaling. The elevated endurance apparent in the Hb9:CHT mice provides strong evidence that modulation of CHT expression/activity at the

NMJ can both decrease or increase endurance. Whether this effect arises as a result of developmental changes in the strength and stability of NMJ signaling or is a feature of ongoing NMJ activity during the challenge protocol is unknown, but should be amenable to study in transgenic models where CHT expression is controlled in an inducible manner. If the latter explanation holds, pharmacological induction of increased CHT activity could represent a novel therapeutic strategy to ameliorate deficits in NMJ signaling, as seen in myasthenic syndromes (Schwab, 1957; Sussman, 2008).

To complement the behavioral challenge of the treadmill and to monitor physiological features of motor neuron signaling arising from a neuromuscular challenge, we assessed the magnitude of evoked stimulation and the rate of recovery from depression that arises from high frequency (50 Hz) stimulation. As CMAP measures the summation of action potentials of the muscle rather than the signal from individual nAChRs, we did not expect to see differences between genotypes in the basal CMAP amplitude. Our amplitudes were evoked using supramaximal stimulation, reducing concerns that results derived from variations in initiation of axonal action potentials. However, we observed a striking bimodal distribution in the basal CMAP amplitude, and the predicted enhanced recovery phenotype was only observed in the "high-CMAP" group. Given that the tibial nerve was supramaximally stimulated and muscles are thought to have a strong safety factor (Wood and Slater, 2001), it was surprising to see a population with increased CMAP amplitude. An elevated CMAP amplitude, caused by increased fidelity of neuromuscular transmission, would be expected if the safety factor of the studied

muscle in CHT+/+ mice is low enough such that stimulation of all motor axons does not necessarily result in action potentials of all muscle fibers. Our recording setup primarily recorded from the FDB, which has been suggested to have a lower safety factor compared to the better studied diaphragm (Molenaar, 2008). However, increased CMAP amplitude is usually associated with pathological conditions that reduce ACh release where CMAP can be elevated by repetitive nerve stimulation (i.e. Lamber-Eaton myasthenic syndrome). In non-pathological conditions, increased CMAP amplitude has been best described only under a few conditions, but all relate to periods of increased use. During timescales on the order of minutes, exercise has been shown to increase CMAP amplitude in response to exercise (Lentz and Nielsen, 2002). Several explanations have been offered for the increase in CMAP including increased muscle excitability (Hicks, 1989), increased number of muscle action potentials (Lee, 1977), and increased synchronization of muscle action potentials (Asawa, 2004). As an alternative hypothesis to improved neuromuscular transmission, increased CHT could alter the excitability of the muscle. It has recently been shown that increased quantal size at the NMJ can alter the steady-state electrical properties of the muscle membrane (Fong). As the expected mechanism for increased cholinergic signaling with elevated CHT is an increase in quantal size (Figure 20), we cannot rule out this change as an explanation of the increased CMAP amplitude.

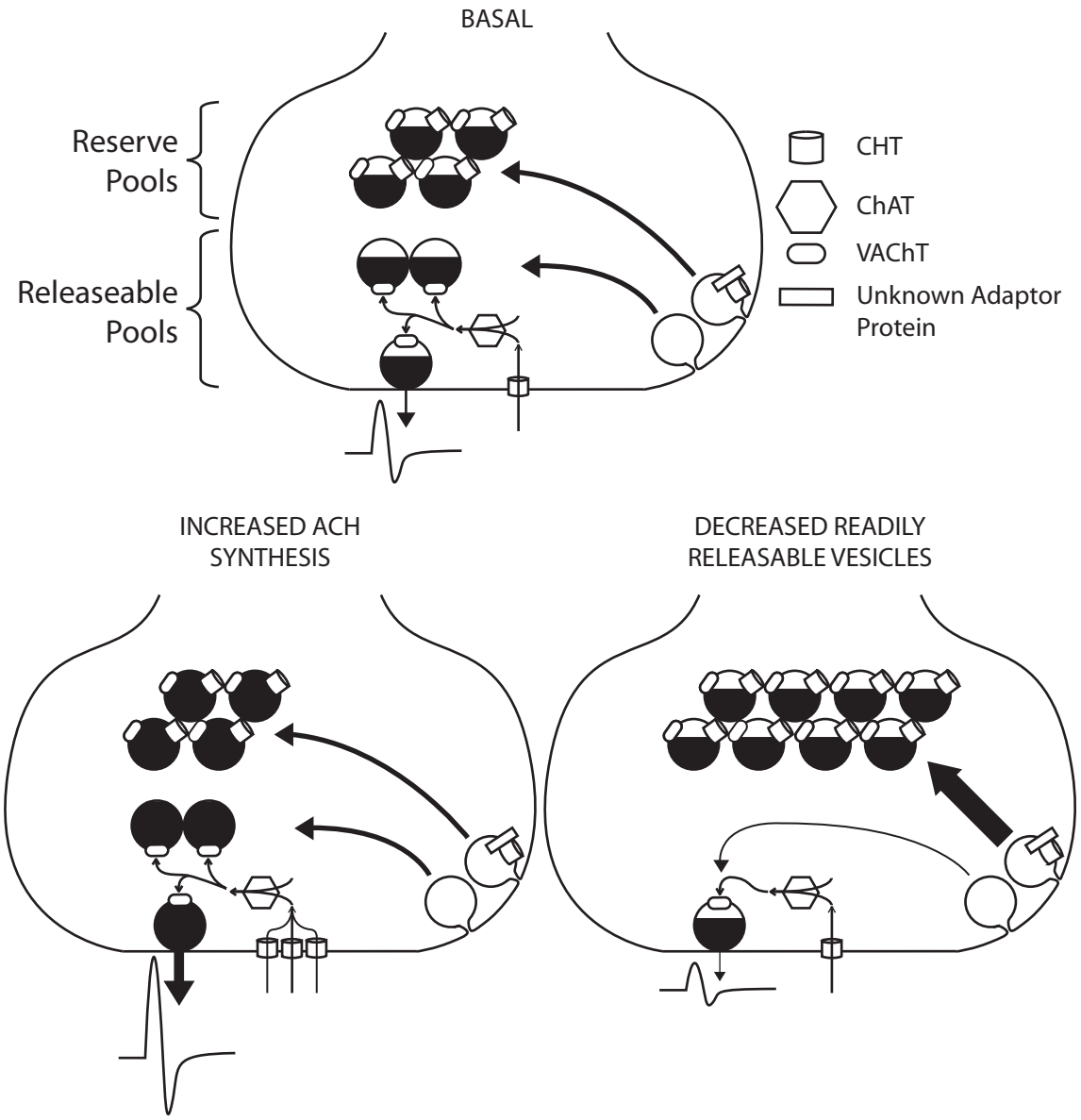

Fig. 20. Proposed model of bimodal distribution of electromyography data. In a wild-type synapse, CHT imports choline that is rapidly synthesized into ACh and packaged into vesicles for release and postsynaptic effect. In CHT+/+;Hb9:CHT mice with an elevated basal response, increased plasma membrane CHT increases both choline transport and ACh synthesis. The distribution of vesicles in the elevated condition is minimally affected, if at all, but the amount of ACh per vesicle is substantially elevated. Conversely, in the CHT+/+;Hb9:CHT mice with reduced response, ACh release is reduced by the lack of readily releasable or recycling vesicles. Vesicles are instead shunted to the reserve pool by the presence of CHT, probably by the interaction of CHT with an unknown adaptor protein.

Possible mechanisms of bimodal CMAP

Previous studies have documented that altered ACh vesicular content can alter the amount of ACh released (Yu and Van der Kloot, 1991; Gras, 2008). Extended periods of stimulation, even at frequencies as low as 10Hz, lead to the emergence of larger quantal sizes (Yu and Van der Kloot, 1991), suggesting that elevating quantal size could be dependent on the history of motor activity of each mouse. As these increases were shown to be HC-3 sensitive, it is reasonable to speculate that increased CHT could increase the variability between animals by increasing the effect of animal experience on measured neuromuscular function. As noted above, we recognize that the effects we observed could be due either to a developmental effect of elevated ACh synthesis and release or elevated ACh signaling at the time of stimulation. Further studies are needed to address this issue that utilize temporally controlled CHT expression.

The generation of a population of animals with low basal CMAP amplitudes was surprising given the expectation of a gain of function. Similar amplitudes obtained from recordings at multiple sites in the same animal convinced us that the changes observed are reflections of stable physiological characteristics as opposed to experimental artifacts. The vesicular localization of CHT at the NMJ and other cholinergic synapses has been postulated to relate to the functionally defined reserve pool of cholinergic synaptic vesicles (Ferguson, 2003; Ferguson and Blakely, 2004; Nakata, 2004). Potentially, elevated CHT could negatively impact the size of CMAPs if elevated CHT increases the abundance of reserve pool vesicles at the expense of the readily releasable pool (Figure 20). In preliminary studies examining

the NMJs of nematodes genetically deprived of the CHT homolog CHO-1, we have observed a loss of synaptic vesicles within 100nm of the plasma membrane (D.S. Matthies and R.D. Blakely, unpublished findings). Increasing the ratio of reserve pool to releasable pool vesicles would reduce the amount of ACh available for release during lighter periods of stimulation and thereby reduce overall stimulation if the mobilization of reserve pool vesicles is too slow to compensate. The two hypotheses we present to explain high and low CMAP values may interrelate as newly synthesized ACh is thought to preferentially load more rapidly recycling vesicles (Gracz, 1988; Bonzelius and Zimmermann, 1990). Possibly, only in mice where there is a sufficiently large population of recycling vesicles can elevated ACh synthesis "win out" and result in an elevation in cholinergic signaling. Although we did not observe a group of CHT+/+;Hb9:CHT mice with reduced endurance to match our findings of reduced CMAP levels, we utilized a cutoff for non-performance in this task that could have masked such an effect. Indeed, retrospective analysis of treadmill times for the nonperforming group reveals a broader distribution of running times than seen in the CHT+/+ mice that might reflect incorporation of mice with a negative shift in endurance. Future experiments will directly assess the relationship between changes in treadmill running time and changes in CMAP amplitude.

An alternative hypothesis for the bimodal distribution of the CMAP is a potential compensatory effect occurring at the neuromuscular junction. In CHT+/- mice, M1 and M2 muscarinic ACh receptor levels are reduced in a brain region-specific manner (Bazalakova, 2006), and these animals display a reduced locomotor

sensitivity to the muscarinic antagonist scopolamine. Both M1 and M2 receptors have been identified on motor neuron presynaptic terminals, where they may also be influenced by elevations in CHT expression. At the NMJ, M1 facilitates ACh release whereas M2 inhibits ACh release and functional interactions between these receptors have been described (Oliveira and Correia-de-Sa, 2006). At low frequencies of stimulation, M1 stimulation of release predominates whereas at higher stimulation frequencies, M2-mediated suppression is dominant. If prior experience can alter the balance between M1 and M2 signaling, then the effects of altered CHT expression should lead to enhanced or suppressed neuromuscular transmission. It is unlikely that the transgene initiates any RNA level feedback regulation as our construct uses the CHT cDNA and therefore lacks potential 3'-untranslated region regulatory elements associated with cholinergic signaling. Finally, differences in the ratio of ACh and ATP storage and release could drive signaling toward enhanced or diminished signaling.

If the two populations identified in CMAP responses derive from contributions of CHT to fundamentally different components of presynaptic signaling capacity (e.g. ACh synthesis and alterations in availability of releasable versus reserve vesicle pools), we hypothesized that these differences might be observable in the kinetic properties of evoked responses. In support of this idea, CHT+/+ and CHT-/- mice display differences in the kinetics of rundown of both spontaneous and evoked ACh release (Ferguson, 2004). In the context of our manipulations, we reasoned that if the high-CMAP group derives from NMJ signaling that is dominated by elevated ACh synthesis and release, recycling vesicles might be

more rapidly refilled after acute depletion, leading to a more rapid recovery. In contrast, if the low-CMAP group derives from a reduction in the availability of readily releasable vesicles, the kinetics of recovery might not be impacted by CHT overexpression. Indeed, we found a statistically significant enhanced rate of recovery in the high-, but not the low-CMAP group. Importantly, this difference was observed in the context of equivalent percentage suppression of CMAP in both groups induced by high frequency stimulation. Altered recovery kinetics of heart rate in the cardiovascular system have been associated with changes in mortality (Cole, 1999) and we have demonstrated reductions in HR recovery in CHT+/- mice (English, 2010). As with our discussion of the origins of differences in basal CMAP values, we recognize that at present, there are likely other explanations for the kinetic differences we observed. Two approaches are currently being pursued to gain finer resolution of the effects of CHT overexpression. One is a quantitative, optical evaluation of presynaptic vesicle cycling rates where CHT overexpression is achieved in NMJ synaptopHluorin mice (Wyatt and Balice-Gordon, 2008; Gaffield, 2009). These studies offer an opportunity to assess the impact of CHT on the segregation of synaptic vesicle pools. The second is a quantal analysis of miniature end-plate potentials (Everett and Ernst, 2004) that can report on the ACh content of single synaptic vesicles. Given the range of disorders that display reduced cholinergic signaling, ranging from neuromuscular disorders to Alzheimer's Disease, the results of these studies should not only clarify molecular contributions to cholinergic signaling but also lay a foundation for new, cholinomimetic therapeutics.

CHAPTER IV

IMPACT OF ELEVATED CHT ON HACU AND BEHAVIOR

Introduction

Previous attempts to elevate synaptic choline availability

Studying the NMJ as a way of understanding the synaptic function of CHT is useful because of how well-studied this synapse at both the molecular and physiological level. However, the greatest potential clinical usefulness of targeting CHT will be a potential enhancement of central ACh synapses that are affected by more prevalent diseases such as Alzheimer's and ADHD. I therefore endeavored to develop a mouse that could express CHT in all locations that have endogenous CHT. This includes the NMJ, central cholinergic synapses, and well as PNS and non-neuronal cholinergic systems.

Several diseases are treated through the augmentation of cholinergic signaling. The most common mechanism of cholinergic enhancement is AChE inhibition. AChE inhibitors are the preferred treatment for Alzheimer's Disease (Birks, 2006) and are also used to treat many myasthenic disorders (Schwab, 1957; Sussman, 2008). Attempts have been made to increase cholinergic signaling by precursor loading, similar to the levodopa strategy used to treat Parkinson's disease. However, the clinical utility of the ACh precursor loading strategy has been equivocal at best where there seem to be a strong dependence on the form of

choline administered (for example, free choline versus choline alphoscerate) (Amenta, 2001). Emerging data suggest that the problem has not been the concept supporting ACh precursor loading, but rather a poor choice of precursors, in the effectiveness of the precursor loading strategy. Due to the necessary active transport of free choline across biological membranes and the rate-limiting nature of CHT in ACh synthesis, precursors such as choline and lecithin (phosphotidylcholine) that supply free choline to the neuronal extracellular space would not be effective in increasing ACh availability. However, precursors that potentially have higher direct availability in the presynaptic terminal have been shown to increase ACh synthesis and are beginning to show clinical usefulness for AD (De Jesus Moreno Moreno, 2003). Importantly, no efforts have been made to increase the plasma membrane availability of CHT or to increase the activity of CHT in a therapeutic setting.

Strategy for the study of overexpression of CHT

The strategy for this mouse was to create a transgene that contained a large region of genomic DNA that contained the CHT gene as well as substantial 3' and 5' flanking sequences. For the vast majority of genes studied, the necessary and sufficient regulatory elements are located within tens of kilobases of the gene (Gong, 2003). It is important to note that many of the more distal regulatory elements can be found either upstream or downstream of the gene (Higgs, 2008). As a result of the mouse genome sequencing effort, such genomic clones are readily available commercially. Standard pronuclear injection of the DNA results in extra copies of

genomic fragments being randomly inserted into the mouse genome. Due to the size and scope of BAC transgenes, they are usually immune to insertion-site effects and expression is directly related to the number of copies inserted (Chandler, 2007).

Although the long term goal of the BAC-CHT mouse is to study the possibility of a CHT activiating therapeutic, the focus of the current study is the basic characterization of phenotypes caused by the central overexpression of CHT. In order to validate the transgene, immunodetection experiments were done to assess CHT levels and localize elevated CHT to the synapse. Despite the increased synaptic CHT, basal HACU measurements showed no differences between BAC-CHT mice and CHT+/+ mice. An initial battery of behavioral tests showed differences in both memory and anxiety related tasks. The phenotypes observerd with the lack of change in HACU raise many of the same questions addressed with the CHT+/- mice making the BAC-CHT mouse a fruitful model for future research.

Materials and Methods

Generation of BAC-CHT mice

BAC clone (RP24-290K23) was obtained from the BACPAC Resources Center at the Children's Hospital Oakland Research Institute supplied in DH10B bacterial cells. The BAC was purified and electroporated (GenePulser, BioRad; Hercules, CA) into SW102 cells for recombineering (200Ω, 25μF, and 1.8V). DNA was prepared from BAC-SW102 cells for injection by CsCl purification. Circular DNA was injected into one-cell embryos of C57BL/6 mice by the Vanderbilt Center for Stem Cell

Biology Embryonic Stem Cell/Transgenic Mouse Shared Resource. Possible founder animals were screened by PCR.

BAC DNA preparation for injection

Single colonies of BAC-SW102 from Luria Broth (LB) plates with chloramphenicol (CAM, LB/CAM) were picked and incubated shaking overnight at 30° in 5mL of LB with 12.5μg/mL of CAM. 1mL of the culture in the morning was then transferred to each of 4 1L flasks of LB with 12.5μg/mL CAM. Cultures were grown to an optical density of 0.6 at 600nm (typically 20 hours). Cultures were then divided into 250mL bottles and centrifuged using a SLA-1500 rotor at 4500rpm for 16 minutes at 4°C. Pellets were washed twice with 25mM NaCl and the pellets were frozen without supernatant. The following day, pellets were brought back up to ambient temperature and resuspended in 20mL solution I (10mM ethylenediaminetetraacetic acid (EDTA), pH 8.0). 40mL of solution II (200mM NaOH, 1% SDS) was then added and incubated for 5 minutes at ambient temperature. 30mL of ice-cold solution III (1.875M KOAc, 2M AcOH) was added and incubated at 4°C for 20 minutes. Each bottle was then centrifuged at 10000rpm in an SLA-1500 rotor at 4° for 30 minutes. The supernatant was collected and recentrifuged at 10000rpm in an SLA-1500 rotor at 4°C for 30 minutes. The supernatant was collected and 90mL of ice-cold iPrOH was added and incubated on ice for 10 minutes. This was centrifuged at 10000rpm in an SLA-1500 rotor at 4°C for 10 minutes. The resulting pellet was dried for 10 minutes and resuspended in 9mL of 10mM Tris, 50mM EDTA. The dissolved DNA was then moved to tubes

suitable for an SS34 rotor and 4.5mL of 7.5M KOAc was added. The solution was then placed at -80°C for 15 minutes and then thawed without mixing. The thawed solution was then centrifuged in an SS34 rotor at 3000rpm for 10minutes at 4°C. The supernatants were then pooled and divided into 9mL in SS34 tubes. To each tube, 22.5mL of EtOH was added and centrifuged at 10000rpm in an SS34 rotor at 4°C for 30 minutes. Pellets were dried for 5 minutes and resuspended in 4mL total (to pools samples) of 50mM Tris, 50mM EDTA. 2mL of Tris saturated phenol was added and incubated for 3 minutes at ambient temperature. 2mL of $CHCl_3$ was then added, mixed and centrifuged for 5 minutes at 5175rpm on a SH-3000 rotor. O.1 volume of 3M NaOAc to the aqueous layer followed by 2.5 volumes of EtOH and incubated overnight at -20°. The DNA was then centrifuged for 10 minutes at 5175rpm at 4°C on an SH-3000 rotor. The pellet was then resuspended in 50mM Tris, 25mM EDTA. CsCl was then added (1.1g of CsCl per g of DNA suspension yielding 1.6g/mL final density) and 2mg/mL ethidium bromide. This was centrifuged for 5 minutes at 3000rpm at 20°C on an SH-3000 rotor. The supernatant was taken and completed with 1.6g/mL CsCl and centrifuged for 19 hours at 20°C at 55000g on a Tv-360 rotor. A single DNA band was visible under ultraviolet illumination and was isolated with a 16-gauge needle. Ethidium bromide was extracted 6 times with Tris-EDTA-NaCl saturated butanol until all color was removed. CsCl was removed by dialyzing with a 20kDa molecular weight cutoff membrane. Sample was dialyzed against 10mM Tris, 0.1mM EDTA with 4 changes of buffer at 4°C. Resulting DNA was then used for analysis and injection.

BAC DNA analysis

DNA was characterized and quality determined by "fingerprinting" and pulse field gel electrophoresis. 5uL of DNA were digested with SpeI and bands separated on a 1% agarose Tris-acetate-EDTA linear field gel. The resulting banding pattern was then compared against the predicted banding pattern (fingerprint) using the deposited sequences in the NCBI mouse build 37.1. DNA quality and concentration were determined by digesting with NotI and analyzed using 1% agarose Tris-borate-EDTA pulse field gel (DR2, BioRad). Samples were quantitated against known concentration standards and DNA integrity determined by the lack of degradation products in uncut samples. Founders were screened by PCR using primers 5'-CCTGATGAATGCTCATCCG-3' and 5'-TGGAAGCCATCACAAACG-3' directed against the CAM resistance gene of the BAC vector.

P2 Synaptosomes

Animals were sacrificed by rapid decapitation and brains immediately dissected out and placed on ice. The striatum, hippocampus and cortex were dissected out by hand. For striatum, careful attention was paid to not take basal forebrain (MS-DB) or olfactory tubercle as part of the dissection. This introduces a small bias in the tissue taken to have a greater amount of caudatoputamen (dorsal striatum) as opposed to nucleus accumbens (ventral striatum). Cortex, as dissected, contains the dorsal and lateral (not ventral) aspects of cortex present forward of bregma. Tissue from two animals of the same genotype from the same litter was pooled. Dissected tissue was placed into 5mL ice-cold homogenization buffer

(0.32M Sucrose, 5mM 4-(2-hydroxyethyl)-1-piperazineethanesulfonic acid (HEPES), pH 7.4) and homogenized using a Teflon coated Dounce homogenizer with 10 strokes at 3500 rpm. The homogenate was then centrifuged at 2200rpm at 4°C in an SH-3000 rotor for 10min. The supernatant was then centrifuged at 14000g at 4°C in an SS34 rotor for 10min. The resulting pellet was then resuspended in 1mL of uptake Krebs-Ringer-HEPES (u-KRH, pH 7.4) buffer containing in mM: 130 NaCl, 3 KCl, 2.2 CaCl2, 1.2 $MgSO_4$, 1.2 KH_2PO_4, 10 Glucose, 10 HEPES. Protein was determined by the Bradford method (kit from BioRad). Samples were then diluted to 2mg/mL.

Uptake of [3H]-Choline

Samples were divided into 800μg aliquots (2 for this experiment, remainder used for western blotting) and centrifuged at 3000rpm at 4°C in a sorvall microfuge rotor for 3min. The sample was then resuspended either in u-KRH or stimulation KRH (u-KRH-stim) containing 40mM KCl with an equivalent reduction in NaCl to maintain isoosmolarity. Samples were incubated in a water bath at 37°C for 30 minutes with intermittent shaking. Samples were then centrifuged at 3000rpm at 4°C in a sorvall microfuge rotor for 3min, resuspended in 400μL of u-KRH, recentrifuged at 3000rpm at 4°C in a sorvall microfuge rotor for 3min and again resuspended in 400μL of u-KRH. Uptake was then performed in silicon glass tubes with 100μg of synaptosomes incubated with 100nM [3H]-choline (82.0 Ci/mmol specific activity, Perkin Elmer, Waltham, MA) shaking for 15 minutes at 37°C. Samples were run in triplicate and non-specific binding was determined by parallel

samples containing 1μM HC-3. Synaptosomes were captured and washed 5 times with u-KRH on polyethyleneimine coated glass fiber filters (GF/B, Whatman; Piscataway, NJ) in a Brandel cell harvester (Brandel, Gaithersburg, MD). Filters were dissolved in EcoScint-H (National Diagnostics, Atlanta, GA) and counted in a Packard Bioscience liquid scintillation counter (Perkin Elmer).

Western Blotting

Two types of samples were used, either synaptosomes or whole tissue. Animals were sacrificed and dissected as described for synaptosomes. Whole tissue was minced by hand with razor blades and placed into solubilization buffer (50mM Tris, 250mM NaCl, 0.2% SDS, and 2% Triton X-100, pH 7.8). Synaptosomes were resuspended in solubilization buffer instead of u-KRH. Samples were solubilized overnight at 4°C and cleared by centrifugation at 13000rpm at 4°C in a sorvall microfuge rotor for 30min. Protein in the supernatant was determined by the Bradford method and samples were diluted to 1mg/mL. Samples were prepared for electrophoresis by diluting to 0.5mg/mL with protein sample buffer (78mM Tris, 2.5% SDS, 900mM β-mercaptoethanol, and 25% glycerol at pH 6.8). 5μg samples were run on a 10% acrylamide gel (Nextgel, AMRESCO, Solon, OH) at 150V. Protein was transferred to a polyvinyldifluoride membrane overnight at 150mA. Blots were washed with phosphate buffered saline (PBS) containing 0.2% Tween-20 (PBS-T). Blocking was done for 1 hour at ambient temperature with 5% nonfat dry milk (Carnation) in PBS-T. Blots were then incubated in primary antibody diluted in blocking buffer overnight at 4°C (rabbit anti-CHT 1:2000, (Ferguson, 2003); rabbit

anti-synaptophysin 1:10000, Millipore; and mouse anti-GAPDH, Millipore). Blots were washed 4 times for 7 minutes in PBS-T, incubated in species-appropriate HRP conjugated secondary antibodies raised in goat (1:5000, Jackson ImmunoResearch, West Grove, PA) washed 4 times for 7 minutes in PBS-T and placed into PBS. Blots were developed with Western Lightning reagent (Perkin Elmer) exposed to Hyperfilm ECL (GE Healthcare, Piscataway, NJ).

Immunofluorescence

Animals were anesthetized with 10mg of pentobarbital and transcardially perfused with 4% paraformaldehyde in PBS. Brains were dissected and post fixed for at least 24 hours in 4% paraformaldehyde in PBS. The brains were cryoprotected by overnight incubation at 4°C in 20% sucrose. 40μm slices were taken using a freezing microtome and organized so that every 12th section was stained for a given protocol. Slices were stored at -20°C in cryoprotectant (30% glycerol, 30% ethylene glycol in 0.1M sodium phosphate pH=7.4) until use. Slices were washed with phosphate buffered saline (PBS) containing 0.2% Triton X-100 (PBS-X). Blocking was done for 1 hour at ambient temperature with 3% normal donkey serum (Jackson ImmunoResearch, West Grove, PA) in PBS-X. Sections were then incubated in primary antibody diluted in blocking buffer overnight at 4°C (rabbit anti-CHT 1:500 (Ferguson, 2003) and goat anti-ChAT 1:500, Millipore). Sections were washed 4 times for 7 minutes in PBS-X, incubated in species appropriate fluorescent label conjugated secondary antibodies raised in goat (1:250, Jackson ImmunoResearch) and diluted in blocking buffer, washed 4 times for 7

minutes in PBS-X and placed mounted on Superfrost slides (Fisher, Pittsburgh, PA) and coverslipped with Aqua Polymount (Polysciences, Inc, Warrington, PA) or Vectashield (Vector Labs, Burlingame, CA). Imaging was done either using a Zeiss LSM Meta 510 laser scanning confocal microscope.

Immunohistochemistry

Tissue was prepared, sliced, and stored as for immunofluorescence. Section were stained using the ABC kit (Vector Labs) using manufacturers instructions with minor modifications. Slices were preincubated with 3% H_2O_2 to quench endogenous peroxidase activity then washed with PBS. Blocking was done for 1 hour at ambient temperature with horse serum at half recommended concentration in PBS-X. Sections were then incubated in primary antibody diluted in blocking buffer overnight at 4°C (rabbit anti-CHT 1:500 (Ferguson, 2003). Sections were washed 4 times for 7 minutes in PBS-X, incubated in biotin labeled universal secondary antibody diluted in PBS-X, then washed 4 times for 7 minutes in PBS-X. Avidin-HRP was incubated on the sections for 30 minutes and color developed with 0.2mg/mL diaminobenzidene in 0.03% H_2O_2 until color was suitably developed by visual observation (usually about 7 minutes, the extended development was for 20 minutes). Tissue was placed mounted on Superfrost slides dried, dehydrated through graded EtOH (2 minutes each, 50%, 70%, 95%, and 2x100%) and xylenes (2 times for 10 minutes) and coverslipped with Permount (Fisher). Imaging was done using a Zeiss Axiophot upright microscope.

Y-maze

A single cohort of male mice was used for Y-maze, elevated plus maze, and the Crawley task (in this order). Mice were between 11 weeks and 12 weeks old during the Y-maze test. Each mouse was tested twice in the Y-maze separated by 1 week, although all analysis was done only on the first trial. For the experiment, the mouse was placed in the middle of a 3-armed maze with 30cm x 5cm arms radiating from the center spaced by equal angles. Walls were 10cm high and made of clear Plexiglas with a clear Plexiglas top. The maze was divided into the three arms and the mouse considered to have changed arms only when it made a complete, four pawed, entry into a different arm. Each trial lasted 7 minutes as was scored by a blind observer watching by live video feed in the next room. The maze was washed with 70% EtOH between trials.

Elevated plus maze (EPM)

Mice were between 12 weeks and 13 weeks old during the EPM test. For the experiment, the mouse was placed in the middle of a 4-armed maze radiating from the center in the shape of a plus symbol (+). Opposite arms were the same and either without walls or with black plastic walls 15 cm high. The maze was 40cm elevated from the floor. Each arm was 30cm long and 5cm wide. The maze was divided into the 5 zones (each arm and the center) and the mouse considered to be in an arm zone only when it had all four paws in the arm, otherwise it was considered to be in the center. Data was analyzed as the time spent in the open arms relative to time spent in any arm. Each trial lasted 7 minutes and was scored

by the ANYmaze software (Stoelting, Wood Dale, IL) and corrected as necessary by a blind observer. The maze was washed with 70% EtOH between trials.

Crawley task

Prior to the experiment, 2 stimulus mice were placed in pencil cups in the outer chambers of the maze 3 times for 10 minutes separated by 10 minutes to acclimate them to the chamber and handling. Mice were between 13 weeks and 15 weeks old during the Crawley task. For the experiment, the mouse was placed in the middle of a 3 chamber box and the experiment conduct largely as described in Nadler et al. (Nadler, 2004). The box was 40cm wide and 50cm long divided into 3 equal chambers along the long axis with both internal walls and external walls 30cm high. In the center of the internal walls was a gap 10cm wide with a removable wall that could serve as a door. Each chamber was its own zone and the mouse considered to be in a zone based on the position of the center of its body. Data was analyzed by the time spent in each zone. The experiment was divided into 3 phases. During the first phase, the mouse was allowed to explore the box with the doors open for 10 minutes with no pencil cups. The mouse was then placed in the middle chamber with the doors shut while the initial stimulus mouse and an empty pencil cup were placed in the outer chambers. Pencil cups were placed to the side of the chamber equidistant to 3 walls. Cups were always on the same side of the maze but which side and which cup contained the mouse were randomized. The doors were lifted and the mouse allowed to explore for 10 minutes. The mouse was then returned to the center chamber and the other stimulus mouse was placed under the

previously empty pencil cup. To prevent the test mouse from climbing on top of the pencil cups, styrofoam cups filled with water were placed on top. The pencil cups in the outer chamber were placed off to one side equidistant from 3 walls. Location of the stimuli (social, novel mouse) was varied pseudorandomly as was which mouse was the novel mouse. The experiment was analyzed with the ANYmaze software and corrected as necessary by a blind observer. The chamber was washed with 70% EtOH between trials and the pencil cups were washed with MB-10 for 3 minutes and thoroughly dried. The inanimate object pencil cup never contained a mouse.

Results

Generation of BAC-CHT mouse

To generate the BAC-CHT mouse, we selected a construct (RP24-290K23) that contains 45kb upstream and 90kb downstream of the mCHT genomic locus (Figure 21A). This construct was selected over another construct (RP24-267H21) due to a possible gene copy of ARMCX3 present 50kb upstream of CHT. As we used the entire, circular, BAC construct for generation of the mice, we were able to screen founders using PCR directed against bacterial sequences. For this we used the CmR gene and identified 2 founder animals out of 16 screened although 1 of the founders died before it could be bred (Figure 21B, data not shown). Unlike the Hb9:CHT mice, validation of overexpression in the BAC-CHT is possible due the higher central

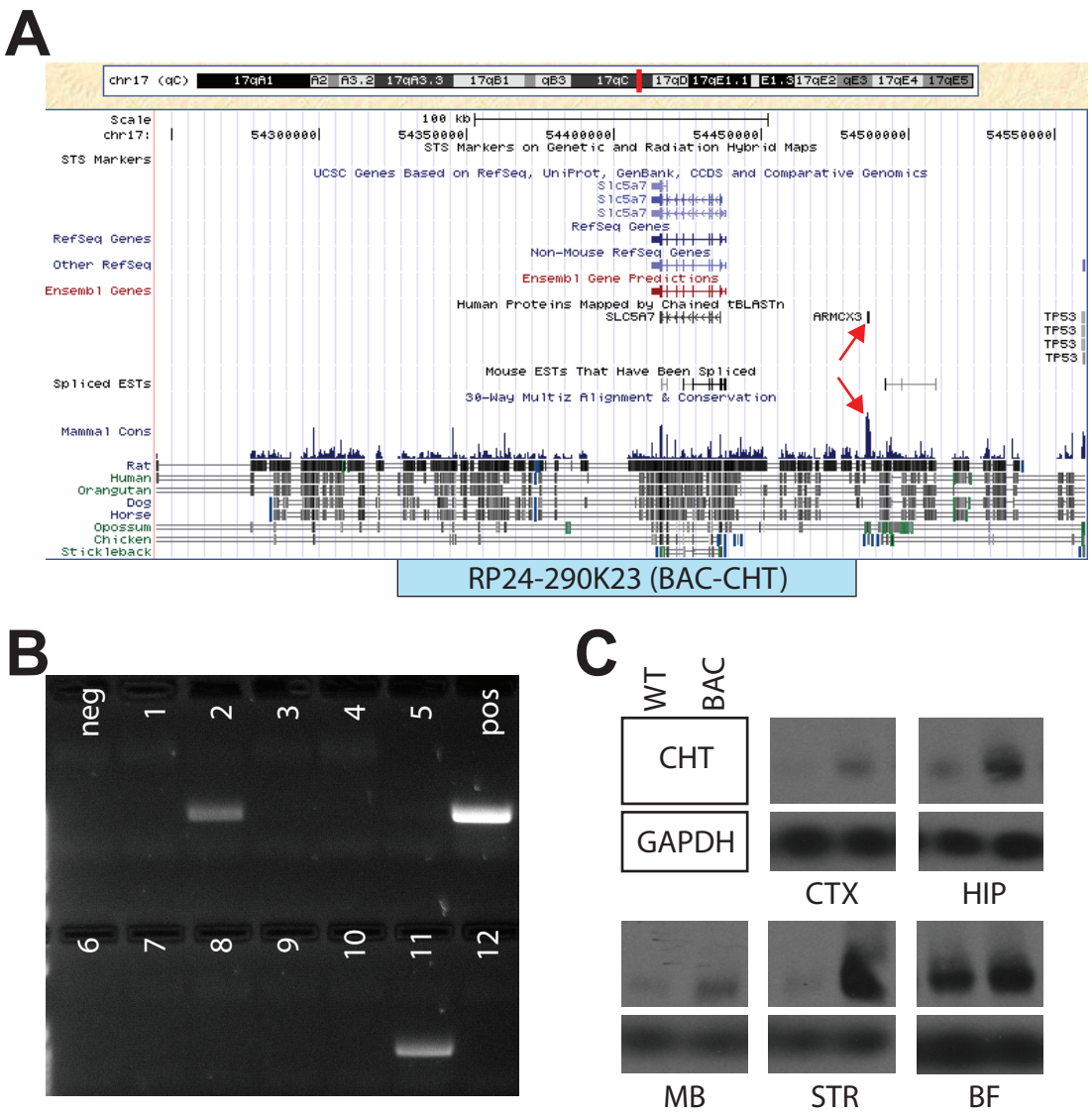

Figure 21. Generation of the BAC-CHT mouse. (A) Screen capture from the University of California at Santa Cruz genome browser of the genomic region of CHT. The region covered by the BAC clone is indicated underneath. Red arrows indicate the possible conflicting gene upstream from CHT (CHT is on the minus strand). Note particularly that the region has a high degree of mammalian conservation. (B) Agarose gel of screening PCR for BAC-CHT founders. Founder number 2 died prior to being received in the lab and therefore founder number 11 provided the only established line. (C) Western blots of extracts from different brain regions establish a large diversity of overexpression (CTX, frontal cortex; HIP, hippocampus; MB, midbrain; STR, striatum; BF, basal forebrain). All brain regions have elevated CHT although there is considerable variability in the degree of overexpression.

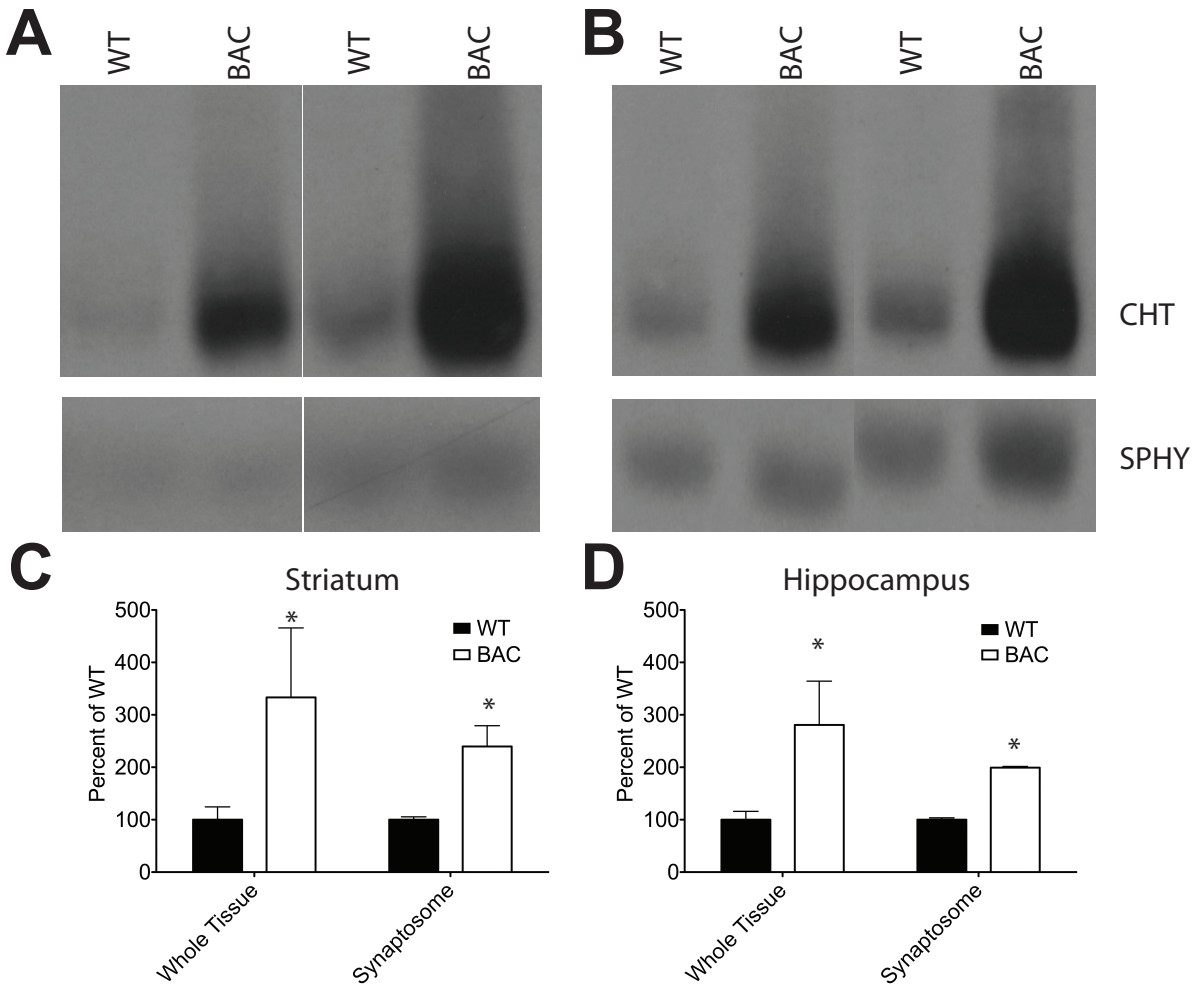

Figure 22. Quantification and localization of overexpression of BAC-CHT mice. (A) and (B) Representative western blots of either whole extract or synaptosomes from the striatum (A) or hippocampus (B) of BAC-CHT mice show strong elevation of CHT. Synaptophysin is used as a loading control. (C) and (D) quantification of n=3 for each group showing the amount of elevation (2-way ANOVA (genotype x preparation), P(genotype)=0.0292 (striatum) and P(genotype)=0.0302 (hippocampus), all post hoc comparisons P>0.05 by Bonferroni posttest). *P<0.05

nervous system localization of expression. Elevated levels of CHT were observed in all brain regions examined (Figure 21C), and could be localized to synapses based on the elevation seen in synaptosomes (Figure 22). To control for the amount of protein loaded, blots were probed for synaptophysin or GAPDH and neither showed elevation.

Characterization of elevated CHT levels

To better assess the localization of CHT, we used immunohistochemical and immunofluorescent techniques. The difference in expression levels was large enough that it was difficult to treat tissue similarly and directly observe differences. When using imunohistochemical techniques, a standard procedure revealed clear cell bodies (striatum) and terminals (cortex) in the BAC-CHT mice (Figure 23A-C). Using the same procedure revealed only faint cell bodies in the WT (Figure 23D). In the medial habenula, increasing the incubation times in the WT (compare Figure 23E to 23F) could darken the staining and reveal some cell bodies, but still not to the level of the BAC-CHT (Figure 23G). Similarly, using immunofluorescence, it was necessary to increase the detector gain to achieve CHT labeling intensity near the level of BAC-CHT in all areas with the representative of the hippocampus presented (Figure 24, compare B, BAC and C, WT which are taken at different detector gains).

No change in basal and stimulated HACU in BAC-CHT mice

Despite the strong elevation of protein levels observed in BAC-CHT mice, no basal change in uptake values has yet been observed (Figure 25). As CHT is present

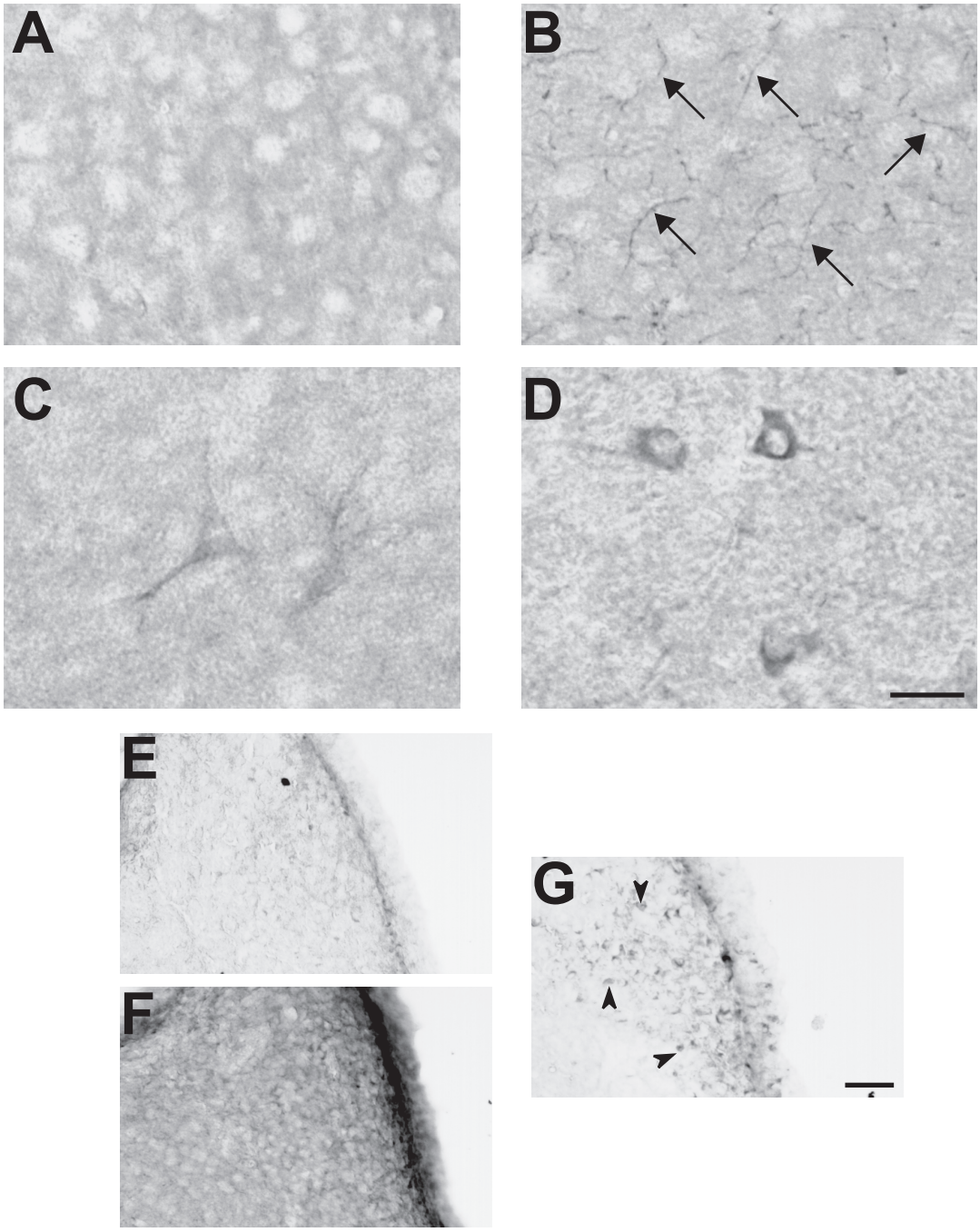

Figure 23. BAC-CHT produces increased density of CHT in soma and synapses. In motor cortex (A) and (B), and striatum (C) and (D), CHT appears higher in BAC-CHT (B and D) over WT (A and C), particularly in the cortex where CHT positive fibers (representatives shown by arrows) are not visible at all in the WT (A). In the medial habenula, CHT positive cell bodies (representatives shown by arrowheads) are readily apparent in BAC-CHT (G) but are faint in WT (E) even if the adjacent WT section is nearly 3-fold over developed (F). Scale bars are 50μm.

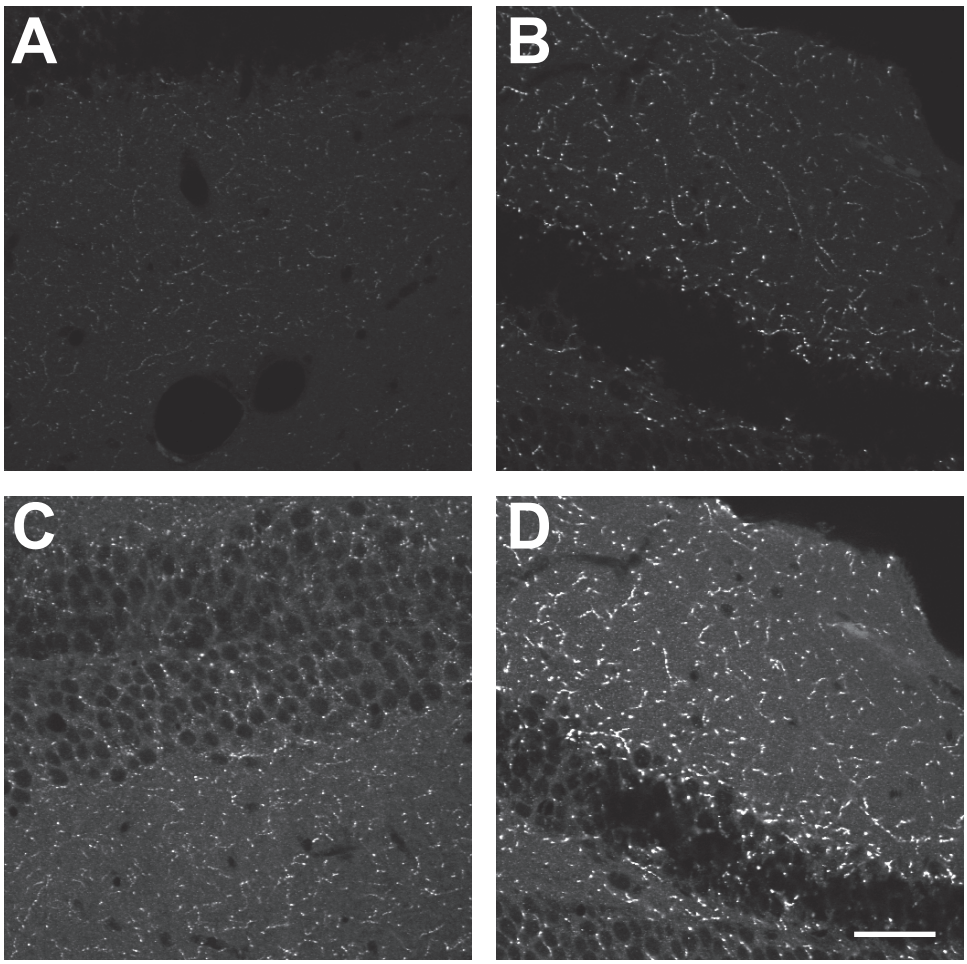

Figure 24. BAC-CHT elevates levels of CHT in the hippocampus. When imaging conditions are optimized to visualize CHT in the BAC-CHT mouse (A and B), cholinergic fibers are barely visible in the WT (A). Conversely, optimization of imaging for WT (C and D), results in several points of saturation in the BAC-CHT mouse. Scale bars are 20μm.

mainly on synaptic vesicles, I hypothesized that elevated uptake might only be observable under conditions that drive CHT to the plasma membrane. Under basal uptake conditions, BAC-CHT uptake was equivalent to WT in both the hippocampus (WT 0.121 +/- 0.030 pmol/mg/min; BAC-CHT 0.138 +/- 0.047 pmol/mg/min, P>0.10 two-way repeated-measures ANOVA) and cortex (WT 0.099 +/- 0.022 pmol/mg/min; BAC-CHT 0.144 +/- 0.033 pmol/mg/min, P>0.10 two-way repeated-measures ANOVA). Pretreatment of synaptosomes with elevated KCl stimulated synaptic vesicle release and increased transport activity both genotypes (Hippocampus P=0.0042, Cortex P=0.0093). However, no interaction effect was observed (P>0.10 two-way repeated-measures ANOVA, genotype x stimulation interaction) indicating that the level of stimulation is not different between genotypes. The possibilty of differences in HACU elicicted by stimulation was further tested by directly comparing fold stimulation for each genotype. The BAC-CHT mice did not show a greater amount of transport stimulation compared to WT mice (Hippocampus: 218.4% +/- 25.37%; BAC-CHT 258.2% +/- 30.42%, P>0.10 Student's t-test, Cortex: WT 194.4% +/- 3.3%; BAC-CHT 202.5% +/- 14.1%, P>0.10 Student's t-test).

Effect of elevated CHT on cholinergically mediated behaviors

Despite the lack of observed change in uptake, the function of CHT in regulating vesicle pools lead us to test cholinergically mediated behaviors. The most straightforward experiment is the Y-maze test of spatial working memory, which

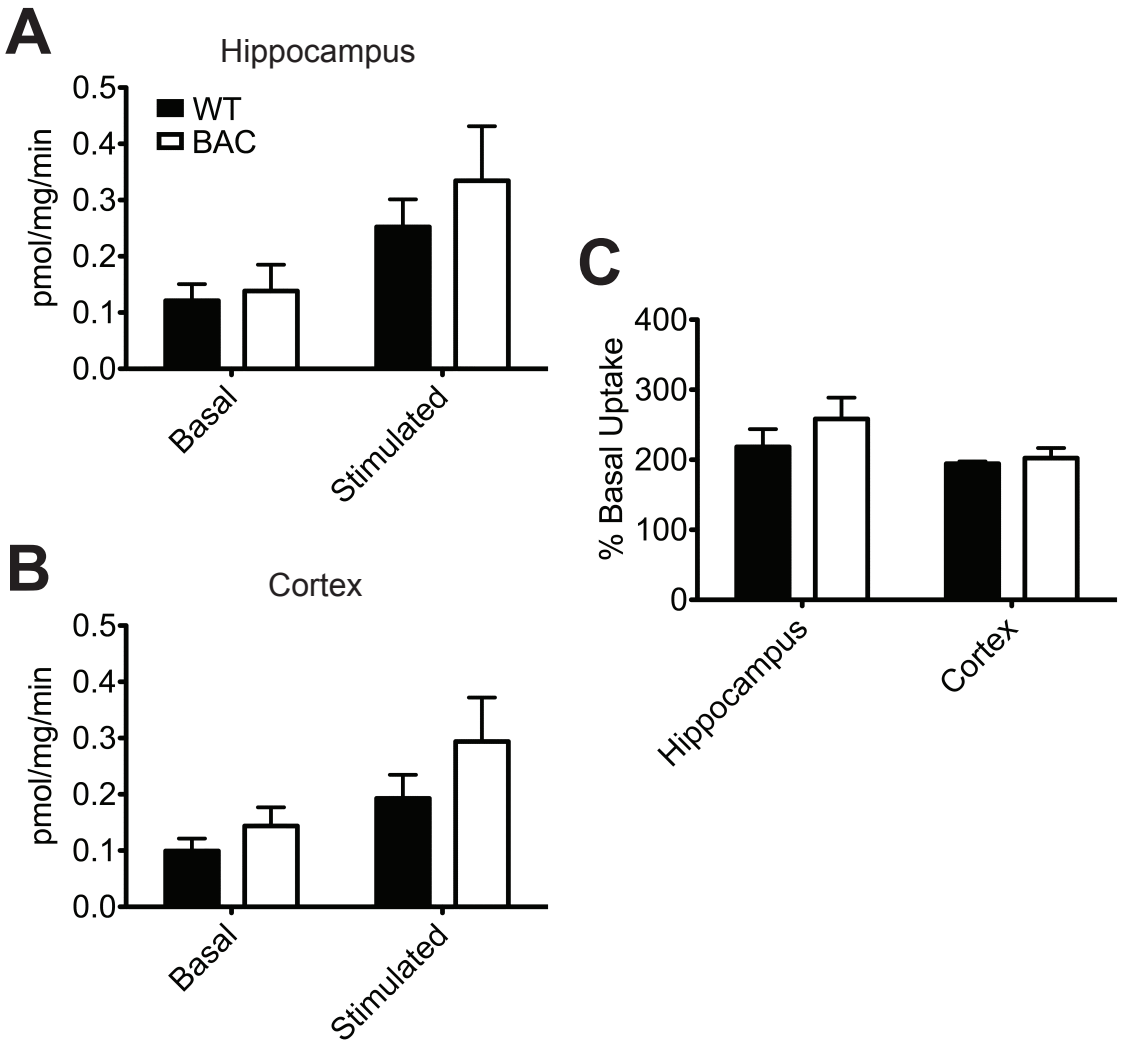

Figure 25. HACU is not elevated in BAC-CHT mice. (A) and (B) Uptake of [3H]-choline is not altered by the BAC in either the hippocampus (A) or cortex (B) under either basal or stimulated conditions (P>0.05, 2-way ANOVA). (C) The degree of stimulation was also not different between genotypes in either location tested (n=3 for all samples, P>0.05, Student's t-test).

measures the spontaeous alternation behavior (SAB) of the mouse. SAB has long been established to be sensitive to pharmacological manipulation of cholinergic pathways, particulary by the use of antagonists to mAChRs such as scopolamine (Squire, 1969). Previous studies have used SAB to study potential cognitive enhancers (Spowart-Manning and van der Staay, 2004) suggesting that the Y-maze is potentially useful approach to examine improvements in memory in th BAC-CHT mice. BAC-CHT mice had a small but significant reduction in spontaneous alternation (WT: 71.1% +/- 3.0%, BAC-CHT: 63.2% +/- 2.2%, *P*=0.0409 Student's t-test) (Figure 26A). The total number of alternations was not different between genotypes (WT: 29.8 +/- 1.4%, BAC-CHT: 25.5 +/- 1.7, *P*=0.0905 Student's t-test) (Figure 26B).

Anxiety is a behavior with a known cholinergic component and is particularly relevant as anxiety is modulated by the use of nicotine, although the effects are complex (Picciotto, 2002). Altered anxiety-like behaviors have been observed with cholonergic manipulations in mice, such as an increase in open-arm time in the elevated plus maze (EPM) measure of anxiety in β3 nAChR knockout mice (Booker, 2007). Anxiety-like traits were measured using the EPM. BAC-CHT mice spent a significantly lower amount of time in the open arms relative to the open arms (WT: 42.5% +/- 5.4%, BAC-CHT: 30.0% +/- 3.1%, *P*=0.0399 Student's t-test) (Figure 27B). As with the Y-maze, an internal locomotor control did not show any differences between genotype indicating that the phenotype is not an artifact of general locomotor activity (Figure 27C).

Although many behaviors are clearly cholinergic based on the pharmacology, several of these behaviors have been resistant to change with genetic manipulations. However, a deficit in social memory has been observed with reductions in cholinergic function established in mice with reduced VAChT expression (Prado, 2006), and therefore, the Crawley task for sociability and social memory was performed. In the first experimental phase, the preference of the mouse for a social versus a non-social stimulus is tested (Figure 28A). There was no genotype effect detected (2-way ANOVA, genotype effect $P>0.1$), although this may be a deficit in some portion of the experimental setup as there was no preference for the social stimulus in the WT mice (2-way ANOVA, chamber effect $P<0.0001$, Bonferroni post-test, WT social versus WT non-social $P>0.05$). For both genotypes, a preference for the stimuli over the center, no stimulus chamber, was observed (two-way ANOVA, Bonferroni post-test, all comparisons versus center $P<0.001$).

A similar lack of WT effect was also observed in the second phase of the experiment, which tests the preference of a mouse for a novel social stimulus compared to a social stimulus that the mouse has already been exposed to (2-way ANOVA, chamber effect $P<0.0001$, Bonferroni post-test, WT novel social versus WT previous social $P>0.05$) (Figure 28B). However, there was an effect observed only in the BAC-CHT mice of a preference for the social stimulus (two-way ANOVA, chamber effect $P<0.0001$, Bonferroni post-test, BAC-CHT social versus WT non-social $P<0.01$). Again, there was a strong preference for stimuli over the center (two-way ANOVA, Bonferroni post-test, BAC previous social versus center $P<0.01$, all other comparisons versus center $P<0.001$).

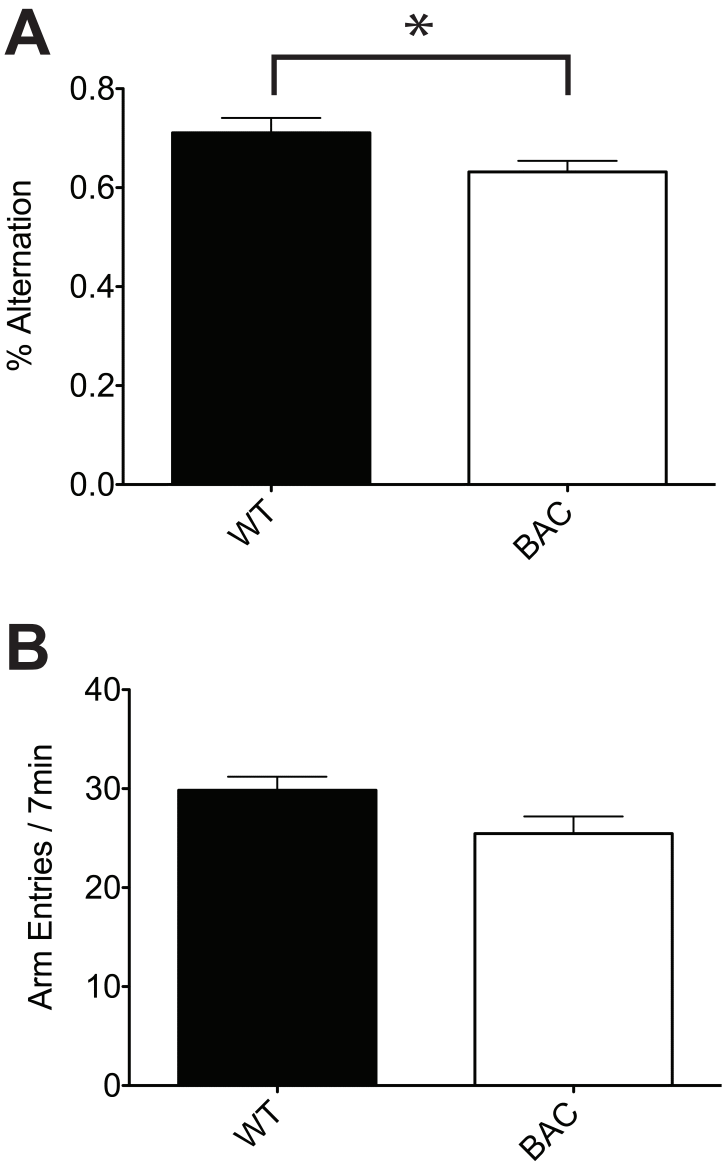

Figure 26. BAC-CHT mice have a mild impairment in spatial working memory. (A) Comparison of WT and BAC-CHT mice shows a reduction in the percent alternation while travelling in the Y-maze. (B) No difference in the total number of alternations was observed. (WT n=12, BAC n=20, **P*<0.05).

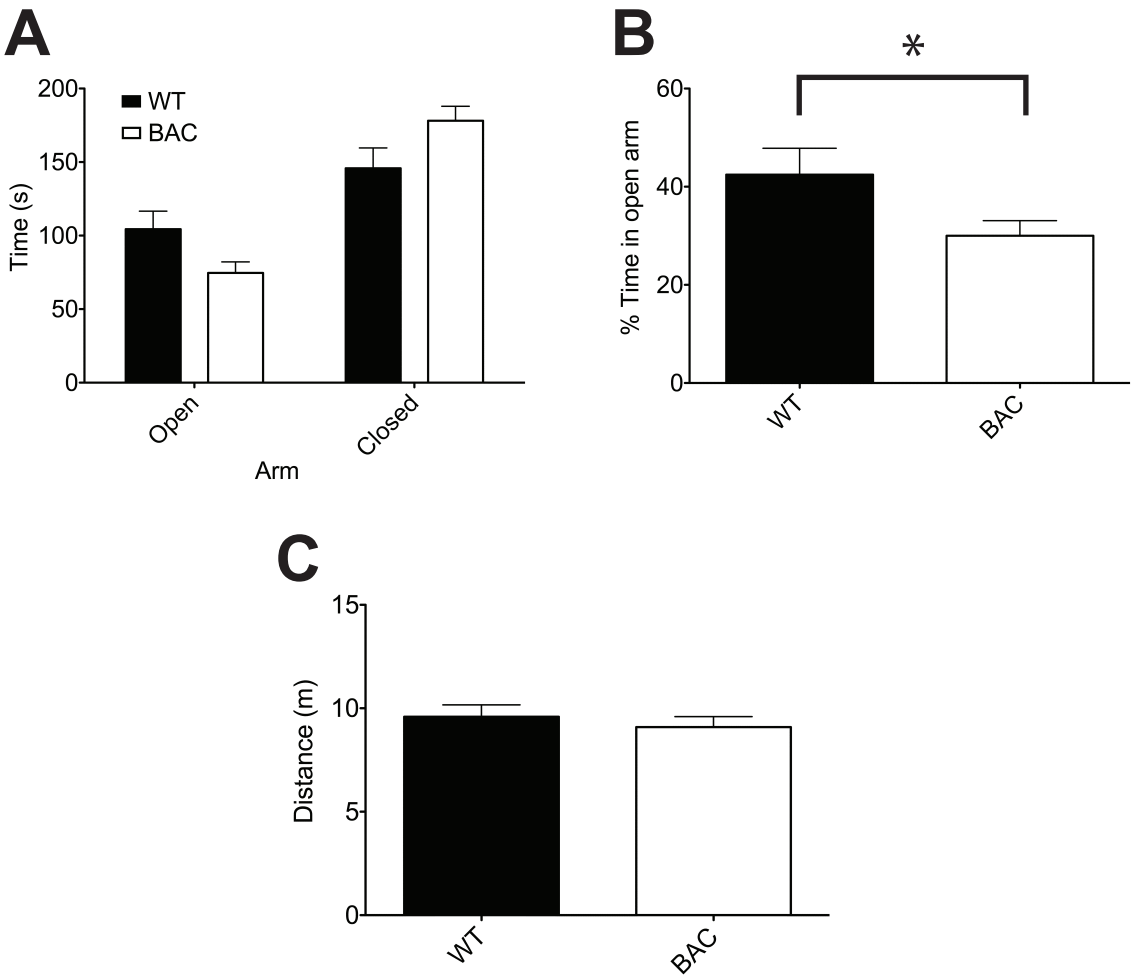

Figure 27. BAC-CHT mice have increased anxiety-like behaviors. (A) Absolute time spent in each arm showing the allocation of arm time that results in reduced open arm time. (B) The percent time in the open arm was reduced in the BAC-CHT mice. (C) Total distance traveled was not different between mice. (WT n=16, BAC n=21, *P<0.05).

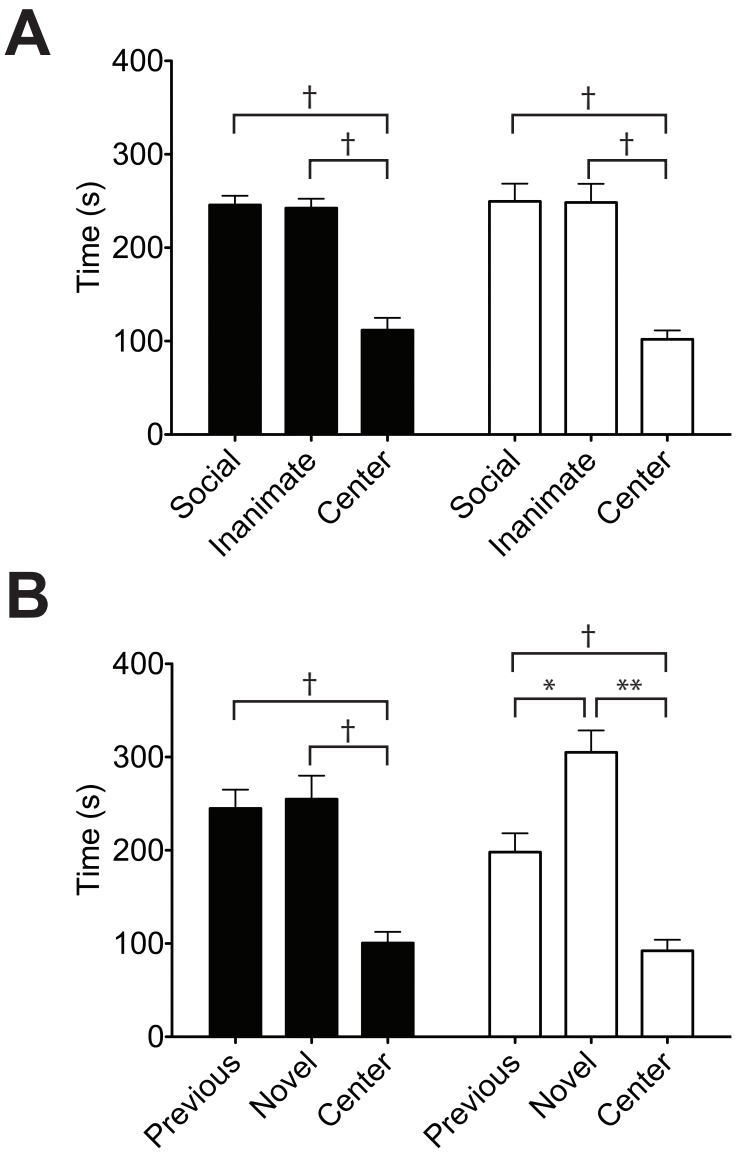

Figure 28. BAC-CHT mouse may have elevated social memory. (A) Test of mouse preference for a social stimulus revealed no effect in either WT or BAC-CHT mouse although both prefer a stimulus to the empty center chamber (2-way ANVOA, †,P<0.001 Bonferroni posttest). (B) While the WT mice did not prefer the novel social stimulus, the BAC-CHT mouse had a preference for the novel social stimulus over a previously experienced mouse (WT n=15, BAC n=18, 2-way ANVOA, *P<0.05, **P<0.01, †P<0.001 Bonferroni post-test).

Discussion

Use of BAC transgenic mice to study overexpression

Use of the BAC approach for induced overexpression has been successful in several contexts. Similar to the strategy I employed for CHT, overexpression of the dopamine transporter (DAT), a presynaptic neurotransmitter transporter similar to CHT, resulted in increased dopamine transport and amphetamine-induced behaviors (Salahpour, 2008). In several cases, overexpression has been attempted to show that the normal function of a protein may be part of the etiology of a given disease, such as the role of the α1G T-type calcium channel in pure absence epilepsy (Ernst, 2009) or of tau protein in Alzheimer's disease (Adams, 2009). Others have used the BAC overexpression approach to introduce possible pathogenic mutations in mice, although this is difficult due to the altered expression levels unless the mutation is autosomal dominant (Li, 2010). Potential therapeutic targets have been tested, including for Alzheimer's disease where ABCA1 (ATP binding cassete transporter, sub-family A, member 1), a protein involved in apolipoprotein E regulation, was overexpressed to test for a reduction in amyloid burden. However, despite the increase in ABCA1 protein on a wild-type background, no increase was observed in an Alzheimer's disease model (APP/PS1) and consequently, no therapeutic effect (Hirsch-Reinshagen, 2007).

Relationship between elevated protein and lack of change in HACU

These initial experiments with the BAC-CHT mouse have established the possibility of this mouse for understanding the role of CHT in cholinergic function. Possessing strongly elevated CHT in all cholinergic systems (far above the Hb9:CHT mouse), we will be able to test hypotheses related the cellular function of CHT as well as the ability of CHT to facilitate cholinergic signaling. This chapter presented some of the initial characterization of overexpression, as well as transport activity and behavior. Although the biochemical data do not lead to simple interpretations, they do lend support to the idea that CHT has a role in synaptic vesicle cycling in addition to transporting choline across the plasma membrane. Specifically, the lack of change in HACU despite a large increase in CHT protein suggests a function for CHT beyond choline uptake. Given the ACh release data from the CHT+/- mice, the most likely hypothesis explaining the disrepency between CHT protein and HACU is that CHT modulates vesicle cycling.

After establishing a founder line, initial experiments focused on determining the localization and amount of increased CHT. It is clear from the immunostaining and immunohistochemistry experiments that CHT density is far greater in all brain regions examined. More quantifiable western blotting showed similar results in striatum and hippocampus with an approximately 3-fold increase in CHT, although basal forebrain overexpression did not appear as great, possibly due to a higher density of cholinergic somata relative to cholinergic terminals. Remaining to be tested is the subsynaptic localization of this change. As CHT resides predominantly on synaptic vesicles, and this proportion is regulated by activity of the neuron, it is

entirely plausible that all of the excess CHT resides on the plasma membrane, synaptic vesicle, or other membrane cycling organelle.

The lack of data regarding the subsynaptic localization of excess CHT provides one possible hypothesis for why no increase in transport activity was observed. Furthermore, no additional elevation of transport activity over CHT+/+ mice was observed despite strong stimulation of HACU in cortex and hippocampus. Biochemical experiments using subcellular fractionation to separate synaptic membranes and organelles will identify the location of the excess CHT (Ferguson, 2003). If excess CHT is present anywhere except the plasma membrane, then it will not be detected in a transport assay. The initial hypothesis was that it resided on synaptic vesicles and could be driven to the surface by synaptic stimulation. However, CHT may be present on endosomes or other intracellular vesicles. If CHT is present on intacellular vesicles other than synaptic vesicles, it will be trafficked to the plasma membrane more slowly and by different mechanisms than synaptic stimulation. [3H]-HC-3 binding or synaptosomal surface biotinylation experiments will help address which of these hypotheses is correct.

Several possibilities exist for why an increase in CHT protein does not immediately cause an increase in detectable transport activity. First, the amount of CHT that is transport competent at the plasma membrane could be regulated. This type of regulation has been observed in other presynaptic neurotransmitter transporters (Zhu, 2005; Steiner, 2008), although it has not been directly examined for CHT. Therefore, increased CHT may be present on the plasma membrane although it cannot transport choline. Regulation of the choline transport

competence of individual CHT molecules may occur because the excess CHT is unable to be activated by a limited supply of activating facotrs. Although very few proteins that bind to CHT have been identified (Xie and Guo, 2004), one intriguing possibility for regulating CHT is APP (Wang, 2007). Because of the degradation of cholinergic neurons, but with an increase in HACU, observed in Alzheimer's Disease (Bissette, 1996), drugs that could activate CHT might act by altering interactions with APP.

A second hypothesis is that the excess CHT is present on organelles that are not releasable under the experimental conditions. These organelles might be endosomes, endocytic vesicles, or even synaptic vesicles that belong to the reserve pool and are not releasable with intense stimulation (Gaffield and Betz, 2007), such as KCl induced depolarization. Subcellular fractionation and immunolabeled electron microscopy experiments will be able to show which specific organelles contain CHT as well as the proportion of CHT at the surface (Ferguson, 2003; Holmstrand, 2010). Given that the immunofluorescence and immunoblotting experiments showed localization of overexpression of CHT at synapses, it is unlikely that the excess CHT is unable to leave the soma or resides in a non-traditional organelle.

Either of these possibilities suggest interesting consequences for the way we understand CHT regulation and function. To date, the only demonstrated physiological cause of increased surface CHT is neuronal activity. However, administration of mAChR antagonists or *in vitro* synaptic stimulation with elevated KCl can also increase [3H]-HC-3 binding (Lowenstein and Coyle, 1986; Saltarelli,

1987). Several studies have shown that the increased transport correlates with an increase in HC-3 binding although this is not conclusive evidence of increased surface expression due to the possibility that HC-3 only binds active CHT molecules (Simon, 1976). However, HC-3 is not membrane permeant and is only capable of binding surface CHT molecules so that it is often interpreted that this increased HC-3 binding is showing elevated surface expression. Therefore, strong regulation of CHT molecules at the surface would be a novel and interesting finding in the BAC-CHT mice, and further experiments will pursue this possibility.

Effects of elevated CHT on behavior in the absence of elevated HACU

Given the complex regulation of CHT, and the results of this regulation on the effects of CHT overexpression, it was difficult to make solid predictions about the effects on behavior. We generated this mouse with the expectation that we would be able to observe behavioral effects associated with increased cholinergic function. However, given the results on expression and transport activity, when these experiments were initiated, the hypotheses had been refined. No basal effect was expected in most tasks, particularly tasks that are simpler for the mouse to perform. However, similar to the CHT+/- mice (Bazalakova, 2006), we did expect to see phenotypes when demanding tasks were performed or challenges were added to basic tasks.

The original concept for this mouse was to mimic the effects of a potential CHT activating therapeutic. Preliminary clinical studies using ACh precursors suggest that strategies, such as CHT activation, that elevate ACh synthesis could be

effective in treating cognitive dysfunction (De Jesus Moreno Moreno, 2003). However, the data presented here regarding CHT function suggest that CHT overexpression and pharmacological activation may have different effects. Elevating the amount of CHT protein should not only increase the amount of CHT that can transport choline, but also the amount of CHT that can send vesicles to the reserve pool, such as hypothesized in Chapter III to explain the bimodal CMAP distribution). Conversely, a CHT activating drug would not likely affect the total amount of protein. Therefore, if it increases the amount of CHT on the surface, it will have to reduce the amount in another pool. Whereas increased CHT expression will not likely affect the stoichiometry of Na^+ and choline in the CHT transport process, there is preliminary evidence that this may be a mechanism for pharmacological CHT activators (Alicia Ruggiero, personal communication).

As the goal of this mouse and of a pharmacological activator is to increase ACh release, it is useful to hypothesize what results would be obtained with the BAC-CHT mice in the release paradigms used in chapter II. Specifically, is there a condition where increased ACh release would be observed? Given the impairment in a simple behavior like spontaneous alternation, one would speculate that basally loaded, Ca^{2+}-mediated release should be reduced. Increased release after stimulation in the presence of Sr^{2+} would be expected, but if there is a basal reduction, it might only return ACh release to CHT+/+ levels. The stimulated labeling condition would offer the best opportunity to observe an increase in ACh release; as both functions of CHT would be expected to increase ACh release in response to greater CHT levels. Increased HACU from more transporters on the

surface, and the specific labeling of a larger reserve SV pool would both point in the direction of increased ACh release. Experiments such as the slice release will also fill a noticeable gap between synaptosome-based approaches and behavior because the slices are a more intact preparation that can more faithfully recaptiulate synaptic functions related to behavior.

CHAPTER V

CONCLUDING REMARKS AND FUTURE DIRECTIONS

The use of CHT overexpression (Hb9:CHT and BAC-CHT) and underexpression (CHT+/-) models demonstrate an important role of CHT in supporting cholinergic signaling. Whereas the previous chapters have focused on narrowly defined and specific functions of CHT, it is important to consider how changes in CHT activity or levels fit into the context of a functioning cholinergic synapse. In particular, I consider the idea that CHT localizes to reserve pool vesicles because it is required for their formation or whether it is a passive rider on otherwise defined vesicles.

Due to the multitude of compensatory changes and functional regulation of proteins involved in ACh release, it is unlikely that genetic or pharmacological manipulations of CHT have only the effects described thus far. This discussion will focus on exploring the model presented in chapter III and how it informs the results obtained from BAC-CHT and CHT+/- mice. Specific consideration will be given to the ways CHT might be altered in either a therapeutic or pathological context either as a primary manipulation or in response to other changes.

LOCALIZATION OF CHT TO THE RESERVE POOL

Weak localization hypothesis: CHT as a free rider

If CHT is found to be a marker for cholinergic reserve pool SV, then it can be there in one of two manners. First, it can be found on vesicles on the reserve pool without affecting the function of the vesicles. Second, it can be a required component of the reserve pool, where a reserve pool vesicle does not get formed if CHT is lacking. Because CHT is found on only a subset of vesicles (Ferguson, 2003), it cannot be the case that CHT is required for general SV formation in the same manner as VAChT.

The first hypothesis, which posits **no function** in the reserve pool for CHT, makes several predictions about several of the experiments in this dissertation. The final release experiment, where [3H]-ACh loading of vesicles was stimulated, should have had one of two outcomes. The most likely would be a deficit in ACh release (as seen), paired with a reduction in the amount of [3H] loaded (not observed). This result would suggest that the deficit in ACh release is due to reduced HACU, and not some other function. The other outcome would be no deficit in release if the stimulation conditions were not enough to result in a change in the amount of transporter choline. At baseline, CHT+/- mice have equal uptake to CHT+/+ mice, which would require stimulation or another intervention to cause a difference in HACU. As the result obtained was a deficit in release with no change in [3H]-ACh content, this experiment argues against the hypothesis that the only function of CHT is HACU.

Two other experiments argue against this hypothesis, although more indirectly. If the sole function of CHT is HACU, and changes in HACU have a direct impact on cholinergic function (e.g. in the absence of compensatory changes), the increases in CHT should enhance ACh-dependant behavior. However, in two clear examples, this was not the case. The BAC-CHT spontaneous alternation task showed a reduction in cholinergic function due to elevated CHT levels. Such reduction in spontaneous alternation are usually interpreted as reductions in cholinergic signaling (). The CMAP analysis of the Hb9:CHT mice similarly produced results at odds with the hypothesis that increased CHT should simply enhance cholinergic function. However, as these are all genetic models and therefore come with several caveats, it is difficult to rule out the potential of compensation for increased cholinergic tone.

Strong localization hypothesis: CHT defines reserve pool vesicles

The second hypothesis is that CHT, in addition to supporting HACU, **defines reserve pool vesicles**. This strong hypothesis does not specify many details. For example, the presence of CHT could recruit other reserve pool proteins to form a reserve pool vesicle or vesicles could be formed at random and assigned to a pool based on the presence of CHT. However, this hypothesis does require that reserve pool vesicles be impaired due to lack of CHT either by their non-existence or conversion into another form of organelle, such as an RRP vesicle.

The data in this dissertation support this latter hypothesis. That CHT has more than one function is immediately evident in the two populations of basal

CMAP amplitude. If overexpression of CHT causes more reserve pool vesicles to form, it should reduce cholinergic function in some circumstances. This was observed in spontaneous alternation of the BAC-CHT mouse. Because overexpression should reduce cholinergic function only in some circumstances, it will be necessary to develop *a priori* predictions for future experiments about the directionality of effect. For example, mAChR antagonists can increase ACh release and would have a dose-dependent shift in action with higher levels of CHT. Specifically, lower doses of scopolamine should be less effective in inducing ACh release due to fewer vesicles being available for release. This hypothesis compares well with the CHT+/- model of cholinergic hypofunction where mice were less behaviorally sensitive to scopolamine (Bazalakova, 2006).

Most convincingly, there is a pool of ACh that is reduced in CHT+/- mice that is only loaded if stimulated beforehand. The strong hypothesis predicts that reserve pool ACh should be reduced because there are fewer reserve pool vesicles. As the stimulation would be expected to load the reserve pool whereas other conditions would not, this specificity argues for an impaired reserve pool capacity in the CHT+/- mice. This hypothesis further predicts that the reduction can occur without changes in HACU. Although HACU was not directly measured, there was no change in the total [3H] in the sample, suggesting that HACU and ACh synthesis was not altered.

Relations between the CHT models, disease states, and therapeutics

Hb9:CHT mice and myasthenic disorders

Use of Hb9:CHT mice showed that elevation of CHT at the neuromuscular junction can facilitate cholinergic function, although multiple effects are possible. An increase in running endurance was observed in these mice as the behavioral readout of cholinergic function. However, the attempt to examine this effect at the physiological level revealed the complex nature of CHT manipulations. In particular, the same genetic change can cause opposite effects on CMAP in different animals.

As discussed in chapter III, compromise of cholinergic transmission at the NMJ is the pathological insult causing myasthenic disorders. Although the most common of these, myasthenia gravis (MG), is an autoimmune disorder with reduced density and function of postsynaptic nAChR, there are presynaptic etiologies as well. Two of these, Lambert-Eaton myasthenic syndrome (LEMS) and congenital myasthenic syndrome with episodic apnea (CMS-EA), cause known deficits in the amount of ACh released. Although it has not been rigorously tested yet, it should be expected that a sufficiently large reduction in the levels of CHT should cause a similar myasthenic deficit and has been demonstrated in mice with reduced VAChT (Prado, 2006).

LEMS, like MG, is an autoimmune disorder, but the target is the voltage gated Ca^2 channel responsible for synaptic vesicle release (Motomura, 1997). Impaired function of the channel causes impaired release of synaptic vesicles upon initial action potentials. However, repetitive nerve stimulation (RNS) results in

progressively elevated intraterminal Ca^{2+} concentration resulting in progressively larger CMAP (Oh, 2007). This increment is not present in unaffected terminals where maximally effective Ca^{2+} concentrations are achieved with the first stimulation. Interestingly, an increment-like effect was seen at baseline in one group of Hb9:CHT mice. As the mechanisms of the CMAP elevation in the Hb9:CHT mice are postulated to be enhancement of neuromuscular coupling (as opposed to downstream from Ca^{2+} channel activation), elevation of CMAP through elevated transport could potentially improve neuromuscular transmission is conditions such as LEMS.

CMS-EA has multiple identified mechanistic etiologies, but is primarily a genetic deficit. Mutations in ChAT are one of the identified and validated causes of the disease (Ohno, 2001; Schara, 2010). Unlike LEMS, we would not expect elevated CHT activity to be therapeutic in these individuals. Whereas CHT is rate-limiting in normal, healthy NMJs, in individuals with CMS-EA due to ChAT mutations, ChAT is rate-limiting. Therefore, elevation of precursor availability would not affect end ACh synthesis and cholinergic function.

BAC-CHT mice and Alzheimer's Disease

As with the Hb9:CHT mice, studies of the BAC-CHT mice (Chapter IV) produced observable effects, but not in the manner predicted by a simple "hypercholinergic" hypothesis. The first indication that the link between elevated CHT and cholinergic function would be complex was that greatly elevated CHT did not result in elevated HACU. An initial behavioral battery (Y-maze, EPM) followed

this trend where the mice appeared to have decreased cholinergic function instead of increased, however, in a more difficult task (social memory), BAC-CHT mice were able to perform where the wild-type could not. Using the model presented in Chapter III, these behavioral results suggest that BAC-CHT mice can fall into a "low-CMAP-like" group (now referred to as high-reserve) or, cholinergic function may be elevated as with the high-CMAP mice (now high-ACh)

There are several possible explanations for the differences between behaviors in the BAC-CHT mice as being hypo- or hypercholinergic. First, as each of these behaviors engages different neural pathways (Lalonde, 2002; Singewald, 2007), the synapses involved may be high-reserve or high-ACh depending on the brain region similar to differences in the increase in surface CHT in response to scopolamine (Lowenstein and Coyle, 1986). Second, as this was the same cohort of mice, it is possible that age became a factor. Cholinergic tone is known to decrease with age, and it is plausible that the elevated CHT cannot compensate until the system has been compromised enough. This hypothesis is particularly attractive in that it explains the lack of WT effect in the social task and suggests that CHT is a viable target for diseases associated with age such as Alzheimer's. Experiments tracking the same memory task during aging, or using the BAC-CHT mouse on an Alzhemeir's Disease mouse model, would help understand the assocation between elevated CHT and aging. Third, the complexity of the task may play a role in determining whether the phenotype of the BAC-CHT mice for a given behavior is hypo- or hypercholinergic. If central terminals have a strong propensity to become high-reserve after addition of CHT, then I would predict that BAC-CHT mice

performing demanding tasks would appear to be hypercholinergic, whereas with simple tasks, the BAC-CHT mice would look hypocholinergic. There is no *a priori* reason to think that the tasks chosen here fall into one group or the other, but other tasks can be chosen or manipulated to achieve these goals.

Part of the rationale of making this mouse was to show the possibilities that would exist for a small molecule activator of CHT. However, it is important to note the differences between the two to highlight both likely discrepancies between the genetic model and a drug as well as potential advantages of the genetic model. Whereas a small molecule activator would be expected to solely increase transport, it would not be expected to have any influence on the vesicle pool trafficking mediated by CHT. Therefore, the small molecule would behave exclusively like the high-ACh group. This increase in cholinergic tone would likely be beneficial on its own, but would also augment the brains own compensatory increase in CHT activity (Slotkin, 1994) and may address part of the underlying pathology (Ehrenstein, 1997). Although this procholinergic expectation is useful clinically, genetic overexpression has a greater utility for understanding the complete biological functions of CHT. As the work in this dissertation and previous work illustrate, CHT likely has a role or roles at the synapse beyond choline transport.

CHT+/- mice and genetic deficiencies of CHT

The CHT+/- mice were used to show the impact of CHT on ACh release and provide initial experimental evidence for the nature of the linkage between CHT function (both transport and trafficking) and ACh release. The ACh release

experiments demonstrated that CHT supports release from a mechanism engaged only after stimulation. This mechanism is likely the reserve pool of vesicles that is only released and refilled after strong stimulation. Given the role cholinergic deficits play in many pathological conditions, it is tempting to use the CHT+/- mice as a model of one or more of these diseases. However, due to the subtle nature of the phenotypes identified thus far, it is unlikely that this current mouse would be useful as a disease model (Bazalakova, 2006). This models most immediate utility in examining human conditions is to known human coding variations in CHT. One such mutation, I89V, results in a 50% loss of transport activity and thus could be well modeled by CHT+/- mice (Okuda, 2002). To date, there has been very little phenotypical characterization of I89V, limited to associations in depression and ADHD (Hahn, 2008; English, 2009). Further work characterizing parallel phenotypes in I89V carriers and CHT+/- mice would advance our understanding greatly.

Further analysis of CHT in cholinergic systems

Future study of the effect of CHT on the physiology of cholinergic synapses

Use of the mouse models presented in this dissertation will provide great insights into the regulation of CHT as a transporter and the role of CHT in vesicle trafficking. The subsynaptic localization of extra (BAC-CHT) or missing (CHT+/-) CHT at the synapse has not yet been studied, but is important to understanding how HACU is elevated in response to stimulation as well as how CHT follows or

determines vesicle identity. Although both models have clear phenotypes, neither is matched by changes in measured HACU suggesting strict regulation of the amount or activity of CHT at the plasma membrane. Treatments that alter these properties (neuronal activity, inhibition of endocytosis, etc.) may reveal differences that have thus far been elusive, particularly changes in HACU in the appropriate direction.

Although the current hypothesis of CHT includes its function in determining reserve pool vesicles, this idea has yet to be directly tested. The closest measurement thus far is the ACh release experiments presented in chapter II. However, both relied on indirect methods of accessing the reserve pool and will benefit from a more straightforward approach. More direct approaches will require the use of optical and electrophysiological tools that allow reserve pool kinetics to be directly measured. In particular, with the collaboration of Dr. Rita Balice-Gordon, synpatopHlourin (spH) mice (Wyatt and Balice-Gordon, 2008) have already been bred to the Hb9:CHT mice and are also to be established into the BAC-CHT background. SpH is a pH-sensitive GFP fused to VAMP in the synaptic vesicle lumen. When exposed to the extracellular space (pH=7.4), spH fluoresces, but when in the synaptic vesicle (pH=5), its fluorescence is quenched. As a vesicular measure of release at cholinergic synapses, spH fluorescence can show alterations in the releasability of vesicle pools more directly than bulk ACh output. Initial experiments that focus on the fraction of vesicles released at different stimulation frequencies will be interesting and lead to more involved stimulation paradigms and other manipulations

Electrophysiology will also be an excellent way to address the questions studied in this dissertation. The model presented in Chapter III makes very specific predictions for the study of mini end plate potentials (mEPPs) at the NMJ. High-CMAP mice should show elevated mEPP amplitude (each vesicle contains more ACh) whereas low-CMAP mice should show reduced mEPP frequency (fewer RRP vesicles available for spontaneous release). CHT-/- mice have no reported changes in either mEPP amplitude or frequency immediately after birth (when ACh levels are equivalent to CHT+/+ mice) but is substantially lower 4 hours after birth when the ACh supply has been exhausted (Ferguson, 2004). The CHT-/- result is not inconsistent with the hypothesis since the small size of the RRP suggests that the maximal size is limited by a mechanism other than CHT. Additionally, pairing stimulated recording of end plate potentials (EPP) with the spH would be able to show the role of CHT in sustaining cholinergic signaling. There is a dissociation between the summed EPP and fluorescence (Tabares, 2007) that could be exacerbated or relieved by reduction or addition of CHT.

Behavioral impacts of the complex functions of CHT

Because CHT appears to have at least two important functions in supporting cholinergic signaling, the design of behavioral experiments will need to be considered carefully. The most important consideration is the demand the task places on the cholinergic system being investigated (Bazalakova, 2006). This distinction was partially evident with the study of the BAC-CHT mice where the mice performed opposite to expectations in the simple spontaneous alternation

task, and it was clearly evident in the more demanding treadmill task for the Hb9:CHT mice. Although many behaviors will be useful to study, I will focus on only two: memory and attention.

Deficits in memory are the most common feature of Alzheimer's disease and are known to be cholinergically based (Luth, 2003; Schliebs and Arendt, 2006). Furthermore, memory tasks are easily modifiable (by changing the salience of the memory or the duration until recall) to be made more or less taxing on cholinergic function. Experiments performed to directly compare the CHT+/-, WT, and BAC-CHT mice will also illustrate during which stages the cholinergic system is most vulnerable to challenge and most receptive to augmentation.

Attentional tasks have many of the same advantages as memory tasks, but have the added advantage of currently established links to CHT (Apparsundaram, 2005a). Furthermore, memory is, by definition, a delayed task that will likely involve postsynaptic mechanisms, which in the case of ACh has been demonstrated through mAChR (Dickinson, 2009). However, attentional tasks have more immediate demands on cholinergic signaling and would be more likely to elicit changes in the dynamic properties proposed for CHT, particularly as distratctors are added (Sarter, 2009).

In addition to the intrinsic demands of each task, pharmacological challenges may elicit relevant phenotypes from mice with altered CHT levels. Drugs directly acting on AChRs or AChE may reveal changes to the cholinergic system that are not otherwise evident (Bazalakova, 2006). Cholinergic pathways also interact with other systems in ways that are relevant to disease and can be tested by

pharamcologically challenging behavior. For example, attentional deficits casued by prolonged amphetamine adminstration that mimicks some aspects of schizophrenia may be improved by manipulations, such as the BAC-CHT mouse, that elevate ACh release (Sarter, 2009)

Conclusion

In conclusion, studies in altered expression levels of CHT have provided new insight into how CHT acts at the synapse and how these changes affect cholinergic functions. Hopefully, this and future work will lead to novel treatments for cholinergic deficits based on the idea that CHT can be a target for augmentation of cholinergic signaling. The mouse models presented here should also be excellent tools for the continued study of CHT and its role at cholinergic synapses.

REFERENCES

Abramson, J., I. Smirnova, V. Kasho, G. Verner, H. R. Kaback and S. Iwata (2003). Structure and mechanism of the lactose permease of Escherichia coli. *Science.* **301**, 610-5.

Abramson, J. and E. M. Wright (2009). Structure and function of Na(+)-symporters with inverted repeats. *Curr Opin Struct Biol.* **19**, 425-32.

Adams, S. J., R. J. Crook, M. Deture, S. J. Randle, A. E. Innes, X. Z. Yu, W. L. Lin, B. N. Dugger, M. McBride, M. Hutton, D. W. Dickson and E. McGowan (2009). Overexpression of wild-type murine tau results in progressive tauopathy and neurodegeneration. *Am J Pathol.* **175**, 1598-609.

Allen, D. D. and P. R. Lockman (2003). The blood-brain barrier choline transporter as a brain drug delivery vector. *Life Sci.* **73**, 1609-15.

Amenta, F., L. Parnetti, V. Gallai and A. Wallin (2001). Treatment of cognitive dysfunction associated with Alzheimer's disease with cholinergic precursors. Ineffective treatments or inappropriate approaches? *Mech Ageing Dev.* **122**, 2025-40.

Anderson, C. R., A. Bergner and S. M. Murphy (2006). How many types of cholinergic sympathetic neuron are there in the rat stellate ganglion? *Neuroscience.* **140**, 567-76.

Anglister, L., B. Haesaert and U. J. McMahan (1994). Globular and asymmetric acetylcholinesterase in the synaptic basal lamina of skeletal muscle. *J Cell Biol.* **125**, 183-96.

Apparsundaram, S., S. M. Ferguson and R. D. Blakely (2001). Molecular cloning and characterization of a murine hemicholinium-3-sensitive choline transporter. *Biochem Soc Trans.* **29**, 711-6.

Apparsundaram, S., S. M. Ferguson, A. L. George, Jr. and R. D. Blakely (2000). Molecular cloning of a human, hemicholinium-3-sensitive choline transporter. *Biochem Biophys Res Commun.* **276**, 862-7.

Apparsundaram, S., V. Martinez, V. Parikh, R. Kozak and M. Sarter (2005a). Increased Capacity and Density of Choline Transporters Situated in Synaptic Membranes of the Right Medial Prefrontal Cortex of Attentional Task-Performing Rats. *J. Neurosci.* **25**, 3851-3856.

Apparsundaram, S., V. Martinez, V. Parikh, R. Kozak and M. Sarter (2005b). Increased capacity and density of choline transporters situated in synaptic

membranes of the right medial prefrontal cortex of attentional task-performing rats. *J Neurosci.* **25**, 3851-6.

Arber, S., B. Han, M. Mendelsohn, M. Smith, T. M. Jessell and S. Sockanathan (1999). Requirement for the homeobox gene Hb9 in the consolidation of motor neuron identity. *Neuron.* **23**, 659-74.

Asawa, T., M. Shindo and H. Momoi (2004). Compound muscle action potentials during repetitive nerve stimulation. *Muscle Nerve.* **29**, 724-8.

Barker, L. A. and T. W. Mittag (1975). Comparative studies of substrates and inhibitors of choline transport and choline acetyltransferase. *J Pharmacol Exp Ther.* **192**, 86-94.

Bazalakova, M. H. and R. D. Blakely (2006). The high-affinity choline transporter: a critical protein for sustaining cholinergic signaling as revealed in studies of genetically altered mice. *Handb Exp Pharmacol.* 525-44.

Bazalakova, M. H., J. Wright, E. J. Schneble, M. P. McDonald, C. J. Heilman, A. I. Levey and R. D. Blakely (2006). Deficits in acetylcholine homeostasis, receptors and behaviors in choline transporter heterozygous mice. *Genes Brain Behav.*

Bazelyansky, M., E. Robey and J. F. Kirsch (1986). Fractional diffusion-limited component of reactions catalyzed by acetylcholinesterase. *Biochemistry.* **25**, 125-30.

Beeri, R., N. Le Novere, R. Mervis, T. Huberman, E. Grauer, J. P. Changeux and H. Soreq (1997). Enhanced hemicholinium binding and attenuated dendrite branching in cognitively impaired acetylcholinesterase-transgenic mice. *J Neurochem.* **69**, 2441-51.

Berse, B., W. Szczecinska, I. Lopez-Coviella, B. Madziar, V. Zemelko, R. Kaminski, K. Kozar, K. S. Lips, U. Pfeil and J. K. Blusztajn (2005). Expression of high affinity choline transporter during mouse development in vivo and its upregulation by NGF and BMP-4 in vitro. *Brain Res Dev Brain Res.* **157**, 132-40.

Betz, W. J. and G. S. Bewick (1992). Optical analysis of synaptic vesicle recycling at the frog neuromuscular junction. *Science.* **255**, 200-3.

Betz, W. J., F. Mao and C. B. Smith (1996). Imaging exocytosis and endocytosis. *Curr Opin Neurobiol.* **6**, 365-71.

Bhagwandin, A., K. Fuxe and P. R. Manger (2006). Choline acetyltransferase immunoreactive cortical interneurons do not occur in all rodents: a study of the phylogenetic occurrence of this neural characteristic. *J Chem Neuroanat.* **32**, 208-16.

Birks, J. (2006). Cholinesterase inhibitors for Alzheimer's disease. *Cochrane Database Syst Rev.* CD005593.

Birks, R. and F. MacIntosh (1961). Acetylcholine metabolism of a sympathetic ganglion. *Can J Physiol Pharmacol.* **39**, 787-827.

Bissette, G., F. J. Seidler, C. B. Nemeroff and T. A. Slotkin (1996). High affinity choline transporter status in Alzheimer's disease tissue from rapid autopsy. *Ann N Y Acad Sci.* **777**, 197-204.

Black, S. A., F. M. Ribeiro, S. S. Ferguson and R. J. Rylett (2010). Rapid, transient effects of the protein kinase C activator phorbol 12-myristate 13-acetate on activity and trafficking of the rat high-affinity choline transporter. *Neuroscience.* **167**, 765-73.

Bonzelius, F. and H. Zimmermann (1990). Recycled synaptic vesicles contain vesicle but not plasma membrane marker, newly synthesized acetylcholine, and a sample of extracellular medium. *J Neurochem.* **55**, 1266-73.

Booker, T. K., C. M. Butt, J. M. Wehner, S. F. Heinemann and A. C. Collins (2007). Decreased anxiety-like behavior in beta3 nicotinic receptor subunit knockout mice. *Pharmacol Biochem Behav.* **87**, 146-57.

Brandon, E. P., W. Lin, K. A. D'Amour, D. P. Pizzo, B. Dominguez, Y. Sugiura, S. Thode, C. P. Ko, L. J. Thal, F. H. Gage and K. F. Lee (2003). Aberrant patterning of neuromuscular synapses in choline acetyltransferase-deficient mice. *J Neurosci.* **23**, 539-49.

Brandon, E. P., T. Mellott, D. P. Pizzo, N. Coufal, K. A. D'Amour, K. Gobeske, M. Lortie, I. Lopez-Coviella, B. Berse, L. J. Thal, F. H. Gage and J. K. Blusztajn (2004). Choline transporter 1 maintains cholinergic function in choline acetyltransferase haploinsufficiency. *J Neurosci.* **24**, 5459-66.

Brock, M., A. C. Nickel, B. Madziar, J. K. Blusztajn and B. Berse (2007). Differential regulation of the high affinity choline transporter and the cholinergic locus by cAMP signaling pathways. *Brain Res.* **1145**, 1-10.

Byun, N. and E. Delpire (2007). Axonal and periaxonal swelling precede peripheral neurodegeneration in KCC3 knockout mice. *Neurobiol Dis.* **28**, 39-51.

Chandler, K. J., R. L. Chandler, E. M. Broeckelmann, Y. Hou, E. M. Southard-Smith and D. P. Mortlock (2007). Relevance of BAC transgene copy number in mice: transgene copy number variation across multiple transgenic lines and correlations with transgene integrity and expression. *Mamm Genome.* **18**, 693-708.

Chang, C. C., S. J. Hong, H. L. Lin and M. J. Su (1985). Acetylcholine hydrolysis during neuromuscular transmission in the synaptic cleft of skeletal muscle of mouse and chick. *Neuropharmacology.* **24**, 533-9.

Cole, C. R., E. H. Blackstone, F. J. Pashkow, C. E. Snader and M. S. Lauer (1999). Heart-rate recovery immediately after exercise as a predictor of mortality. *N Engl J Med.* **341**, 1351-7.

Coleman, W. L., C. A. Bill, F. Simsek-Duran, G. Lonart, D. Samigullin and M. Bykhovskaia (2008). Synapsin II and calcium regulate vesicle docking and the cross-talk between vesicle pools at the mouse motor terminals. *J Physiol.* **586**, 4649-73.

Coleman, W. L. and M. Bykhovskaia (2009). Rab3a-mediated vesicle recruitment regulates short-term plasticity at the mouse diaphragm synapse. *Mol Cell Neurosci.* **41**, 286-96.

Collier, B. and H. S. Katz (1974). Acetylcholine synthesis from recaptured choline by a sympathetic ganglion. *J Physiol.* **238**, 639-55.

Cousin, M. A. (2000). Synaptic vesicle endocytosis: calcium works overtime in the nerve terminal. *Mol Neurobiol.* **22**, 115-28.

Coyle, J. T., D. L. Price and M. R. DeLong (1983). Alzheimer's disease: a disorder of cortical cholinergic innervation. *Science.* **219**, 1184-90.

Danglot, L. and T. Galli (2007). What is the function of neuronal AP-3? *Biol Cell.* **99**, 349-61.

Dani, J. A. and D. Bertrand (2007). Nicotinic acetylcholine receptors and nicotinic cholinergic mechanisms of the central nervous system. *Annu Rev Pharmacol Toxicol.* **47**, 699-729.

De Jesus Moreno Moreno, M. (2003). Cognitive improvement in mild to moderate Alzheimer's dementia after treatment with the acetylcholine precursor choline alfoscerate: a multicenter, double-blind, randomized, placebo-controlled trial. *Clin Ther.* **25**, 178-93.

De Paepe, B., J. L. De Bleecker and R. Van Coster (2009). Histochemical methods for the diagnosis of mitochondrial diseases. *Curr Protoc Hum Genet.* **Chapter 19**, Unit19 2.

Dickinson, B. A., J. Jo, H. Seok, G. H. Son, D. J. Whitcomb, C. H. Davies, M. Sheng, G. L. Collingridge and K. Cho (2009). A novel mechanism of hippocampal LTD involving muscarinic receptor-triggered interactions between AMPARs, GRIP and liprin-alpha. *Mol Brain.* **2**, 18.

Dowdall, M. J. and H. Zimmermann (1974). Evidence for heterogeneous pools of acetylcholine in isolated cholinergic synaptic vesicles. *Brain Res.* **71**, 160-6.

Ehrenstein, G., Z. Galdzicki and G. D. Lange (1997). The choline-leakage hypothesis for the loss of acetylcholine in Alzheimer's disease. *Biophys J.* **73**, 1276-80.

English, B. A., M. Appalsamy, A. Diedrich, A. M. Ruggiero, D. Lund, J. Wright, N. R. Keller, K. M. Louderback, D. Robertson and R. D. Blakely (2010). Tachycardia, reduced vagal capacity, and age-dependent ventricular dysfunction arising from diminished expression of the presynaptic choline transporter. *Am J Physiol Heart Circ Physiol.* **299**, H799-810.

English, B. A., M. K. Hahn, I. R. Gizer, M. Mazei-Robison, A. Steele, D. M. Kurnik, M. A. Stein, I. D. Waldman and R. D. Blakely (2009). Choline transporter gene variation is associated with attention-deficit hyperactivity disorder. *J Neurodevelop Disord.* **1**, 252-63.

Ernst, W. L., Y. Zhang, J. W. Yoo, S. J. Ernst and J. L. Noebels (2009). Genetic enhancement of thalamocortical network activity by elevating alpha 1g-mediated low-voltage-activated calcium current induces pure absence epilepsy. *J Neurosci.* **29**, 1615-25.

Everett, A. W. and E. J. Ernst (2004). Increased quantal size in transmission at slow but not fast neuromuscular synapses of apolipoprotein E deficient mice. *Exp Neurol.* **185**, 290-6.

Faham, S., A. Watanabe, G. M. Besserer, D. Cascio, A. Specht, B. A. Hirayama, E. M. Wright and J. Abramson (2008). The crystal structure of a sodium galactose transporter reveals mechanistic insights into Na+/sugar symport. *Science.* **321**, 810-4.

Ferguson, S. M., M. Bazalakova, V. Savchenko, J. C. Tapia, J. Wright and R. D. Blakely (2004). Lethal impairment of cholinergic neurotransmission in hemicholinium-3-sensitive choline transporter knockout mice. *Proc Natl Acad Sci U S A.* **101**, 8762-7.

Ferguson, S. M. and R. D. Blakely (2004). The choline transporter resurfaces: new roles for synaptic vesicles? *Mol Interv.* **4**, 22-37.

Ferguson, S. M., V. Savchenko, S. Apparsundaram, M. Zwick, J. Wright, C. J. Heilman, H. Yi, A. I. Levey and R. D. Blakely (2003). Vesicular Localization and Activity-Dependent Trafficking of Presynaptic Choline Transporters. *J. Neurosci.* **23**, 9697-9709.

Fernandez-Alfonso, T. and T. A. Ryan (2004). The kinetics of synaptic vesicle pool depletion at CNS synaptic terminals. *Neuron.* **41**, 943-53.

Fong, S. W., I. S. McLennan, A. McIntyre, J. Reid, K. I. Shennan and G. S. Bewick TGF-beta2 alters the characteristics of the neuromuscular junction by regulating presynaptic quantal size. *Proc Natl Acad Sci U S A.* **107**, 13515-9.

Frick, K. M., L. A. Burlingame, S. S. Delaney and J. Berger-Sweeney (2002). Sex differences in neurochemical markers that correlate with behavior in aging mice. *Neurobiol Aging.* **23**, 145-58.

Gaffield, M. A. and W. J. Betz (2007). Synaptic Vesicle Mobility in Mouse Motor Nerve Terminals with and without Synapsin. *J. Neurosci.* **27**, 13691-13700.

Gaffield, M. A., S. O. Rizzoli and W. J. Betz (2006). Mobility of synaptic vesicles in different pools in resting and stimulated frog motor nerve terminals. *Neuron.* **51**, 317-25.

Gaffield, M. A., L. Tabares and W. J. Betz (2009). The spatial pattern of exocytosis and post-exocytic mobility of synaptopHluorin in mouse motor nerve terminals. *J Physiol.* **587**, 1187-200.

Garcia, R. A., D. E. Laney, S. M. Parsons and H. G. Hansma (1998). Substructure and responses of cholinergic synaptic vesicles in the atomic force microscope. *J Neurosci Res.* **52**, 350-5.

Gates, J., Jr., S. M. Ferguson, R. D. Blakely and S. Apparsundaram (2004). Regulation of choline transporter surface expression and phosphorylation by protein kinase C and protein phosphatase 1/2A. *J Pharmacol Exp Ther.* **310**, 536-45.

Geldenhuys, W. J., V. K. Manda, R. K. Mittapalli, C. J. Van der Schyf, P. A. Crooks, L. P. Dwoskin, D. D. Allen and P. R. Lockman (2010). Predictive screening model for potential vector-mediated transport of cationic substrates at the blood-brain barrier choline transporter. *Bioorg Med Chem Lett.* **20**, 870-7.

Gitler, D., Q. Cheng, P. Greengard and G. J. Augustine (2008). Synapsin IIa controls the reserve pool of glutamatergic synaptic vesicles. *J Neurosci.* **28**, 10835-43.

Gong, S., C. Zheng, M. L. Doughty, K. Losos, N. Didkovsky, U. B. Schambra, N. J. Nowak, A. Joyner, G. Leblanc, M. E. Hatten and N. Heintz (2003). A gene expression atlas of the central nervous system based on bacterial artificial chromosomes. *Nature.* **425**, 917-25.

Gracz, L. M., W. C. Wang and S. M. Parsons (1988). Cholinergic synaptic vesicle heterogeneity: evidence for regulation of acetylcholine transport. *Biochemistry.* **27**, 5268-74.

Gras, C., B. Amilhon, E. M. Lepicard, O. Poirel, J. Vinatier, M. Herbin, S. Dumas, E. T. Tzavara, M. R. Wade, G. G. Nomikos, N. Hanoun, F. Saurini, M. L. Kemel, B. Gasnier, B. Giros and S. El Mestikawy (2008). The vesicular glutamate

transporter VGLUT3 synergizes striatal acetylcholine tone. *Nat Neurosci.* **11**, 292-300.

Greengard, P., F. Valtorta, A. J. Czernik and F. Benfenati (1993). Synaptic vesicle phosphoproteins and regulation of synaptic function. *Science.* **259**, 780-5.

Haberberger, R. V., U. Pfeil, K. S. Lips and W. Kummer (2002). Expression of the high-affinity choline transporter, CHT1, in the neuronal and non-neuronal cholinergic system of human and rat skin. *J Invest Dermatol.* **119**, 943-8.

Haga, T. (1971). Synthesis and release of (14 C)acetylcholine in synaptosomes. *J Neurochem.* **18**, 781-98.

Hagler, D. J., Jr. and Y. Goda (2001). Properties of synchronous and asynchronous release during pulse train depression in cultured hippocampal neurons. *J Neurophysiol.* **85**, 2324-34.

Hahn, M. K., J. U. Blackford, K. Haman, M. Mazei-Robison, B. A. English, H. C. Prasad, A. Steele, L. Hazelwood, H. M. Fentress, R. Myers, R. D. Blakely, E. Sanders-Bush and R. Shelton (2008). Multivariate permutation analysis associates multiple polymorphisms with subphenotypes of major depression. *Genes Brain Behav.* **7**, 487-95.

Happe, H. K. and L. C. Murrin (1995). In situ hybridization analysis of CHOT1, a creatine transporter, in the rat central nervous system. *J Comp Neurol.* **351**, 94-103.

Harrington, A. M., J. M. Hutson and B. R. Southwell Cholinergic neurotransmission and muscarinic receptors in the enteric nervous system. *Prog Histochem Cytochem.* **44**, 173-202.

Harrington, A. M., J. M. Hutson and B. R. Southwell (2007). High affinity choline transporter immunoreactivity in rat ileum myenteric nerves. *Cell Tissue Res.* **327**, 421-31.

Harrington, A. M., M. Lee, S. Y. Ong, E. Yong, P. Farmer, C. J. Peck, C. W. Chow, J. M. Hutson and B. R. Southwell (2010). Immunoreactivity for high-affinity choline transporter colocalises with VAChT in human enteric nervous system. *Cell Tissue Res.* **341**, 33-48.

Hicks, A., J. Fenton, S. Garner and A. J. McComas (1989). M wave potentiation during and after muscle activity. *J Appl Physiol.* **66**, 2606-10.

Higgs, D. R., D. Vernimmen and B. Wood (2008). Long-range regulation of alpha-globin gene expression. *Adv Genet.* **61**, 143-73.

Hirsch-Reinshagen, V., J. Y. Chan, A. Wilkinson, T. Tanaka, J. Fan, G. Ou, L. F. Maia, R. R. Singaraja, M. R. Hayden and C. L. Wellington (2007). Physiologically regulated transgenic ABCA1 does not reduce amyloid burden or amyloid-beta peptide levels in vivo. *J Lipid Res.* **48**, 914-23.

Holmstrand, E. C., J. Asafu-Adjei, A. R. Sampson, R. D. Blakely and S. R. Sesack (2010). Ultrastructural localization of high-affinity choline transporter in the rat anteroventral thalamus and ventral tegmental area: differences in axon morphology and transporter distribution. *J Comp Neurol.* **518**, 1908-24.

Hoover, D. B., C. E. Ganote, S. M. Ferguson, R. D. Blakely and R. L. Parsons (2004). Localization of cholinergic innervation in guinea pig heart by immunohistochemistry for high-affinity choline transporters. *Cardiovasc Res.* **62**, 112-21.

Horiguchi, K., S. Horiguchi, N. Yamashita, K. Irie, J. Masuda, H. Takano-Ohmuro, T. Himi, M. Miyazawa, Y. Moriwaki, T. Okuda, H. Misawa, H. Ozaki and K. Kawashima (2009). Expression of SLURP-1, an endogenous alpha7 nicotinic acetylcholine receptor allosteric ligand, in murine bronchial epithelial cells. *J Neurosci Res.* **87**, 2740-7.

Inazu, M., H. Takeda and T. Matsumiya (2005). Molecular and functional characterization of an Na+-independent choline transporter in rat astrocytes. *J Neurochem.* **94**, 1427-37.

Ivy, M. T., R. F. Newkirk, M. R. Karim, C. M. Mtshali and J. G. Townsel (2001). Hemicholinium-3 mustard reveals two populations of cycling choline cotransporters in Limulus. *Neuroscience.* **102**, 969-78.

Iwamoto, H., R. D. Blakely and L. J. De Felice (2006). Na+, Cl-, and pH dependence of the human choline transporter (hCHT) in Xenopus oocytes: the proton inactivation hypothesis of hCHT in synaptic vesicles. *J Neurosci.* **26**, 9851-9.

Jope, R. S. and D. J. Jenden (1980). The utilization of choline and acetyl coenzyme A for the synthesis of acetylcholine. *J Neurochem.* **35**, 318-25.

Kaja, S., R. C. van de Ven, J. G. van Dijk, J. J. Verschuuren, K. Arahata, R. R. Frants, M. D. Ferrari, A. M. van den Maagdenberg and J. J. Plomp (2007). Severely impaired neuromuscular synaptic transmission causes muscle weakness in the Cacna1a-mutant mouse rolling Nagoya. *Eur J Neurosci.* **25**, 2009-20.

Kawashima, K., K. Yoshikawa, Y. X. Fujii, Y. Moriwaki and H. Misawa (2007). Expression and function of genes encoding cholinergic components in murine immune cells. *Life Sci.* **80**, 2314-9.

Klein, J., A. Koppen and K. Loffelholz (1998). Regulation of free choline in rat brain: dietary and pharmacological manipulations. *Neurochem Int.* **32**, 479-85.

Krishnaswamy, A. and E. Cooper (2009). An activity-dependent retrograde signal induces the expression of the high-affinity choline transporter in cholinergic neurons. *Neuron.* **61**, 272-86.

Kuromi, H. and Y. Kidokoro (2002). Selective replenishment of two vesicle pools depends on the source of Ca2+ at the Drosophila synapse. *Neuron.* **35**, 333-43.

Lalonde, R. (2002). The neurobiological basis of spontaneous alternation. *Neurosci Biobehav Rev.* **26**, 91-104.

Lee, C., A. Barnes, E. Yang and R. L. Katz (1977). Neuromuscular facilitation during train-of-four and tetanic stimulation in healthy volunteers: observations with half-refractory paired responses. *Br J Anaesth.* **49**, 555-60.

Lee, N. Y., H. M. Choi and Y. S. Kang (2009). Choline transport via choline transporter-like protein 1 in conditionally immortalized rat syncytiotrophoblast cell lines TR-TBT. *Placenta.* **30**, 368-74.

Lentz, M. and J. F. Nielsen (2002). Post-exercise facilitation and depression of M wave and motor evoked potentials in healthy subjects. *Clin Neurophysiol.* **113**, 1092-8.

Lerman, I., B. C. Harrison, K. Freeman, T. E. Hewett, D. L. Allen, J. Robbins and L. A. Leinwand (2002). Genetic variability in forced and voluntary endurance exercise performance in seven inbred mouse strains. *J Appl Physiol.* **92**, 2245-2255.

Li, X., J. C. Patel, J. Wang, M. V. Avshalumov, C. Nicholson, J. D. Buxbaum, G. A. Elder, M. E. Rice and Z. Yue (2010). Enhanced striatal dopamine transmission and motor performance with LRRK2 overexpression in mice is eliminated by familial Parkinson's disease mutation G2019S. *J Neurosci.* **30**, 1788-97.

Lightfoot, J. T., M. J. Turner, K. A. Debate and S. R. Kleeberger (2001). Interstrain variation in murine aerobic capacity. *Med Sci Sports Exerc.* **33**, 2053-7.

Lin, W., B. Dominguez, J. Yang, P. Aryal, E. P. Brandon, F. H. Gage and K. F. Lee (2005). Neurotransmitter acetylcholine negatively regulates neuromuscular synapse formation by a Cdk5-dependent mechanism. *Neuron.* **46**, 569-79.

Lips, K. S., U. Pfeil, K. Reiners, C. Rimasch, K. Kuchelmeister, R. C. Braun-Dullaeus, R. V. Haberberger, R. Schmidt and W. Kummer (2003). Expression of the high-affinity choline transporter CHT1 in rat and human arteries. *J Histochem Cytochem.* **51**, 1645-54.

Loewi, O. (1921). Über humorale übertragbarkeit der Herznervenwirkung. *Pflügers Archiv European Journal of Physiology.* **189**, 239-242.

Lowenstein, P. R. and J. T. Coyle (1986). Rapid regulation of [3H]hemicholinium-3 binding sites in the rat brain. *Brain Res.* **381**, 191-4.

Luth, H. J., J. Apelt, A. O. Ihunwo, T. Arendt and R. Schliebs (2003). Degeneration of beta-amyloid-associated cholinergic structures in transgenic APP SW mice. *Brain Res.* **977**, 16-22.

Madziar, B., S. Shah, M. Brock, R. Burke, I. Lopez-Coviella, A. C. Nickel, E. B. Cakal, J. K. Blusztajn and B. Berse (2008). Nerve growth factor regulates the expression of the cholinergic locus and the high-affinity choline transporter via the Akt/PKB signaling pathway. *J Neurochem.* **107**, 1284-93.

Mandl, P., J. P. Kiss and E. S. Vizi (2003). Functional neurochemical evidence for the presence of presynaptic nicotinic acetylcholine receptors at the terminal region of myenteric motoneurons: a study with epibatidine. *Neurochem Res.* **28**, 407-12.

Maouche, K., M. Polette, T. Jolly, K. Medjber, I. Cloez-Tayarani, J. P. Changeux, H. Burlet, C. Terryn, C. Coraux, J. M. Zahm, P. Birembaut and J. M. Tournier (2009). {alpha}7 nicotinic acetylcholine receptor regulates airway epithelium differentiation by controlling basal cell proliferation. *Am J Pathol.* **175**, 1868-82.

Massett, M. P. and B. C. Berk (2005). Strain-dependent differences in responses to exercise training in inbred and hybrid mice. *Am J Physiol Regul Integr Comp Physiol.* **288**, R1006-1013.

Mayser, W., P. Schloss and H. Betz (1992). Primary structure and functional expression of a choline transporter expressed in the rat nervous system. *FEBS Lett.* **305**, 31-6.

McLachlan, E. M. (1977). The effects of strontium and barium ions at synapses in sympathetic ganglia. *J Physiol.* **267**, 497-518.

Mellott, T. J., N. W. Kowall, I. Lopez-Coviella and J. K. Blusztajn (2007). Prenatal choline deficiency increases choline transporter expression in the septum and hippocampus during postnatal development and in adulthood in rats. *Brain Res.* **1151**, 1-11.

Meriggioli, M. N. and D. B. Sanders (2009). Autoimmune myasthenia gravis: emerging clinical and biological heterogeneity. *Lancet Neurol.* **8**, 475-90.

Michel, V., Z. Yuan, S. Ramsubir and M. Bakovic (2006). Choline transport for phospholipid synthesis. *Exp Biol Med (Maywood).* **231**, 490-504.

Misawa, H., H. Fujigaya, T. Nishimura, Y. Moriwaki, T. Okuda, K. Kawashima, K. Nakata, A. M. Ruggiero, R. D. Blakely, F. Nakatsu and H. Ohno (2008).

Aberrant trafficking of the high-affinity choline transporter in AP-3-deficient mice. *Eur J Neurosci.* **27**, 3109-17.

Misgeld, T., R. W. Burgess, R. M. Lewis, J. M. Cunningham, J. W. Lichtman and J. R. Sanes (2002). Roles of neurotransmitter in synapse formation: development of neuromuscular junctions lacking choline acetyltransferase. *Neuron.* **36**, 635-48.

Mobley, W. C., J. L. Rutkowski, G. I. Tennekoon, K. Buchanan and M. V. Johnston (1985). Choline acetyltransferase activity in striatum of neonatal rats increased by nerve growth factor. *Science.* **229**, 284-7.

Molenaar, P. C. (2008). A relative weak leg muscle in the rolling Nagoya mouse as a model for Lambert-Eaton myasthenic syndrome. *J Neuroimmunol.* **201-202**, 166-71.

Motomura, M., B. Lang, I. Johnston, J. Palace, A. Vincent and J. Newsom-Davis (1997). Incidence of serum anti-P/O-type and anti-N-type calcium channel autoantibodies in the Lambert-Eaton myasthenic syndrome. *J Neurol Sci.* **147**, 35-42.

Murakami, H., N. Sawada, N. Koyabu, H. Ohtani and Y. Sawada (2000). Characteristics of choline transport across the blood-brain barrier in mice: correlation with in vitro data. *Pharm Res.* **17**, 1526-30.

Nachshen, D. A. and M. P. Blaustein (1982). Influx of calcium, strontium, and barium in presynaptic nerve endings. *J Gen Physiol.* **79**, 1065-87.

Nadler, J. J., S. S. Moy, G. Dold, D. Trang, N. Simmons, A. Perez, N. B. Young, R. P. Barbaro, J. Piven, T. R. Magnuson and J. N. Crawley (2004). Automated apparatus for quantitation of social approach behaviors in mice. *Genes Brain Behav.* **3**, 303-14.

Nagy, G., K. Reim, U. Matti, N. Brose, T. Binz, J. Rettig, E. Neher and J. B. Sorensen (2004). Regulation of releasable vesicle pool sizes by protein kinase A-dependent phosphorylation of SNAP-25. *Neuron.* **41**, 417-29.

Nakata, K., T. Okuda and H. Misawa (2004). Ultrastructural localization of high-affinity choline transporter in the rat neuromuscular junction: enrichment on synaptic vesicles. *Synapse.* **53**, 53-6.

Neves, G., A. Neef and L. Lagnado (2001). The actions of barium and strontium on exocytosis and endocytosis in the synaptic terminal of goldfish bipolar cells. *J Physiol.* **535**, 809-24.

Nguyen, M. L., G. D. Cox and S. M. Parsons (1998). Kinetic parameters for the vesicular acetylcholine transporter: two protons are exchanged for one acetylcholine. *Biochemistry.* **37**, 13400-10.

O'Regan, S. and B. Collier (1981). Factors affecting choline transport by the cat superior cervical ganglion during and following stimulation, and the relationship between choline uptake and acetylcholine synthesis. *Neuroscience.* **6**, 511-20.

Oh, S. J., Y. Hatanaka, G. C. Claussen and E. Sher (2007). Electrophysiological differences in seropositive and seronegative Lambert-Eaton myasthenic syndrome. *Muscle Nerve.* **35**, 178-83.

Ohno, K., A. Tsujino, J. M. Brengman, C. M. Harper, Z. Bajzer, B. Udd, R. Beyring, S. Robb, F. J. Kirkham and A. G. Engel (2001). Choline acetyltransferase mutations cause myasthenic syndrome associated with episodic apnea in humans. *Proc Natl Acad Sci U S A.* **98**, 2017-22.

Okuda, T., T. Haga, Y. Kanai, H. Endou, T. Ishihara and I. Katsura (2000). Identification and characterization of the high-affinity choline transporter. *Nat Neurosci.* **3**, 120-5.

Okuda, T., M. Okamura, C. Kaitsuka, T. Haga and D. Gurwitz (2002). Single nucleotide polymorphism of the human high affinity choline transporter alters transport rate. *J Biol Chem.* **277**, 45315-22.

Oliveira, L. and P. Correia-de-Sa (2006). Dissociation between M1-facilitation of acetylcholine release and crosstalk with A2A- and M2-receptors on rat motoneurons. *Signal Transduct.* **6**, 19-31.

Otsu, Y. and T. H. Murphy (2004). Optical postsynaptic measurement of vesicle release rates for hippocampal synapses undergoing asynchronous release during train stimulation. *J Neurosci.* **24**, 9076-86.

Parikh, V., S. Apparsundaram, R. Kozak, J. B. Richards and M. Sarter (2006). Reduced expression and capacity of the striatal high-affinity choline transporter in hyperdopaminergic mice. *Neuroscience.* **141**, 379-89.

Pfeil, U., R. V. Haberberger, K. S. Lips, L. Eberling, V. Grau and W. Kummer (2003). Expression of the high-affinity choline transporter CHT1 in epithelia. *Life Sci.* **72**, 2087-90.

Picciotto, M. R., D. H. Brunzell and B. J. Caldarone (2002). Effect of nicotine and nicotinic receptors on anxiety and depression. *Neuroreport.* **13**, 1097-106.

Prado, V. F., C. Martins-Silva, B. M. de Castro, R. F. Lima, D. M. Barros, E. Amaral, A. J. Ramsey, T. D. Sotnikova, M. R. Ramirez, H. G. Kim, J. I. Rossato, J. Koenen, H.

Quan, V. R. Cota, M. F. Moraes, M. V. Gomez, C. Guatimosim, W. C. Wetsel, C. Kushmerick, G. S. Pereira, R. R. Gainetdinov, I. Izquierdo, M. G. Caron and M. A. Prado (2006). Mice deficient for the vesicular acetylcholine transporter are myasthenic and have deficits in object and social recognition. *Neuron.* **51**, 601-12.

Rassadi, S., A. Krishnaswamy, B. Pie, R. McConnell, M. H. Jacob and E. Cooper (2005). A null mutation for the alpha3 nicotinic acetylcholine (ACh) receptor gene abolishes fast synaptic activity in sympathetic ganglia and reveals that ACh output from developing preganglionic terminals is regulated in an activity-dependent retrograde manner. *J Neurosci.* **25**, 8555-66.

Ribeiro, F. M., J. Alves-Silva, W. Volknandt, C. Martins-Silva, H. Mahmud, A. Wilhelm, M. V. Gomez, R. J. Rylett, S. S. Ferguson, V. F. Prado and M. A. Prado (2003). The hemicholinium-3 sensitive high affinity choline transporter is internalized by clathrin-mediated endocytosis and is present in endosomes and synaptic vesicles. *J Neurochem.* **87**, 136-46.

Ribeiro, F. M., S. A. Black, S. P. Cregan, V. F. Prado, M. A. Prado, R. J. Rylett and S. S. Ferguson (2005a). Constitutive high-affinity choline transporter endocytosis is determined by a carboxyl-terminal tail dileucine motif. *J Neurochem.* **94**, 86-96.

Ribeiro, F. M., S. A. G. Black, S. P. Cregan, V. F. Prado, M. A. M. Prado, R. J. Rylett and S. S. G. Ferguson (2005b). Constitutive high-affinity choline transporter endocytosis is determined by a carboxyl-terminal tail dileucine motif. *Journal of Neurochemistry.* **94**, 86-96.

Ribeiro, F. M., M. Pinthong, S. A. Black, A. C. Gordon, V. F. Prado, M. A. Prado, R. J. Rylett and S. S. Ferguson (2007). Regulated recycling and plasma membrane recruitment of the high-affinity choline transporter. *Eur J Neurosci.* **26**, 3437-48.

Richards, D. A., C. Guatimosim and W. J. Betz (2000). Two endocytic recycling routes selectively fill two vesicle pools in frog motor nerve terminals. *Neuron.* **27**, 551-9.

Richards, D. A., C. Guatimosim, S. O. Rizzoli and W. J. Betz (2003). Synaptic vesicle pools at the frog neuromuscular junction. *Neuron.* **39**, 529-41.

Rizzoli, S. O. and W. J. Betz (2004). The structural organization of the readily releasable pool of synaptic vesicles. *Science.* **303**, 2037-9.

Rizzoli, S. O. and W. J. Betz (2005). Synaptic vesicle pools. *Nat Rev Neurosci.* **6**, 57-69.

Robinson, P. J. and P. R. Dunkley (1983). Depolarization-dependent protein phosphorylation in rat cortical synaptosomes: the effects of calcium, strontium and barium. *Neurosci Lett.* **43**, 85-90.

Rommelspacher, H., A. M. Goldberg and M. J. Kuhar (1974). Action of hemicholinium-3 on cholinergic nerve terminals after alteration of neuronal impulse flow. *Neuropharmacology.* **13**, 1015-23.

Rotundo, R. L. (2003). Expression and localization of acetylcholinesterase at the neuromuscular junction. *J Neurocytol.* **32**, 743-66.

Salahpour, A., A. J. Ramsey, I. O. Medvedev, B. Kile, T. D. Sotnikova, E. Holmstrand, V. Ghisi, P. J. Nicholls, L. Wong, K. Murphy, S. R. Sesack, R. M. Wightman, R. R. Gainetdinov and M. G. Caron (2008). Increased amphetamine-induced hyperactivity and reward in mice overexpressing the dopamine transporter. *Proc Natl Acad Sci U S A.* **105**, 4405-10.

Saltarelli, M. D., P. R. Lowenstein and J. T. Coyle (1987). Rapid in vitro modulation of [3H]hemicholinium-3 binding sites in rat striatal slices. *Eur J Pharmacol.* **135**, 35-40.

Sarter, M., V. Martinez and R. Kozak (2009). A neurocognitive animal model dissociating between acute illness and remission periods of schizophrenia. *Psychopharmacology (Berl).* **202**, 237-58.

Schara, U., H. J. Christen, H. Durmus, M. Hietala, K. Krabetz, C. Rodolico, G. Schreiber, H. Topaloglu, B. Talim, W. Voss, H. Pihko, A. Abicht, J. S. Muller and H. Lochmuller (2010). Long-term follow-up in patients with congenital myasthenic syndrome due to CHAT mutations. *Eur J Paediatr Neurol.* **14**, 326-33.

Schatz, C. R. and R. W. Veh (1987). High-resolution localization of acetylcholinesterase at the rat neuromuscular junction. *J Histochem Cytochem.* **35**, 1299-307.

Scheuber, A., R. Rudge, L. Danglot, G. Raposo, T. Binz, J. C. Poncer and T. Galli (2006). Loss of AP-3 function affects spontaneous and evoked release at hippocampal mossy fiber synapses. *Proc Natl Acad Sci U S A.* **103**, 16562-7.

Schikorski, T. and C. F. Stevens (2001). Morphological correlates of functionally defined synaptic vesicle populations. *Nat Neurosci.* **4**, 391-5.

Schliebs, R. and T. Arendt (2006). The significance of the cholinergic system in the brain during aging and in Alzheimer's disease. *J Neural Transm.* **113**, 1625-44.

Schmitt, B. M., D. Gorbunov, P. Schlachtbauer, B. Egenberger, V. Gorboulev, E. Wischmeyer, T. Muller and H. Koepsell (2009). Charge-to-substrate ratio during organic cation uptake by rat OCT2 is voltage dependent and altered by exchange of glutamate 448 with glutamine. *Am J Physiol Renal Physiol.* **296**, F709-22.

Schwab, R. S., K. E. Osserman and J. E. Tether (1957). Treatment of myasthenia gravis; prolonged action with multiple-dose tablets of neostigmine bromide and mestinon bromide. *J Am Med Assoc.* **165**, 671-4.

Schwartz, P., E. Vanoli, M. Stramba-Badiale, G. De Ferrari, G. Billman and R. Foreman (1988). Autonomic mechanisms and sudden death. New insights from analysis of baroreceptor reflexes in conscious dogs with and without a myocardial infarction. *Circulation.* **78**, 969-979.

Shao, X. M. and J. L. Feldman (2005). Cholinergic neurotransmission in the preBotzinger Complex modulates excitability of inspiratory neurons and regulates respiratory rhythm. *Neuroscience.* **130**, 1069-81.

Simon, J. R., S. Atweh and M. J. Kuhar (1976). Sodium-dependent high affinity choline uptake: a regulatory step in the synthesis of acetylcholine. *J Neurochem.* **26**, 909-22.

Simon, J. R. and M. G. Kuhar (1975). Impulse-flow regulation of high affinity choline uptake in brain cholinergic nerve terminals. *Nature.* **255**, 162-3.

Singewald, N. (2007). Altered brain activity processing in high-anxiety rodents revealed by challenge paradigms and functional mapping. *Neurosci Biobehav Rev.* **31**, 18-40.

Slotkin, T. A., C. B. Nemeroff, G. Bissette and F. J. Seidler (1994). Overexpression of the high affinity choline transporter in cortical regions affected by Alzheimer's disease. Evidence from rapid autopsy studies. *J Clin Invest.* **94**, 696-702.

Song, P., H. S. Sekhon, Y. Jia, J. A. Keller, J. K. Blusztajn, G. P. Mark and E. R. Spindel (2003). Acetylcholine is synthesized by and acts as an autocrine growth factor for small cell lung carcinoma. *Cancer Res.* **63**, 214-21.

Spowart-Manning, L. and F. J. van der Staay (2004). The T-maze continuous alternation task for assessing the effects of putative cognition enhancers in the mouse. *Behav Brain Res.* **151**, 37-46.

Squire, L. R. (1969). Effects of pretrial and posttrial administration of cholinergic and anticholinergic drugs on spontaneous alternation. *J Comp Physiol Psychol.* **69**, 69-75.

Steiner, J. A., A. M. Carneiro and R. D. Blakely (2008). Going with the flow: trafficking-dependent and -independent regulation of serotonin transport. *Traffic.* **9**, 1393-402.

Stevens, C. F. and J. H. Williams (2007). Discharge of the readily releasable pool with action potentials at hippocampal synapses. *J Neurophysiol.* **98**, 3221-9.

Sudhof, T. C. (2004). The synaptic vesicle cycle. *Annu Rev Neurosci.* **27**, 509-47.

Sugita, S., O. H. Shin, W. Han, Y. Lao and T. C. Sudhof (2002). Synaptotagmins form a hierarchy of exocytotic Ca(2+) sensors with distinct Ca(2+) affinities. *Embo J.* **21**, 270-80.

Sussman, J. D., Z. Argov, D. McKee, E. Hazum, S. Brawer and H. Soreq (2008). Antisense treatment for myasthenia gravis: experience with monarsen. *Ann N Y Acad Sci.* **1132**, 283-90.

Sweet, D. H., D. S. Miller and J. B. Pritchard (2001). Ventricular choline transport: a role for organic cation transporter 2 expressed in choroid plexus. *J Biol Chem.* **276**, 41611-9.

Tabares, L., R. Ruiz, P. Linares-Clemente, M. A. Gaffield, G. Alvarez de Toledo, R. Fernandez-Chacon and W. J. Betz (2007). Monitoring synaptic function at the neuromuscular junction of a mouse expressing synaptopHluorin. *J Neurosci.* **27**, 5422-30.

Thaler, J., K. Harrison, K. Sharma, K. Lettieri, J. Kehrl and S. L. Pfaff (1999). Active suppression of interneuron programs within developing motor neurons revealed by analysis of homeodomain factor HB9. *Neuron.* **23**, 675-87.

Tillotson, D. L. and A. L. Gorman (1983). Localization of neuronal Ca2+ buffering near plasma membrane studied with different divalent cations. *Cell Mol Neurobiol.* **3**, 297-310.

Tomi, M., K. Arai, M. Tachikawa and K. Hosoya (2007). Na(+)-independent choline transport in rat retinal capillary endothelial cells. *Neurochem Res.* **32**, 1833-42.

Trommershauser, J., R. Schneggenburger, A. Zippelius and E. Neher (2003). Heterogeneous presynaptic release probabilities: functional relevance for short-term plasticity. *Biophys J.* **84**, 1563-79.

Van der Kloot, W. (2003). Loading and recycling of synaptic vesicles in the Torpedo electric organ and the vertebrate neuromuscular junction. *Prog Neurobiol.* **71**, 269-303.

Vaseghi, M. and K. Shivkumar The Role of the Autonomic Nervous System in Sudden Cardiac Death. *Prog Cardiovasc Dis.* **50**, 404-419.

Vernino, S., S. Hopkins and Z. Wang (2009). Autonomic ganglia, acetylcholine receptor antibodies, and autoimmune ganglionopathy. *Auton Neurosci.* **146**, 3-7.

Volpicelli, L. A. and A. I. Levey (2004). Muscarinic acetylcholine receptor subtypes in cerebral cortex and hippocampus. *Prog Brain Res.* **145**, 59-66.

Volpicelli-Daley, L. A., A. Hrabovska, E. G. Duysen, S. M. Ferguson, R. D. Blakely, O. Lockridge and A. I. Levey (2003). Altered striatal function and muscarinic cholinergic receptors in acetylcholinesterase knockout mice. *Mol Pharmacol.* **64**, 1309-16.

von Engelhardt, J., M. Eliava, A. H. Meyer, A. Rozov and H. Monyer (2007). Functional characterization of intrinsic cholinergic interneurons in the cortex. *J Neurosci.* **27**, 5633-42.

Wang, B., L. Yang, Z. Wang and H. Zheng (2007). Amyolid precursor protein mediates presynaptic localization and activity of the high-affinity choline transporter. *Proc Natl Acad Sci U S A.* **104**, 14140-5.

Wessler, I. and H. Kilbinger (1986). Release of [3H]acetylcholine from a modified rat phrenic nerve-hemidiaphragm preparation. *Naunyn Schmiedebergs Arch Pharmacol.* **334**, 357-64.

Wessler, I., C. J. Kirkpatrick and K. Racke (1999). The cholinergic 'pitfall': acetylcholine, a universal cell molecule in biological systems, including humans. *Clin Exp Pharmacol Physiol.* **26**, 198-205.

Wessler, I. and J. Sandmann (1987). Uptake and metabolism of [3H]choline by the rat phrenic nerve-hemidiaphragm preparation. *Naunyn Schmiedebergs Arch Pharmacol.* **335**, 231-7.

Whitehouse, P. J., D. L. Price, R. G. Struble, A. W. Clark, J. T. Coyle and M. R. Delon (1982). Alzheimer's disease and senile dementia: loss of neurons in the basal forebrain. *Science.* **215**, 1237-9.

Wilson, J. M., R. Hartley, D. J. Maxwell, A. J. Todd, I. Lieberam, J. A. Kaltschmidt, Y. Yoshida, T. M. Jessell and R. M. Brownstone (2005). Conditional rhythmicity of ventral spinal interneurons defined by expression of the Hb9 homeodomain protein. *J Neurosci.* **25**, 5710-9.

Wilson, M. H. and M. R. Deschenes (2005). The neuromuscular junction: anatomical features and adaptations to various forms of increased, or decreased neuromuscular activity. *Int J Neurosci.* **115**, 803-28.

Wood, S. J. and C. R. Slater (2001). Safety factor at the neuromuscular junction. *Prog Neurobiol.* **64**, 393-429.

Woolf, N. J. (1991). Cholinergic systems in mammalian brain and spinal cord. *Prog Neurobiol.* **37**, 475-524.

Wyatt, R. M. and R. J. Balice-Gordon (2008). Heterogeneity in synaptic vesicle release at neuromuscular synapses of mice expressing synaptopHluorin. *J Neurosci.* **28**, 325-35.

Xie, J. and Q. Guo (2004). Par-4 inhibits choline uptake by interacting with CHT1 and reducing its incorporation on the plasma membrane. *J Biol Chem.* **279**, 28266-75.

Yamamura, H. I. and S. H. Snyder (1973). High affinity transport of choline into synaptosomes of rat brain. *J Neurochem.* **21**, 1355-74.

Yu, S. P. and W. Van der Kloot (1991). Increasing quantal size at the mouse neuromuscular junction and the role of choline. *J Physiol.* **433**, 677-704.

Yuan, Z., A. Tie, M. Tarnopolsky and M. Bakovic (2006). Genomic organization, promoter activity, and expression of the human choline transporter-like protein 1. *Physiol Genomics.* **26**, 76-90.

Yuan, Z., L. Wagner, A. Poloumienko and M. Bakovic (2004). Identification and expression of a mouse muscle-specific CTL1 gene. *Gene.* **341**, 305-12.

Zengel, J. E. and K. L. Magleby (1977). Transmitter release during repetitive stimulation: selective changes produced by Sr2+ and Ba2+. *Science.* **197**, 67-9.

Zengel, J. E. and K. L. Magleby (1981). Changes in miniature endplate potential frequency during repetitive nerve stimulation in the presence of Ca2+, Ba2+, and Sr2+ at the frog neuromuscular junction. *J Gen Physiol.* **77**, 503-29.

Zhang, W., A. S. Basile, J. Gomeza, L. A. Volpicelli, A. I. Levey and J. Wess (2002). Characterization of central inhibitory muscarinic autoreceptors by the use of muscarinic acetylcholine receptor knock-out mice. *J Neurosci.* **22**, 1709-17.

Zhao, Y. and M. Klein (2004). Changes in the readily releasable pool of transmitter and in efficacy of release induced by high-frequency firing at Aplysia sensorimotor synapses in culture. *J Neurophysiol.* **91**, 1500-9.

Zhu, C. B., A. M. Carneiro, W. R. Dostmann, W. A. Hewlett and R. D. Blakely (2005). p38 MAPK activation elevates serotonin transport activity via a trafficking-independent, protein phosphatase 2A-dependent process. *J Biol Chem.* **280**, 15649-58.